EVALUATION OF OOCYTE COMPETENCY IN BOVINE AND CANINE SPECIES VIA NON-INVASIVE ASSESSMENT OF OOCYTE QUALITY

A Dissertation

by

LAURI WILLINGHAM-ROCKY

Submitted to the Office of Graduate Studies of
Texas A&M University
in partial fulfillment of the requirements for the degree of

DOCTOR OF PHILOSOPHY

December 2008

Major Subject: Veterinary Anatomy

EVALUATION OF OOCYTE COMPETENCY IN BOVINE AND CANINE SPECIES VIA NON-INVASIVE ASSESSMENT OF OOCYTE QUALITY

A Dissertation

by

LAURI WILLINGHAM-ROCKY

Submitted to the Office of Graduate Studies of
Texas A&M University
in partial fulfillment of the requirements for the degree of

DOCTOR OF PHILOSOPHY

Approved by:

Co-Chairs of Committee,	Robert C. Burghardt
	Mark E. Westhusin
Committee Members,	Duane C. Kraemer
	Katrin Hinrichs
Head of Department,	Evelyn Tiffany-Castiglioni

December 2008

Major Subject: Veterinary Anatomy

ABSTRACT

Evaluation of Oocyte Competency in Bovine and Canine Species via Non-Invasive Assessment of Oocyte Quality.

(December 2008)

Lauri Willingham-Rocky, B.S., University of North Texas;

M.S., Texas A&M University

Co-Chairs of Advisory Committee: Dr. Robert C. Burghardt
Dr. Mark E. Westhusin

Traditional methods of oocyte selection for in vitro studies have proven inefficient with respect to achieving a level of predictability for competency. In this study, a novel method of oocyte selection was implemented that identified a relationship between oocyte morphological parameters (as defined by a ratio of a shape factor (SF) to average fluorescence intensity (AFI) and AFI, followed by in vitro fertilization (IVF) and in vitro culture (IVC) using the Well of Well (WOW) method to evaluate oocyte competency. Specifically, we used non-cytotoxic fluorescent molecular probes and multiphoton microscopy to non-invasively characterize spatial localization and functional activity of mitochondria, mitochondrial membrane potential ($\Delta\psi m$), and intracellular calcium activity ($[Ca^{2+}]_i$) using rhodamine 123, JC-1 and Fluo-4, AM, respectively in bovine and canine in vitro matured (IVM) oocytes. Comparison of morphological grading with fluorescence intensity yielded similar trends between all grades of oocytes for both species with no visually obvious, distinct characteristic staining that

would permit classification of each oocyte as a specific morphological grade. Our studies confirmed that oocyte mitochondria were homogeneously distributed but primarily localized to the peri- and sub-cortical regions of the oocyte at MII stage for both species. Further, heterogeneously polarized mitochondria were localized to the peri- and sub- cortical regions of the oocyte for both species. In bovine oocytes labeled with Fluo-4, AM, levels of $[Ca^{2+}]_i$ were either unremarkable, or very low and limited to the peri-cortical areas, just beneath the oolema. For canine MII stage oocytes, levels of $[Ca^{2+}]_i$ were within the same range of AFI as bovine. Ranges of fluorescence intensity compatible for optimal embryo development for bovine and optimal fertilization for canine oocytes were 30-300 and 20-35, and 20-30 and 20-25.5 for rhodamine 123 and Fluo-4, AM, respectively. The optimal range for bovine oocytes imaged with JC-1 was 1.25-2.25 and $\leq$6 for canine.

DEDICATION

This dissertation is dedicated to my two “perfectly competent” oocytes, who have blossomed into two “perfectly beautiful” little girls, Avery & Ella Paige, and to my husband, Jonathan, who never let me give up, giving me the motivation to finish this chapter of my life.

ACKNOWLEDGEMENTS

While the completion of this dissertation brings closure to this chapter of my life, I cannot move on without expressing the most heartfelt gratitude and respect to Dr. Robert Burghardt, who has been a model mentor and advisor. Thank you for your patience, guidance, leadership, motivation and counseling. More importantly, thanks for not giving up on me!

I am also very grateful to Dr. Rola Barhoumi Mouneimne for her collaboration, patience and guidance. Her contributions to this project and to my graduate career are invaluable.

The support of my co-chair, Dr. Mark Westhusin and fellow committee members, Drs. Duane Kraemer and Katrin Hinrichs is also greatly appreciated. Thank you for your continued guidance and support of my research and graduate path.

Further, this project would not have been possible without the help and support of many people who spent countless hours assisting me with my research. Thank you to Drs. Chuck Long, Carol Hanna, and Taeyoung Shin, and also to Christy Bormann, Jane Pryor, Sharon Kolenda and J. Matthew Wright, D.V.M. and Dr. Dana Dean for their technical assistance.

Lastly, thank you to BioArts Research Coporation for funding this research.

TABLE OF CONTENTS

CHAPTER Page

CHAPTER Page

LIST OF FIGURES

FIGURE Page

FIGURE Page

FIGURE Page

FIGURE Page

LIST OF TABLES

TABLE Page

CHAPTER I

INTRODUCTION

1.1 Overview

High oocyte quality is linked to the production of superior embryos. Oocyte properties correlated with improved embryo development have been extensively studied, yet oocyte-grading criteria remain imprecise with respect to the correlation between "good" oocytes and developmental competence. Experimentally, the morphology of ovarian follicles and oocytes in the bovine has been linked to the prediction of embryo developmental competence (Gandolfi *et al.,* 1997; Wurth and Kruip, 1992). Some of these criteria include oocyte size, shape, color, stage of meiosis (metaphase II with first polar body extrusion), zona pellucida integrity, cumulus cell layers, and follicle size (Leibfried and First, 1979). While these characteristics have been a useful guideline for numerous in vitro experiments, many oocytes that appear healthy and normal are incapable of supporting embryo development (Rocha *et al.,* 1998). These findings are indicative of an obvious lack of understanding of the functional aspects of oocyte physiology which contribute to developmental competence.

Methods of morphological oocyte selection present major limitations for efficiently identifying reliable criteria of oocyte competency, especially in canids.

This dissertation follows the style of Molecular Reproduction and Development.

A more mechanistic physiological approach of assessing oocyte quality that has no adverse effects would greatly enhance this area of research. Recent technological advances in microscopy (e.g. computer controlled instruments, laser light sources, sensitive detectors, biosensor technologies, image processing software) offer new avenues to assess both morphological and functional properties of living cells and tissues. These technologies have been used to describe a number of functional properties of mammalian oocytes and embryos but have not yet been applied to the assessment of mammalian oocyte quality in a non-invasive fashion. These approaches might also be useful for competence assessment in the canine oocyte, the maturation of which is poorly understood relative to other mammalian species.

1.2 Canine female reproduction

Historically, the dog has played an integral role in the initial discovery of many facets of mammalian reproduction. Antoine von Leeuwenhoek, coined by some as “the father of microscopy,” used semen from dogs during the late 1600’s to describe the extent of spermatozoa dissemination into the female genital tract, and what capacity they had for survival under these conditions (Castellani, 1973). Almost 100 years later in Italy, Lazzaro Spallanzani used semen siphoned from a naturally bred bitch to inseminate a different bitch in heat. This breeding resulted in the birth of 3 pups and is the first recorded attempt of mammalian artificial insemination and also assisted reproduction in

the dog (Harrop, 1956). Also, Ernest Von Baer used ova collected from dog ovaries to first describe the mammalian female gamete in the early 1900's (O'Malley, 1956). While the dog has contributed to the foundation of these scientific "firsts" for mammalian reproduction, progress in understanding canine reproductive physiology and assisted reproduction in the bitch lags far behind the technological advances reported for other mammalian species that include protocols for in vitro maturation (IVM), in vitro fertilization (IVF), in vitro culture (IVC), intracytoplasmic sperm injection (ICSI), and embryo/gamete cryopreservation. Currently, clinical assisted reproduction in the dog is limited to semen collection and freezing, artificial insemination, and heterologous embryo transfer. However, the application of modern advances in assisted reproductive technology such as somatic cell nuclear transfer, or "cloning" may potentially be an alternative to the preservation of superior genetics among various breeds, wild or endangered canids, or those of a beloved pet (Lee *et al.,* 2005; Jang *et al.,* 2007; Jang *et al.,* 2008a, Jang *et al.,* 2008b).

Domestic canines (*Canis familiaris)* are classified as monoestrous, meaning one estrus phase is exhibited per breeding season, unlike most mammalian species that are classified as either continuous or seasonal breeders. Wild or rare breed canid bitches such as the gray wolf (*Canis lupus*) and the swift fox (*Vulpes velox*) are seasonal breeders and usually experience estrus only once per annum. Conversely, the domestic bitch is considered a non-seasonal breeder due to her ability to exhibit estrus and produce off spring

at any time of the year. Previous studies of numerous domestic breed bitches conducted in the 1970's reported peak estrous activity during late winter and spring, similar to that observed in non-domestic canids suggesting an evolutionary contribution of domestication (Sokolowski, 1977; Jochle and Andersen, 1977; Christie and Bell, 1971; Tedor and Reif, 1978). Nevertheless, all canids have an extended inter-estrus, or anestrus phase between fertile periods, the duration of which varies among breeds and limits reproductive opportunity to one or two times each year.

From an endocrinology perspective, the canid estrous cycle is comparable to that reported for other mammalian species (*i.e.*: increasing estradiol levels, FSH and LH surges prior to ovulation, progesterone producing corpus luteum, etc.) with a number of species-specific exceptions. Toward the end of proestrus, estradiol levels increase gradually, peaking just prior to onset of estrus (Fig. 1.1). Unlike most mammals where estrogen dominates the pre-ovulatory environment, canine pre-ovulatory follicles begin to luteinize just prior to the LH surge and produce progesterone that is detectable in sera throughout the estrus phase (Feldman and Nelson, 2004).

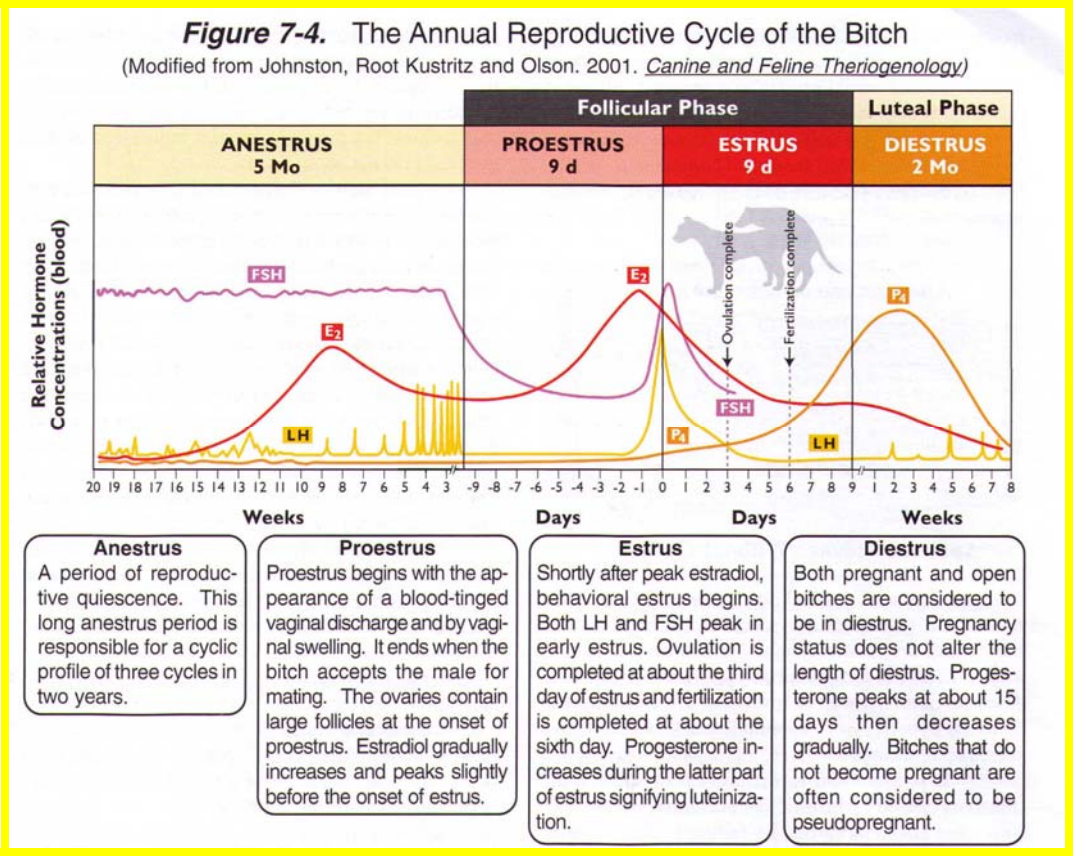

Figure 1.1. Canine estrous cycle (from Senger, 1999).

Ovulation occurs roughly 2-3 days following the LH peak and is correlated with progesterone levels 4-10 ng/ml. Progesterone production from the corpus luteum increases to levels and duration similar to that seen in pregnant bitches, with peak levels occurring 15-30 days following the LH surge and then gradually decreasing (Feldman and Nelson, 2004). A return to anestrus is marked by progesterone levels that are <1-2 ng/ml, and remains persistent for several months until the subsequent cycle begins. This phase is often referred to as a quiescent period of the canine estrous cycle from clinical and behavioral assessment, but not endocrinologically. Small, pulsatile bursts of both LH and

FSH occur throughout anestrus, and increase just prior to the onset of proestrus, while prolactin levels decrease (Kooistra *et al.,* 1999; Corrada *et al.,* 2003). Fluctuations in estradiol concentrations also occur and increase during late anestrus, just prior to initiation of the breeding period (Onclin *et al.,* 2002).

The physiological mechanisms regulating follicle recruitment and the onset of proestrus both at puberty and after the prolonged inter-estrus period are poorly defined for canids. Firstly, primordial follicle development is not completed until ~15-17 days after birth, and follicular growth of primary follicles is not observed until 4-5½ months of age when the bitch becomes sexually mature (Anderson and Simpson, 1973). However, efforts to induce estrus in both prepubertal (120-150 days of age) and adult bitches have been successful using gonadotropins (LH, FSH, hCG, hMG, PMSG, eCG), GnRH and related agonists (deslorelin, luprolide acetate), the synthetic estrogen diethylstilbesterol (DES), prostaglandins (PGF2α), dopamine agonists to decrease prolactin levels (cabergoline, metergoline, or bromocriptine), or combinations thereof (Cain *et al.,* 1989; Inaba *et al.,* 1998; Verstegen *et al.,* 1998; Kooistra *et al.,* 1999; Concannon, 2002b; Marks *et al.,* 2002; Gobello and Corrada, 2003; Beijerink *et al.,* 2004). Results from these experiments were variable with respect to degree of response and reaction times to proestrus. Further, these experiments included the use of drugs that are not approved for veterinary use, are not available in some countries, or involved complex modes of administration (i.e. GnRH infusion pump) (Cain *et al.,* 1989). Also, induction protocols administered

to bitches in earlier stages of anestrus responded slower than those in mid or late anestrus (Wanke *et al.,* 1996; Verstegen *et al.,* 1998). Presently, there is no standard protocol for the induction of estrus in canids recommended for clinical use.

The process of canine oocyte development is even less understood than that reported for other species. The physiology of canine female reproduction presents a challenge due to the uniqueness of the canine estrous cycle which is characterized by a prolonged inter-estrus phase (~6 months) between fertile period and the ovulation of immature ova (Farstad, 2000). Further, oocyte maturation in vivo is delayed roughly 2 days post ovulation and occurs in the oviduct. Therefore, the degree of developmental competence of the canine oocyte at ovulation is unclear. This obscurity has presented major challenges for the development of in vitro maturation and fertilization procedures, resulting in very little advancement of knowledge in terms of defining the morphological and functional aspects of oocyte developmental competence in canines.

The most remarkable dissimilarity in canine reproduction with other species is the process of ovulation and oocyte maturation. Ovulation occurs roughly 2 days following the LH peak, and the resulting ova are at the prophase I (germinal vesicle, GV) stage of meiosis (Concannon *et al.,* 1989). Wildt *et al.,* (1979) showed that 70% of ovulatory follicles ovulate in the first 24-72 hours after the LH peak, but that ovulation at any other time during the end of proestrus and estrus is possible. After ovulation, oocytes must undergo both

nuclear and cytoplasmic maturation in the oviduct over a period of 24-72 hours. Reynaud *et al.,* (2005) showed that in vivo ovulated oocytes did not progress beyond the GV stage until at least 44 hours, and that MII was not observed before 54 hours post-ovulation (Reynaud *et al.,* 2005). This hallmark in canine reproductive physiology is in sharp contrast to that of most other domestic mammalian species wherein ovulation of mature, metaphase II oocytes normally occurs ~30 hours post LH surge. Reports of viability for the canine oocyte have been suggested to span as many as 6-8 days as evidenced by litters produced from single matings 7-8 days post ovulation (Concannon, 2002b; Concannon and Verstegen, 2005). Hence, the degree of developmental competence of the canine oocyte prior to or at ovulation is unclear.

Fertilization occurs in the ampullary region of the oviduct for most mammals and resulting embryos enter the uterus about 3 days later (Wimsatt, 1975). However in canids, fertilization occurs in the distal third of the oviduct and embryos enter the uterus ~9-12 days later at the compact morula or blastocyst stage (Holst and Phemister, 1971; Valtonen and Jalkanen, 1993). Implantation occurs ~17-19 days post ovulation and the blastocysts average 2.5 mm in diameter (Holst and Phemister, 1971). Gestation length for domestic canines has been shown to range from 57-72 days from first mating, and averages 63 days post ovulation (Johnston *et al.,* 2001).

A number of canine IVM/IVF studies have indicated that sperm are able to penetrate the oocyte at the GV stage and form a pronucleus, indicating an

induction of meiotic resumption in in vitro matured oocytes similar to that reported for the human and cow (Chian *et al.,* 1992; Van Blerkom *et al.,* 1994; Farstad, 2000; Saint-Dizier *et al.,* 2001). However, the integrity of this meiotic resumption in vitro is unclear as reported in experiments by Saint-Dizier *et al.,* (2001) wherein 41.7% of fertilized canine oocytes at the GV stage were polyspermic, averaging 3.5 spermatozoa per oocyte, and that all sperm nuclei were moderately decondensed (Saint-Dizier *et al.,* 2001). Contrary to this observation, studies defining in vivo meiotic resumption and fertilization in the bitch reported no sperm penetration in ovulated GV stage oocytes, only 3% fertilization in immature oocytes (GVBD-teleophase I), with fertilization occurring in most cases 90 hours post-ovulation in MII stage oocytes, and no incidence of polyspermy (Reynaud *et al.,* 2005). Thus, the ability of immature oocytes to allow sperm penetration and pronucleus formation in vitro could result from a number of factors including sub-optimal culture conditions, inappropriate sperm numbers, lack of cytoplasmic oocyte maturation, failure to block polyspermy, etc.

The factors that trigger resumption of meiosis after ovulation in the domestic bitch are peculiar, and very limited information is available regarding the cell signaling mechanisms of canine cumulus-oocyte complexes (COC). Krogenæs *et al.,* (1993) reported that the addition of FSH to IVM medium significantly increased cAMP levels, induced greater cumulus expansion, and caused a significant increase in the number of oocytes reaching MII at 48 and 72 hours of culture. Investigation of mitogen activated protein kinase (MAPK)

phosphorylation for IVM oocytes in presence of FSH and in ovulated oocytes matured in vitro as first reported in vixen oocytes occurs after 48-72 hours of culture, but in the absence of FSH in IVM media, phosphorylation is accelerated by at least 24 hours and exceeded phosphorylation levels of the former cultures (Kalab *et al.,* 1997). More recently, the activities of maturation promoting factor (MPF)/MAPK levels, as well as the cytoskeletal and chromatin organization patterns associated with these kinases in in vitro matured oocytes of domestic canines were comparable to those observed in other mammalian species (Saint-Dizier *et al.,* 2004).

Gap junction intercellular communication (GJIC) has also been partially investigated. Functional gap junction channels between cumulus cells and oocytes were reported in experiments using microinjected Lucifer Yellow into the oocyte cytoplasm of COC's during late proestrus, which diffused into the cumulus cells, whereas no dye transfer was detected into oocytes of bitches in anestrus (Luvoni *et al.,* 2001). This observation suggests a functional difference in GJIC between the two estrous cycle stages that may be hormonally influenced. Furthermore, connexin43 (Cx43) protein, the most abundant gap junction protein in the mammalian ovary, was identified in cumulus and corona radiata cells of the Blue fox during IVM experiments and showed a reduction, but not complete uncoupling of GJIC in corona cells after 72 hours of IVM (Srsen *et al.,* 1998). This is in sharp contrast to in vivo matured oocytes of the Blue fox on days 2-3 post-ovulation or for IVM bovine oocytes where gap junctions are

completely disconnected from the oocyte, suggesting the corona radiata cells may regulate the resumption of meiosis during in vitro, but not during in vivo oocyte maturation in this species (Hyttel *et al.,* 1990; Hyttel *et al.,* 1997). Messenger RNA expression profiles for *GJA1*, the gene encoding Cx43, were found to be consistent with those reported for other species and indicated an increased expression during proestrus, a marked decreased expression at estrus, rising levels during diestrus, followed by declining values during anestrus (Willingham-Rocky *et al.,* 2006). Taken together, these data indicate that the molecular events surrounding meiotic resumption and oocyte maturation in canids reported thus far are not significantly different from what is known in other mammals. Conversely, the considerable delay of oocyte maturation in relation to the LH peak or to ovulation in canine oocytes is perplexing, and offers an interesting model to study oocyte competence.

The morphology of canine oocytes is distinctive from that of other carnivores, and mammals in general. The most obvious difference being the appearance of a dense, dark, lipid-rich cytoplasm, which is generally typical of the lower, nonplacental vertebrates, and thus relatively rare among mammalian species (Tesoriero, 1981; Szabo, 1967). Lipids are present in the oocytes of many other mammals (i.e. cow, cat, horse, and human) in varying amounts, but appear intensely concentrated in canid, mustelid and porcine oocytes (Tesoriero, 1981; Lindeberg, 2003; Sturmey and Leese, 2003). Although the functional and biochemical aspects of oocyte lipids in mammals remains to be

elucidated, the general consensus is that lipids, and particularly triglycerides, serve as a metabolic reservoir for both the oocyte during maturation and the developing embryo after fertilization (McEvoy *et al.,* 2000; Tesoriero, 1981). The dark lipid masks the presence of the GV in canine oocytes, which is centrally located prior to the LH surge, and then relocates to a more cortical region as soon as 1 day post LH (Hyttel *et al.,* 1990). In most mammals, excluding rodents, the GV is located eccentrically in growing or fully-grown oocytes (Albertini and Barrett, 2004). The size of canine oocyte is another important morphological factor and is reported to average 112 μm in diameter (excluding the zona pellucida) in sexually mature bitches (Farstad, 2000). A relationship between canine oocyte size and meiotic competency suggests that oocytes ≥110 μm are competent to resume meiosis, but that oocytes ≥120 μm are the most competent and have significantly increased rates of maturation to MII than those of smaller size (Hewitt and England, 1998; Srsen *et al.,* 1998; Farstad, 2000; Otoi *et al.,* 2001). These data suggest a size-related ability of canine oocytes to undergo meiotic maturation, similar to that reported in the cow (Fair *et al.,* 1995; Otoi *et al.,* 1997).

However, IVM of canine oocytes ≥110 μm diameter remains inefficient in contrast to the mouse, cow, pig, sheep and human (Hewitt and England, 1998). Numerous variations in culture conditions and adaptations of the bovine model for in vitro culture have been investigated that include differences in serum type and concentration, temperature, gas composition, the use of bi-phasic culture

systems that incorporated meiotic inhibitors, and addition of hormones, growth factors and other metabolites. Regardless, none of these variations in culture conditions have advanced the rate of maturation to MII above 25%, and they typically achieve 10-15% to MII (Mahi and Yanagimachi, 1976; Yamada *et al.,* 1992; Yamada *et al.,* 1993, Nickson *et al.,* 1993, Hewitt, 1997; Metcalfe, 1999, Otoi *et al.,* 1999, 2000 and 2002; Songsasen *et al.,* 2002; Bolamba *et al.,* 2002; Willingham-Rocky *et al.,* 2002; Rodrigues and Rodrigues, 2003; Songsasen *et al.,* 2003; Willingham-Rocky *et al.,* 2003; Kim *et al.,* 2004). Recent literature suggests that the estrous cycle stage from which canine oocytes are obtained is an important factor in their ability to resume meiosis and attain competency; and that oocytes recovered from bitches during the follicular and luteal phases of the estrous cycle resume meiosis at a significantly higher rate than do oocytes recovered from anestrus bitches (Luvoni *et al.,* 2001; Otoi *et al.,* 2001; Willingham-Rocky *et al.,* 2003; Lee *et al.,* 2006). It is not known whether this is the result of atretic follicles that have lost their ability to maintain oocytes in an incompetent state, or is the result of acquisition of cytoplasmic competence influenced by hormonal exposure in viable follicles.

The production of canine embryos in vitro by IVF, ICSI, or somatic cell nuclear transfer (SCNT) is equally inefficient as IVM of canine oocytes with limited successful outcomes. Although embryo collection and heterologous transfer attempts have been successful, only one clinical pregnancy has been established from IVM/IVF/embryo transfer, but failed to develop to term

(Kraemer *et al.,* 1982; Jalkanen and Lindeberg, 1998; England *et al.,* 2001). SCNT in the dog being the most recently achieved assisted reproductive technique has resulted in numerous clinical pregnancies and live births (Westhusin *et al.,* 2003 and personal communication; Lee *et al.,* 2005; Jang *et al.,* 2007; Kim *et al.,* 2007). The successful pregnancies and births reported in these experiments are the result of two independent laboratories employing the use of both in vitro and in vivo matured ova, and multiple embryo transfers (Westhusin *et al.,* 2003 and personal communication; Lee *et al.,* 2005; Jang *et al.,* 2007; Kim *et al.,* 2007). However, it is important to clarify that all live births resulting from SCNT were the result of using in vivo matured ova after surgical collection (Lee *et al.,* 2005; Jang *et al.,* 2007; Kim *et al.,* 2007).

To achieve the aforementioned results, numerous IVM experiments attempting to increase the rates of maturation in vitro to MII were conducted to improve the understanding of oocyte physiology and the subsequent development of embryos. While the results of these experiments yielded beneficial insight, there has been very little progress made in increasing the rates of maturation in vitro to MII. Therefore, an investigation of the mechanistic and functional parameters associated with the acquisition of oocyte competence is warranted in order to improve our knowledge of canine oocyte maturation, and to use this information for the advancement of reproductive management in canids.

1.3 Mammalian follicular development

The mammalian ovary is heavily populated by large numbers of oocytes at birth, the majority of which are destined for atresia with each passing estrus or menstrual cycle, while only a select few will ovulate over a reproductive lifetime. The reserve of non-ovulating oocytes during this time period allows for in vivo and in vitro research opportunities that will narrow the gaps in our knowledge base of oocyte and embryo physiology. Information gained from such experiments will not only benefit the treatment of those unable to or have difficult reproducing, but will also define species-specific differences, enhance fertility rates and offspring numbers, and aid in selective breeding and improved genetics.

Oogenesis and folliculogenesis are closely coordinated and interdependent events that together regulate the growth and development of the female gamete beginning in early embryo development (day 10 for most domestic species). The dynamics of this synergistic system insures the legacy of the female gamete, as ovarian follicles do not form without oocytes, and oocyte development is dependent on certain factors produced by the somatic cells of the follicle. Therefore, in order to appreciate and understand characteristics of the mature, fertilizable ova that are capable of producing live offspring, it is imperative to understand the origin of female gametes.

Oocytes arise from primordial germ cells that originate from endoderm of the yolk sac and migrate to the genital ridge of the primitive ovary by self-

propulsive, independent morphogenic movement. Response to certain chemotactic substances such as transforming growth factor β1 (TGFβ1), and other intercellular signaling molecules facilitated by gap junctions are also thought to contribute to the PGC migratory process (Picton, 2001; Perez-Armendariz *et al.,* 2003). During their migration, the PGCs undergo rapid mitotic proliferation and begin to differentiate into oogonia. The expansion of oogonia continues until a predetermined, species-specific population has been achieved before entering meiosis which occurs throughout most of fetal life. Initiation of meiotic division promotes the germ cells to primary oocytes that arrest at the first meiotic prophase. The cytoplasm of meiotically arrested oocytes continues to develop, increasing the size of the germ cell (more than 100-fold) as it accumulates the necessary cellular and molecular machinery to sustain its existence (Gosden, 2002).

Concomitant with the onset of germ cell meiosis is the commencement of folliculogensis. The coordinated development of both the oocyte and somatic cells during follicle formation is the result of complex, bi-directional communication between the two cell types via paracrine secreted factors (i.e.: kit ligand and GDF-9), and gap junctional interactions, specifically via connexins 37 (Cx37) and Cx43, that facilitate the intercellular exchange of small molecular weight cell signaling molecules and metabolites (Albertini and Barrett, 2003). It is believed that epithelial cells of mesenchymal origin branch from the medulla of the ovary into the cortex and invade the clusters of oogonia and oocytes,

encasing them in a single, flattened layer of pregranulosa cells that in turn are separated from the differentiating stromal cells (theca cells) by a basement membrane, thus creating primordial follicles (Bukovsky *et al.,* 2005; Skinner, 2005). It is this population of primordial follicles that comprise what is believed to be a finite source of germ cells in the post-natal ovary; the numbers of which vary among species. Germ cells that do not form follicles degenerate.

Initiation and selection of primordial follicle growth remains poorly understood, but begins during the perinatal period in domestic species and humans, and postnatally in rodents, rabbits and canids. Histological assessment of ovarian architecture shows that non-growing primordial follicles are located in avascular, cortical regions of the ovary, while primordial follicles that have exited their quiescent stage are found in the intensely vascularized cortico-medullary border. This implies that follicle growth and development are dependent on certain metabolic factors and nutrients carried via the blood (Picton, 2001). The etiology of this spatial migration is vague, and is further clouded by the fact that not all primordial follicles activate at the same time. However, studies in mice and domestic species have reported spontaneous activation of primordial follicles in in vitro cultured cortical tissue, suggesting a possible growth inhibitory influence from the resting primordial pool in vivo (Fortune, 2003). Nonetheless, growing primordial follicles are classified as having a mixture of flattened and cuboidal granulosa cells, and then graduate to primary follicles when they become completely surrounded by one layer of

cuboidal-shaped granulosa cells. The continuous cycle of follicular recruitment begins during fetal life shortly after completion of follicle formation for most mammals, arresting just prior to birth, and resuming again at puberty where presumptive ova are destined for either ovulation or atresia. This process of selection and recruitment does not cease until the follicular pool has been exhausted.

Once selected, the cohort of primary follicles begins to grow in response to increasing levels of FSH secretion and under permissive conditions, expansion of granulosa cells occurs rapidly, and secondary follicles are formed when two complete layers have been generated around the oocyte (Fig. 1.2). As granulosa cell expansion continues, the cells begin to differentiate into mural granulosa cells found at the periphery of the follicle nearest to the basement membrane, and also into cumulus and corona radiata cells that immediately surround the growing oocyte. Antrum formation occurs during this differential process, and this fluid-filled cavity continues to increase in volume with follicular development. It is at this stage when the follicle unit is considered “activated” because intercellular communication increases among the somatic cells of the follicle and the oocyte (Hyttel *et al.,* 1997). During this pre-antral to antral transition, the oocyte gains meiotic competence necessary for reorganization of chromatin, meiotic resumption, and epigenetic modifications, all of which are associated with the accumulation of certain cell cycle regulatory factors necessary for cytoplasmic and molecular maturation (Matzuk *et al.,* 2002). The

somatic cells of the follicle (granulosa and theca cells) become responsive to gonadotrophins as the respective receptors are synthesized, and estradiol production increases in growing follicles. Increasing estrogen production contributes to the LH surge, followed by ovulation shortly thereafter for most mammals. It is generally thought that the LH surge triggers a myriad of cell signaling events required for finalizing cytoplasmic, nuclear and molecular maturation of the oocyte and follicle cells necessary for the ovulation of a mature egg that is competent to undergo fertilization.

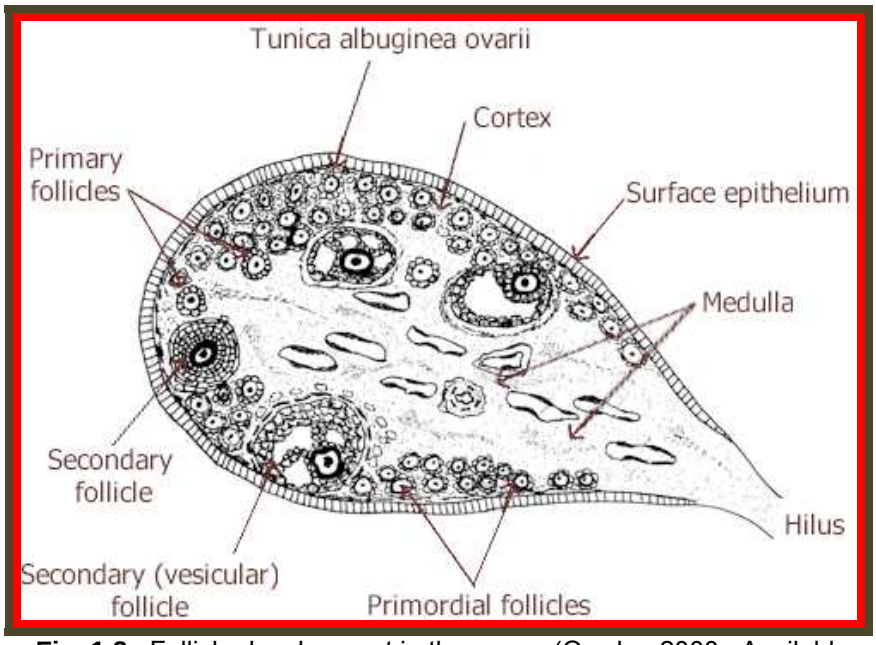

Fig. 1.2. Follicle development in the ovary. (Ownby, 2000. Available: http://instruction.cvhs.okstate.edu/Histology/fr/HiFRp01.htm).

Selection of the ovulatory follicle(s) from the recruited cohort occurs throughout follicular development. Those which escape the alternate pathway of

death grow to the tertiary or Graffian follicle stage and contain an oocyte(s) that is fully grown and is surrounded by a thick zona pellucida. The entire oocyte is surrounded by several layers of cumulus cells, connected to the mural granulosa cells of the follicle by a stalk of cumulus-granulosa cells. At the LH surge, meiotic inhibition is relieved as gap junctions of the somatic cells become disconnected from the oocyte, finalizing oocyte maturation and arresting at the metaphase II stage for most mammals. Ovulation occurs shortly thereafter (species dependent), and the mature, fertilizable ova are transported to the oviduct where it awaits its union with spermatozoa. The residual follicle cells luteinize, forming an endocrine gland that continually secretes progesterone necessary for support and maintenance of the impending pregnancy.

1.4 Mammalian oocyte maturation and mechanisms of developmental competence

While improvements in assisted reproductive technologies (ART) have fairly alleviated the hardships of infertility of humans and animals, limitations in understanding the etiology of infertility problems continue. Mammalian oocytes undergo spontaneous maturation when liberated from antral follicles and cultured in vitro, but in vivo oocyte maturation is under the control of gonadotropins, implying that the constraints limiting meiotic progression in vivo are strongly influenced the by cell signaling products of the somatic cells of the follicle (Pincus and Enzmann, 1935; Edwards 1962). These observations have

launched decades of research dedicated to understanding the functional, physiological and biochemical mechanisms necessary to produce a competent oocyte during oogenesis and folliculogenesis. Studies in mice, cows and other mammals have revealed that oocyte competence is achieved progressively in vivo during oogenesis within the follicle (Thibault *et al,.* 1987; Hyttel *et al.,* 1997; reviewed by Albertini *et al.,* 2003). Furthermore, it has been well established that in vivo matured oocytes are more developmentally competent than in vitro matured oocytes, the cause of which is attributed to the absence of normal preovulatory follicular processes involving progressive changes at the cellular, molecular, and chromosomal stages of oocyte maturation (Lonergan *et al.,* 2003).

Collectively, oocyte developmental competence can be defined as the achievement of nuclear, cytoplasmic and molecular maturation. This process occurs in the ovarian follicle for most mammals and coincides initially with antrum formation at the secondary follicle stage until ovulation in preparation for fertilization and subsequent embryo development. Thus, the oocyte has already accumulated the necessary RNA transcripts and proteins by the end of the growth phase that are required for meiotic and cytoplasmic maturation (Hyttel *et al.,* 1997). On the contrary, acquisition of the cellular and molecular machinery associated with oocyte maturation does not assure developmental competence, hence the rationale for lower in vitro-produced embryo development rates. It is generally believed that oocytes matured in vivo undergo a final maturation phase

within the follicle immediately preceding ovulation in preparation for fertilization that may either be absent or incomplete in IVM oocytes (Hyttel *et al.,* 1997). Consequently, IVF and early cleavage stage bovine embryos can be achieved at rates exceeding 95% from IVM oocytes, but the rate of blastocyst formation plateaus at approximately 30-40%, and these rates have not improved in the last decade (Hyttel *et al.,* 1997; Lonergan *et al.,* 2003).

According to Fair *et al.,* (1995), oocyte meiotic competence is gained in three phases. First, the oocyte acquires the ability to break down the GV, second it achieves the ability to reach metaphase I (MI), and third, gains the ability to progress to MII (Fair *et al.,* 1995). Thus, maternal DNA is transformed from a disbursed configuration in the germinal vesicle (GV) to the highly condensed, yet organized MII chromatin structure following pre-ovulatory LH surge. This process is mediated in part by protein kinases that bring about phosphorylation and dephosphorylation events, hence initiating chromatin condensation, transcriptional repression, histone exchange, and other factors necessary for chromatin remodeling after fertilization (Fan and Sun, 2004). Cytoskeleteal organization of microtubules and centrosome phosphorylation also aid in chromatin condensation and are thought to influence polarity and spatial segregation of cell cycle factors during the critical stages of nuclear maturation (reviewed by Albertini, 2003). A number of oocyte and somatic cell specific gene products such as GDF-9, BMP-15, c-Kit contribute to the acquisition of meiotic arrest at MII which is maintained by inhibitory factors (including cAMP)

contained in the follicular fluid and/or secreted by the somatic cells that transfer information via trans-zonal projections to the developing oocyte until just prior to the LH surge (Hyttel *et al.,* 1997).

Molecular aspects of oocyte maturation have gained more attention recently with the discovery of novel oocyte-derived genes and proteins, the mechanics of countless inter- and intracellular systems affecting oocyte maturation, and the complexity of cell signaling pathway intermediates involved in oocyte maturation. The functions of the oocyte-derived genes have been directly identified via knockout mice that serve as invaluable generalized models for mammalian oocyte physiology in order to reveal the individual contributions to the developing oocyte. To name a few, genes such as *KL*, *Gdf9, Nobox* and *Gja-4* are necessary for oocyte growth, while *Spo11*, *Atm*, *Dmc1, Msh5, Mlh1, and Msh4* mediate recombination of homologous chromosomes and DNA mismatch repair beginning at the primordial to primary oocyte transition (Acevedo and Smith, 2005). Yet these genes do not perform correctly without very specific precursors that are influenced by a series of highly coordinated, complex events between hormones, hormonally responsive follicle cells, and the oocyte (i.e. ligand-receptor binding, upstream signaling cascades, activation of transcription factors, etc.) during meiotic arrest, prior to ovulation.

Cytoplasmic maturation continues during meiotic arrest wherein the oocyte is dependent on the production, modification and redistribution of new gene products and organelles. The oocyte increases both in size (diameter),

and also in volume, or mass during this time, and is dependent upon the replication of mitochondria and associated DNA molecules, as well as accumulation of protein, mRNA transcripts and increased transcriptional and translational activities. Such events are essential for supporting oocyte survival, maturation, fertilization, and early cleavage of embryos until the maternal zygotic transition and activation of the embryonic genome (Van Blerkom, 1991; de Moor and Richter, 1999; Memili and First, 1999; Anderson *et al.,* 2001; Pickard *et al.,* 2001; Stojkovic *et al.,* 2001; and Eichenlaub-Ritter and Peschke, 2002). As a result, nuclear and cytoplasmic maturation are intimately coupled with metabolic and cell-signaling events that occur simultaneously in the oocyte, thus fueling a synergistic relationship.

Additional markers of cytoplasmic maturation include an increase in lipid content, other membrane bound vesicles, glycogen granules, cortical granule synthesis, migration and alignment of the cortical granules at the oolemma, and retraction of trans-zonal projections, resulting in an interruption of GJIC, followed by cumulus cell expansion (Hyttel *et al.,* 1997; Picton *et al.,* 1998; Hendriksen *et al.,* 2000). In addition to the ultrastructural aspects of cytoplasmic maturation, there are a number of well characterized physiological factors that are thought to contribute to oocyte developmental competence. Some of these factors include the spatial distribution and functional properties of mitochondria, glutathione levels, intracellular calcium homeostasis, as well as adverse factors such as

reactive oxygen species (ROS), all of which serve as potential bio-markers of oocyte competence.

Mitochondria are among the most studied organelles in oocytes and are known to be present in large numbers in the mature ovum. They are responsible in part for cellular respiration during the conversion of pyruvate to ATP via oxidative phosphorylation, and also contribute to regulation of calcium homeostasis within the cell, thereby participating in all phases of oocyte maturation and accumulation of energy stores for the developing embryo. ATP is generated within the inner mitochondrial matrix via a proton gradient created by the outward pumping of protons generated from the reduction of NAD^+ to NADPH, and FAD^+ to $FADH_2$ across the inner mitochondrial membrane. The accumulation of protons establishes a high concentration gradient and an electrical gradient between the inner and outer mitochondrial membranes, creating potential energy called the mitochondrial membrane potential ($\Delta\Psi m$). Protons can then begin to diffuse back into the inner mitochondrial membrane via ATP synthase, providing energy to phosphorylate ADP to ATP. ATP is then transported from the inner mitochondrial membrane to the cytosol where it can be utilized to meet the metabolic requirements of the cell.

In oocytes, the efficient production of ATP within the mitochondrial matrix is essential for successful physiological events surrounding embryo development including cell proliferation, DNA replication, and activation of the embryonic genome. Increasing levels of ATP are generated during oocyte

growth as the mitochondria replicate and become primarily localized around the germinal vesicle, and then later disperse during meiotic resumption toward areas potentially requiring higher levels of ATP, such as the peri-cortical region of the cytoplasm in preparation of fertilization as reported for the human, mouse and cow (Van Blerkom *et al.,* 1998; Stojkovic *et al.,* 2001; Van Blerkom *et al.,* 2002; Tarazona *et al.,* 2006). This spatial re-distribution of mitochondria continues with each embryonic division after fertilization.

Stojkovic *et al.,* (2001) reported increased levels of ATP in immature bovine oocytes deemed morphologically favorable (Grades 1 & 2) over those less favorable (Grades 3 & 4), and an overall significant increase in ATP content after IVM in all oocytes, regardless of quality. Further, total blastocyst cell numbers after IVF were higher in embryos derived from Grade 1 & 2 oocytes than those originating from Grade 3 or 4, suggesting a functional diversity amongst oocyte quality and developmental potential. Consequently, a direct relationship between mitochondrial function and oocyte development is hypothesized. The extent to which mitochondria contribute to oocyte competence and embryo development remains obscure, but is of importance in order to better understand oocyte development, and also to learn how mitochondrial dysfunction may be related to oocyte wastage and early embryonic death leading to infertility or other major metabolic diseases (reviewed by Wilding *et al.,* 2001).

Mitochondrial spatial localization and aggregation patterns have most recently been correlated with mitochondrial membrane potential ($\Delta\psi m$) and oocyte developmental competence in human, bovine and rodent oocytes and embryos (Wilding *et al.,* 2001; Van Blerkom *et al.,* 2002). The use of specific potentiometric molecular probes and fluorescence microscopy has facilitated the measurement of such activity throughout oocyte maturation, thereby potentially identifying intracellular areas of metabolic demand. Specifically, areas of heterogeneity with respect to $\Delta\psi m$ have been reported that further support hypotheses surrounding independent, spatial metabolic energy requirements within oocytes and embryos suggesting that oocytes are polarized, and that the cytoplasmic mitochondrial aggregation patterns are directly related to the appearance of the oocyte under the light microscope (Wilding *et al.,* 2001; VanBlerkom *et al.,* 2002). Wilding *et al.,* (2001) further reported that mitochondrial activity is negatively correlated with maternal age which may contribute to lower embryo development and pregnancy rates in women considered to be at an advanced maternal age. Therefore, the measurement of $\Delta\Psi m$ might be used as an indicator of mitochondria health in that it is reflective of the activity and integrity of the mitochondrial membrane. Differences in activity at various stages of meiosis may represent specific energy requirements at each stage.

Maintenance of intracellular calcium homeostasis is a critical element of oocyte physiology that has been well documented throughout oocyte

development and fertilization, but remains ill-defined with regards to certain molecular events surrounding calcium-dependent signaling (Carroll & Swann, 1992; Homa, 1995; and Tosti, 2006). During maturation, free intracellular calcium (Ca^{2+}) is necessary for meiotic progression from one stage to the next and is regulated by certain cell cycle checkpoints that include maturation promoting factor (MPF), mitogen activated protein kinase (MAPK), and emission of the first polar body. Other events in preparation for fertilization require the transient release of intracellular Ca^{2+} from intracellular stores for completion of meiosis and embryonic activation (Whitaker and Patel, 1990; Carroll and Swann, 1992; He *et al.,* 1997). Very slight species-specific differences have been reported between rodents and other mammals regarding the timing of Ca^{2+} transients which may contribute to the variances in oocyte maturation. In mice and hamsters, Ca^{2+} rises prior to GVBD, but in bovine and porcine species, increased intracellular Ca^{2+} levels are not recognized until the GVBD stage and beyond (reviewed by He *et al.,* 1997). These differences between species are thought to be related to LH-induced Ca^{2+} release from adjacent cumulus cells that provide an avenue for transfer of calcium via gap junctions connected directly to the oocyte. For oocytes of domestic species, Ca^{2+} is required for initiation of cyclin synthesis, which occurs after the LH surge. However, for rodent oocytes it is hypothesized that the synthesis of cyclin and associated proteins occurs during follicular development, prior to the LH surge (Homa, 1995). Thus the timing of Ca^{2+} release with respect to the LH surge may be

correlated with the timing of meiotic progression between species. Other studies have confirmed the importance of Ca^{2+} during oocyte maturation by implementing the use of Ca^{2+} chelators that inhibited meiotic progression to GVBD in bovine species, but not in rodents (He at al., 1997; Carroll and Swann, 1992). Hence, the cellular events necessary for GVBD in the mouse are Ca^{2+} independent, while the opposite is true for bovine species. This finding is likely a key factor in the ability of mouse oocytes to spontaneously mature in vitro and remain viable under minimal culture conditions, whereas bovine and other domestic species require hormonal and somatic cell support (Carroll and Swann, 1992). However, the importance of intercellular Ca^{2+} activity cannot solely be defined by the ootcyte's ability to progress beyond GVBD, as its influence on the structural and biochemical modifications of other cytoplasmic and molecular events that occur during oocyte maturation in all mammals should be considered (Homa, 1995; Whitaker, 1996).

Ca^{2+} current activity, intracellular Ca^{2+} stores and COC grade have been correlated with developmental potential in bovine species (Boni *et al.,* 2002). In research presented by Boni *et al.,* (2002), immature bovine COCs were morphologically classified according to criteria set by Wurth and Kruip (1992), matured in vitro, and then 1) evaluated for their developmental potential by either IVF or parthenogenetic activation at both cleavage and blastocyst stages, 2) Ca^{2+} current activity by whole-cell voltage clamp technique, and 3) intracytoplasmic Ca^{2+} stores by microfluorimetric evaluation. Results indicated

that grade B- COCs showed the highest embryo production efficiency, as well as the greatest plasma membrane Ca^{2+} current activity, and the greatest intracellular Ca^{2+} concentration after IVM (Boni *et al.,* 2002). However, Ca^{2+} can also be a limiting factor to the competency of aged mouse oocytes and their ability to undergo normal embryonic development by initiating the Bcl-2 pathway of apoptosis rather than oocyte activation at fertilization, presumably due to aging mitochondria (Gordo, 2002). At any rate, the maintenance of intracellular Ca^{2+} homeostasis is critical for both meiotic progression and cytoplasmic maturation in controlling cell-cycle checkpoints as the oocyte's intracellular Ca^{2+} stores are accumulated.

The prevention of ROS generation within the oocyte is another critical cellular mechanism in achieving oocyte developmental competence. Oxygen is an indispensable element of life's cellular processes, especially as its role of final electron acceptor in the respiratory chain. Oxygen related free radical production resulting from cellular respiration or other metabolic events play key roles in maintaining intracellular homeostasis, certain cell signaling events and mediating stress responses at physiological levels. However, if the generation of free radicals or O_2 concentrations exceed physiological limitations, detrimental cellular damage may occur due to oxidative stress, affecting metabolism, cell signaling, amino acid transport, and DNA associated events, thus upsetting the homeostatic intracellular balance related to cellular disruptions and possibly cell death by altering the cell's reduction-oxidation (redox) state (Burton *et al.,* 2002).

Such imbalances may be prevented or rescued by the cell's inherent antioxidant system(s) to resume normal function. Perhaps the most widely studied of these systems utilizes glutathione (GSH), the major ubiquitous, intracellular thiol redox buffer. Glutathione (the tripeptide, γ- glutamylcysteinylglycine) is synthesized in the cytosol, and participates in numerous detoxifying reactions, namely those involving hydrogen peroxide and other ROS (Burton *et al.,* 2002; Harvey *et al.,* 2002; and Luberda, 2005).

The relevance of GSH and redox state to reproductive function and embryo development has been closely investigated and have revealed that GSH concentrations are higher in the mature oocyte than in immature oocytes and that levels recede after fertilization, suggesting that GSH synthesis may be coupled with cell cycle events (Furnus *et al.,* 1998; Kaneko *et al.,* 2001; Zuelke *et al.,* 2003). Improvements in IVM and subsequent embryo development rates have also been reported from experiments supplementing IVM media with other thiols, or with amino acid precursors to GSH synthesis (Yoshikuni *et al.,* 1988; Yoshida *et al., 1993;* deMatos *et al.,* 1996; Abeydeera *et al.,* 1999; deMatos and Furnus, 2000; Bing *et al.,* 2001; Kim *et al.,* 2004; Kobayashi *et al.,* 2006; Maedomari *et al.,* 2007). Furthermore, the elevated concentration of GSH at MII has been hypothesized to play an important role in male pronucleus formation after fertilization, and hence correlated with improved embryo development in the mouse, hamster, pig and cow (Furnus *et al.,* 1998; deMatos and Furnus, 2000; deMatos *et al.,* 2002; Liu *et al.,* 2002; Zuelke *et al.,* 2003). In contrast,

GSH levels significantly decrease after fertilization and are not remarkable throughout embryo development (Zulke *et al.,* 2003). Thus, high concentrations of GSH are necessary for oocyte maturation and fertilization suggesting the importance of this metabolic pathway to both cytoplasmic and nuclear oocyte maturation necessary for quality embryo development. For this reason, GSH levels may serve as a useful biomarker for evaluating oocyte competency.

1.5 Selection and assessment of mammalian oocyte quality

A relationship between follicle size, oocyte size and developmental competence has been established for many species (mice, cattle, swine, goat, and sheep) based exclusively on morphology (Otoi *et al.,* 1997; Steeves and Gardner 1999; Salamone *et al.,* 2001; Eichenlaub-Ritter and Peschke, 2002). For example in cattle, oocytes considered to be developmentally competent have been identified in follicles that have initiated antrum formation and are at least 3 mm in diameter, with an oocyte of at least 110μm in diameter, excluding the surrounding cumulus cells (Hyttell *et al.,* 1997, Fair *et al.,* 1995). Otoi *et al.,* (1997) reported a relationship between oocyte size and meiotic competence by improved IVM rates to MII in oocytes at 115 μm, 120μm and 125 μm (85%, 96% and 100%, respectively) (Otoi *et al.,* 1997). In contrast, oocytes obtained from small follicles (<3mm) and (≤2mm) in cows and pre-pubertal calves, respectively are able to achieve nuclear maturation to MII but have poor embryo development rates suggesting that developmental competence is acquired

progressively and therefore independent of nuclear maturation. (Damiani *et al.,* 1996; Steeves and Gardner, 1999). Moreover, many studies have revealed that oocytes retrieved from atretic follicles in cattle and horses have better in vitro maturation and/or embryo development than do oocytes from viable follicles (Blondin and Sirard, 1995; Gandolfi *et al.,* 1997; Hinrichs and Williams, 1997; Rocha *et al.,* 1998; Choi *et al.,* 2004).

In addition to size of both the follicle and oocyte, morphological characteristics for oocyte selection and grading depend on several other factors, but most notably, the number of cumulus layers surrounding the oocyte at retrieval. COC morphology of the immature oocyte is related to oocyte developmental competence in the mouse, human, pig, and cow, and subsequently has been categorized into grades, using either a number (1, 2, 3 or 4) or letter system (A, B, C) that are similarly defined. Oocytes designated as “Grade A or 1” have the presence of a clear, compact and multi-layered cumulus and homogenous cytoplasm. “Grade B or 2” oocytes have a cytoplasm that is homogeneous with only few areas showing irregular pigmentation and a darker ooplasm, the fewer cumulus layers than in Grade A/1 COCs but have more than five layers of compact cumulus cells. Grade B oocytes are thought to be derived from mature follicles that can no longer maintain meiotic arrest, and developmental potential of in vitro produced embryos that is surprisingly higher in grade B COC’s in cattle, as is also observed in the horse in expanded COCs (Blondin and Sirard, 1995; Hinrichs and Williams, 1997; Boni *et al.,* 2002).

“Grade C or 3” oocytes have a cytoplasm that is heterogeneous/vacuolated, dark and unevenly pigmented and the zona pellucida is covered by three to five layers of cumulus cells except for small denuded areas. Grades 3 & 4 are often combined as Grade 3 or C, however, Grade 4 can further be defined as having a cytoplasm that is heterogeneously pigmented and cumulus that is completely or in great part absent or expanded, (Wurth and Kruip, 1992; Stojkovic *et al.,* 2001). Other general features of oocyte selection and grading can be assessed in mature, denuded oocytes and include the appearance of a smooth, round ooplasm, visualization of the first polar body, clear peri-vitelline space, absence of vacuoles in the cytoplasm, and an intact, round and clear zona pellucida (Allen *et al.,* 1930; Pincus and Enzmann, 1935; Shettles, 1958; Motlik *et al.,* 1984; Hyttel *et al.,* 1997; and Hendriksen *et al.,* 2000). However, differences can vary among these criteria depending on one’s interpretation during the selection process. Furthermore, selection criteria established for mammals in general may not be applicable to species such as the horse.

The rising interest in using ART has reinforced the importance of identifying egg quality as an indicative marker of embryo quality and its correlation to embryo development, thus improving the rates of pregnancy and live offspring. However, the correlation between “good” oocytes and developmental competence remains obscure, as evidenced by comparatively low live birth rates among species. Currently the molecular properties of oocyte quality are ill defined however decades of research have aided in identifying

several generic morphological parameters that have contributed to an improvement in oocyte selection. On the contrary, a majority of oocytes that are favorable for ART procedures fail to exhibit any marked discrepancies in a given population that would allow an accurate forecast of embryo developmental potential (i.e.: follicle size, oocyte size, shape, color, cytoplasmic granularity, integrity of the zona pellucida and cumulus cell vestments, oocyte age post ovulation, and meiotic status among others) (Allen *et al.,* 1930; Pincus and Enzmann, 1935; Shettles, 1958; Motlik *et al.,* 1984; Hyttel *et al.,* 1997; and Hendriksen *et al.,* 2000).

More recently, the emergence of specialized computer hardware and software programs have been designed to aid in oocyte and embryo assessment/selection that non-invasively detect and/or measure certain morphological features including 3-D imaging of oocyte external and internal architecture, and spindle and zona pellucida integrity (Fertimorph™, MetaMorph™, and OOsight™, respectively). Regardless of the selection criteria reported and imaging technology available for identifying morphological oocyte qualities, there remains no adequate method by which mammalian oocytes can be efficiently evaluated other than by fertilization, and in the end, birth of live, healthy offspring. Further, considering that the majority of oocytes used in current ART procedures across species are in vitro derived, it is imperative that markers of oocyte competency be defined on a more intrinsic, yet non-invasive level to complement the morphological standards.

1.6 Research objectives

As suggested by the few reports mentioned herein, efforts have been made to unravel the mystery of what constitutes a healthy, competent oocyte. However, these methods are generally considered invasive and do not permit intimate evaluation without compromising cellular physiology or vitality. The marriage of two non-invasive selection approaches (morphological and mechanistic) for determining oocyte quality may lead to the development of novel, “cell friendly” methods for oocyte screening and selection. The application of certain microscopy tools such as multiphoton microscopy has already enabled the non-invasive exploration of various biological events in living cells/tissues such as neurons, capillaries, brain tissue, and embryos (Squirrell *et al.,* 1999; Dedov *et al.,* 2001; Larson *et al.,* 2003; McLellan *et al.,* 2003 and Squirrell *et al.,* 2003). Multiphoton microscopy is a promising imaging tool thought to be more advantageous than conventional confocal laser scanning microscopy (CLSM) because it uses two (or more) photons simultaneously to excite a fluorophore, rather than one photon, thereby employing a longer wavelength light, which penetrates to a greater depth and is less destructive than short wavelength light. Additionally, the multiphoton excitation occurs only at the focal point of the sample, thus tissues are exposed to less photo-damage compared to confocal laser scanning microscopy (CLSM) (White and Errington, 2002). Squirrell *et al.,* (1999) have compared the developmental potential of hamster embryos imaged by both CLSM and multiphoton microscopy. They

reported that embryos imaged by CLSM displayed signs of oxidative stress as evidenced by the production of hydrogen peroxide, which was further associated with decreased developmental competence. Embryos imaged using multiphoton microscopy did not indicate comparable signs of oxidative stress and, in fact, were developmentally comparable to non-imaged control embryos. These studies support the use of non-invasive and non-destructive microscopy and imaging techniques for the development of novel and potentially useful oocyte screening methods that might be applied for the selection of competent oocytes.

Establishment of the aforementioned selection criteria has been achieved through the use of optical and electron microscopy, and has provided a foundation from which to generalize mammalian oocyte morphological characteristics based on non-invasive selection of the COC for use in vitro. The gap in understanding more specific functional and mechanistic aspects of oocyte physiology has hindered recognition of true oocyte quality. Therefore, the non-invasive identification of specific molecular markers associated with oocyte quality and/or embryo development will establish an invaluable contribution toward improving embryo development and live birth rates in mammals.

The overall objective of this research project was to gain a better understanding of the physiological aspects of canine oocyte development and to establish better methods to assess mammalian oocyte quality in general. To achieve these goals, we have developed methods that may be generically useful in assessing mammalian oocyte competence and that can ultimately be applied to the evaluation of canine oocyte quality. Specifically, we have:

1. Characterized the spatial distribution of mitochondria and mitochondrial activity, and intercellular Ca^{2+} stores as they relate to morphology of in vitro matured bovine oocytes and established baseline criteria of functional parameters for selection.

2. Evaluated embryonic developmental potential of bovine oocytes from objective 1 via in vitro fertilization to determine optimal oocyte selection.

3. Characterized the spatial distribution of mitochondria and mitochondrial activity and intercellular Ca^{2+} stores in relation to morphology of in vitro matured canine oocytes using criteria from objective 1 that could potentially be used to evaluate developmental competence in this species.

4. Modified a unique IVF/IVC culture system that allowed for the tracking of individual embryos throughout development to the blastocyst stage.

CHAPTER II

GENERAL MATERIALS AND METHODS

2.1 Oocyte collection, in vitro maturation and selection

Given that there is a lack of commercial resources for canine oocytes, as well as defined IVM/IVF protocols for the production of mature canine oocytes and embryos, experiments conducted to fulfill this objective were performed using commercially available bovine oocytes to serve as a reference oocyte model system for studies with canine oocytes. Bovine oocytes were shipped in maturation medium (prepared by the commercial vendor) overnight to the laboratory in a portable incubator at 39°C. Upon arrival, oocytes were transferred into an incubator at 38.5°C with 5% CO_2 and humidified air until the designated maturation time of 24 hours. Oocytes were then pooled and denuded of cumulus cells in a 0.3% solution of hyaluronidase (Sigma-Aldrich, St. Lois MO) in fresh TL Hepes medium supplemented with 3 mg/ml of BSA by vortexing, and washed two additional times in fresh TL Hepes. Oocytes were further segregated into grades I, II, and III according to the cytoplasmic criteria described by Wurth and Kruip (1992), and then transferred to 500 µl of pre-equilibrated holding medium consisting of M-199 medium without phenol red (Sigma-Aldrich, St. Louis, MO), 10% FCS (Hyclone, Logan, UT), and 1% Penicillin-Streptomycin (P/S) comprised of 10,000 units/ml of Penicillin G sodium and 10,000 µg/ml Streptomycin sulfate (Gibco, Grand Island, NY). Briefly, Grade I oocytes exhibited a smooth plasma membrane and consistent, semi-

translucent ooplasm, first polar body and noticeable peri-vitelline space; Grade II oocytes showed a smooth plasma membrane, darker, non-homogeneous ooplasm, presence of first polar body and noticeable peri-vitelline space; and Grade III oocytes showed a non-homogeneous ooplasm, that was often dark, irregularly shaped, and/or vacuolated (Fig. 2.1).

Fig. 2.1. Bovine oocytes graded according to Wurth & Kruip, 1992. (a) Grade I; (b) Grade II, (c) Grade III

For canines, reproductive tracts from normal bitches greater than 6 months of age were collected after routine ovariohysterectomy at private veterinary clinics, placed immediately into physiological saline solution (PSS) at 37°C and transported back to the laboratory in a styrofoam container (allowed to cool to room temperature during transport) for processing. Ovaries were removed from the tract and washed free from blood in fresh PSS, and then repeatedly slashed with a scalpel blade to release oocytes from follicles in fresh TL Hepes medium supplemented with 3 mg/ml of BSA (Sigma-Aldrich, St. Louis, MO) and 1% (P/S). Only oocytes with more than two layers of cumulus and a cytoplasm >110 μm in diameter were selected for use (Hewitt, 1997; Otoi *et al.,* 2000). All oocytes within this size parameter were selected and included

oocytes characterized as having either a) a round, dark, homogenous cytoplasm and an in-tact vitelline membrane, notable peri-vitelline space and/or first polar body, or b) those described as having a non-homogeneous ooplasm that was often irregularly shaped, or vacuolated. Cumulus-oocyte complexes were washed three times in fresh TL Hepes medium before transfer to IVM medium. Oocytes were not sorted into groups and were randomly selected from a pool for experimentation due to the lack of a defined morphological grading criteria for canine oocytes.

Canine oocytes were matured in vitro in medium containing modified tissue culture medium M-199 with Earles salts (Sigma-Aldrich, St. Louis, MO), supplemented with 2.92 mM lactic acid (Sigma-Aldrich, St. Louis, MO), 2.0 mM sodium pyruvate (Sigma-Aldrich, St. Louis, MO), 4.43 mM Hepes (Sigma-Aldrich, St. Louis, MO), 10% heat-inactivated estrus bitch serum (EBS) and P/S (modified from Srsen *et al.*, 1998). The oocytes were cultured in four-well dishes (Nunc, Roskilde) with medium at a ratio of 10 μl per oocyte for ~65 h in an atmosphere of 5% CO_2 in humidified air at 39°C. Oocytes were denuded of surrounding cumulus cells prior to experiment by repeated mechanical pipetting in fresh TL Hepes medium containing 0.5% hyaluronidase, and segregated into two groups before transferring to 500 μl of pre-equilibrated holding medium consisting of M-199 medium, 10% EBS, and 1% Penicillin-Streptomycin (P/S).

2.2 Oocyte imaging

In vitro matured, denuded bovine oocytes were utilized for the establishment of baseline imaging parameters, employing a system with well-defined IVM/IVF/IVC protocols and expected embryo development results for the first part of this experiment. Parallel experiments were conducted using canine oocytes when available. Based upon preliminary analysis of several functional endpoints as biological markers (mitochondrial membrane potential ($\Delta\psi$m), mitochondrial distribution, and mitochondrial Ca^{2+}; cytoplasmic and mitochondrial reduced pyridine nucleotides NADH and NADPH by utilization of the inherent fluorescence of reduced pyridine nucleotides (Patterson *et al.*, 2000); intracellular GSH levels and GST activity, these investigations focused primarily on mitochondrial distribution and function as well as intracellular Ca^{2+} homeostasis.

The loading of fluorescent probes and instrument parameters used to assess functional cellular homeostasis mechanisms were optimized to allow for comparisons across all grades of mature bovine oocytes. Probe selection was based on its effectiveness at low concentrations, non-invasive mode of delivery, and lack adverse influence on metabolism in the determination of a functional endpoint. All fluorescent probes were obtained from Molecular Probes, Inc. and prepared according to the manufacturers instructions (Eugene, OR). Instrument parameters that optimize laser power and detection of emitted fluorescence signals were also determined for each probe. Functional data related to oocyte

grade (morphology) was obtained by laser cytometry using a Bio-Rad Radiance 2000MP multiphoton microscope with a tunable (750-1020 nm) Ti:Sapphire laser. Digital images were rapidly captured of each oocyte in accordance with steady state analysis of each functional endpoint as indicated by its respective molecular probe.

For defining mitochondrial distribution and function, rhodamine 123 and JC-1 (5,5',6,6'-tetrachloro-1,1',3,3'-tetraethylbenzimidazolylcarbocyanine iodide) probes were selected. Rhodamine 123 is a cell permeant dye that is readily sequestered by active mitochondria without cytotoxic effects. Its steady uptake by mitochondria occurs as a consequence of the maintenance of a high electrochemical potential across the mitochondrial membrane (Johnson *et al.*, 1980). Rhodamine 123 was prepared from stock solutions immediately preceding each experiment yielding a final loading concentration of 2.0 μg/ml when added to the holding medium, just prior to addition of oocytes. Oocytes were incubated for either 10 minutes (bovine), or 20 minutes (canine) due to the high concentration of cytoplasmic lipid. Oocytes were imaged using Ti:Sapphire laser at 950 nm excitation wavelength (equivalent to 475 nm wavelength in single photon excitation mode) and an emission wavelength of 525 +/- 25 nm.

JC-1 is a cell permeant dye that accumulates in the mitochondria and is considered a sensitive marker for mitochondrial membrane potential. This newer generation mitochondrial probe was selected because of its ability to exist as a monomer at low concentrations (polarized) yielding green fluorescence,

while at higher concentrations (hyperpolarized) the dye forms J-aggregates that exhibit a broad excitation spectrum yielding red fluorescence (VanBlerkom *et al.*, 2002). JC-1 was prepared from stock solutions in DMSO immediately preceding each experiment yielding a final loading concentration of 2.0 μg/ml when added to the holding medium, just prior to addition of oocytes. Oocytes were incubated for either 10 minutes (bovine), or 20 minutes (canine) due to the high concentration of cytoplasmic lipid. Oocytes stained with JC-1 were excited at 950 nm wavelength and emissions were collected at 520 +/- 25 nm and 590 +/- 25 wavelength.

To evaluate oocyte intracellular calcium activity, the non-ratiometric visible wavelength probe Fluo-4, AM was selected, as it is a cell permeable probe with high affinity for Ca^{2+} and exhibits approximately a 40 fold enhancement of fluorescence intensity with Ca^{2+} binding (Gee *et al.*, 2000). Stock solution of 1.0 mM Fluo-4, AM was prepared in DMSO and diluted immediately preceding staining to yield a final loading concentration of 2.5 μg/ml when added to the holding medium, just prior to the addition of oocytes. Oocytes were incubated for 30 minutes (both bovine and canine) prior to imaging due to the high concentration of cytoplasmic lipid. Oocytes were then imaged with an excitation wavelength of 950 nm and an emission wavelength of 525 +/- 25 nm.

Cellular GSH levels were evaluated with mBCl (monochlorobimane), by laser cytometry. mBCl is a cell-permeant, non-fluorescent probe that forms a

fluorescent adduct with GSH in a reaction catalyzed by glutathione *S*-transferase (Rice *et al.*, 1986; Shrieve *et al.*, 1988). mBCl was prepared according to the manufacturer's specifications and diluted immediately preceding staining from a 50mM stock solution to yield a final loading concentration of 25 μM. Images were collected with an excitation wavelength of 800 nm (equivalent to 400 nm in a single photon excitation system) and an emission wavelength of 460 nm +/- 25 nm. Redox fluorometry based on intrinsic fluorescence of reduced pyridine nucleotides NADH and NADPH was also attempted to examine cellular energy due to the intrinsic fluorescence of NADH and NADPH (Patterson *et al.*, 2000).

For each parameter analyzed, approximately eight IVM, denuded oocytes of known grade for bovine and random selection for canine were placed into 1 ml of fresh holding medium (previously described) containing the specific fluorescent probe at the desired concentration (described above), and incubated at 38.5°C in CO_2 and humidified air for a loading interval specific for that particular probe (as previously indicated). All oocytes were then washed three times in warm, fresh TL Hepes medium (phenol red-free) and placed individually in drops of 4 μl onto the glass bottom of a Lab-Tek 2-well chambered cell culture dish (Nunc International, Rochester, NY), and immediately imaged. Each oocyte was assigned an identification number that continued consecutively from 1-64 for bovine, beginning with Grade I oocytes, followed by Grades II & III. The same procedure was followed for canine oocytes randomly selected, when available except the glass bottom of the Lab-Tek 2-well chambered cell culture

dish was previously coated with poly-L-lysine (Sigma, St. Louis) for a period of 30 minutes, rinsed with fresh TL Hepes medium, and allowed to dry before placing oocytes into droplets for imaging. This procedure was introduced as a method of anchoring the canine oocyte to the surface of the dish for imaging due to the observation that canine oocytes sometimes floated freely within the micro-droplet. Rapid acquisition of digital images of each oocyte were performed with a color CCD camera and R, G, and B color planes were stored in a reference library prior to functional analysis by laser cytometry. These data were used to establish baseline criteria of specific functional characteristics in relation to oocyte quality.

For bovine, a positive oocyte control group that was neither stained nor imaged was also formed and subjected to subsequent fertilization and monitoring of embryonic development in an identical manner to the oocytes prepared for imaging. As a negative control, either two (for rhodamine 123) or three separate groups of oocytes were fertilized and cultured in bulk to address the issue of in vitro fertilization and embryo culture of individual oocytes/embryos vs. bulk fertilization of oocytes/embryos. Bulk culture groups are defined as a) cumulus oocyte complexes (COC), b) denuded oocytes (DO) stripped of their cumulus cells (DO), and/or c) DO co-cultured with cumulus cells (DO+CU). Cumulus cells for co-culture were prepared as described below. Only the COC and DO bulk culture groups were used in the rhodamine 123 experiments.

As a positive control for the canine image analysis experiments, two separate groups from the same population of oocytes for any given experiment were a) neither stained nor imaged, or b) stained only for the reason that there is not a well-defined IVF or activation protocol for the production of canine embryos in vitro and also to rule out any potential adverse effects of probe loading to the oocyte . All canine oocytes were subjected to IVM in bulk, imaged individually and then fixed in a 3.7% formaldehyde-Triton X-100 (Sigma, St. Louis, MO) solution for 15 minutes, washed in a solution of DPBS (Gibco, Grand Island, NY) + 3mg/ml Polyvinylpropinal (PVP) (Sigma, St. Louis, MO) for an additional 15 minutes, and mounted on a glass slide in 15 μl of 1.9μM Hoechst 33342 (Sigma, St. Louis, MO) in glycerol (Sigma, St. Louis, MO). Oocytes were then evaluated under UV light using a Nikon Eclipse TE300 with a Roper Scientific Cool Snap CF Camera and analyzed with the NIS Elements software to determine the stage of meiosis as defined by Hewitt (1997).

Exception was taken in the canine JC-1 experiment whereby all oocytes analyzed using the improved selection method were fertilized using either cryopreserved or freshly collected canine semen, as part of a range-finding, informative study. Semen preparation, IVF, IVC and analysis of embryo development are described below.

2.3 Bovine and canine sperm preparation

Bovine spermatozoa used in these experiments were prepared from cryopreserved bull semen according to Pertoft *et al.* (1978) by density gradient separation using 45%/90% Percoll (Sigma, St. Louis, MO). Sperm concentration used for IVF was $2x10^6$/ml. While semen from two different bulls was used, the source remained consistent throughout any one particular experiment (i.e. all experiments using Fluo-4 and involving IVF were analyzed with semen from the same bull, and all JC-1 experiments involving IVF were analyzed with semen from the same bull, however, the source of semen differed between the two experiments).

Canine spermatozoa used in these experiments were prepared either from cryopreserved dog sperm or from freshly collected dog semen. The cryopreserved semen was prepared according to Pertoft *et al.* (1978) by density gradient separation using 45%/90% Percoll (Sigma, St. Louis, MO), and fertilized at a concentration of either 2×10^6/ml or 5×10^6/ml.

Fresh collected dog semen was extended 1:1 using Biladyl Part A (Minitube, Verona, WI), and slow-cooled overnight at 4°C. The extended semen was then prepared for IVF by density gradient separation using 45%/90% Percoll (Sigma, St. Louis, MO) according to Pertoft *et al.* (1978). Canine oocytes were fertilized in vitro at a concentration of 5×10^6/ml.

2.4 In vitro fertilization and embryo culture

After imaging, both bovine and canine oocytes were fertilized in vitro in a modified Tyrode's-lactate medium defined by Bavister and Yanagimachi (1977) using the "Well of the Well" (WOW) system in 4-well culture dishes (Nalgene-Nunc, Denmark) as described by Vajta *et al.*, (2000), in order to track and maintain oocyte/embryo identification through development (Fig. 2.2). Briefly, mini-wells were made by hand under a dissecting microscope using a blunt tapestry sewing needle (#18) held by a hemostat and gently heated over an open flame from an alcohol lamp (Fig. 2.3). The wells were formed by gently pressing the needle into the bottom of the plastic dish to the level of the needle's bevel, allowing it to cool for easy removal. This process was repeated until six rows of 8 wells were formed, for a total of 48 mini wells with well number 1 being the first well of the first row (from left to right) and well number 48 being the last well of the last row. Only well 1 of the 4-well dish was converted to the WOW system. Wells 2-4 were reserved for washing post culture. The WOW was then washed 3 times with sterile saline solution to flush away any plastic debris or by-products that may have been produced from melting the plastic, and then sterilized under UV light for a minimum of 30 minutes. Fertilization medium was allowed to equilibrate in the WOW dishes for at least 1 hour prior to use. Imaged bovine or canine oocytes were placed in their respective wells according to the numbers assigned immediately preceding imaging. Cumulus cells preserved from denuding the oocytes at the beginning of the experiment were

pelleted in a 15ml conical tube (BD Biosciences, San Jose, CA), and re-suspended in ~100 μl of fertilization medium. Approximately 10 μl of the cumulus cell solution was added to each WOW dish to aid in capacitation of spermatozoa, and to provide essential nutrients and cell signaling molecules for optimal embryo development.

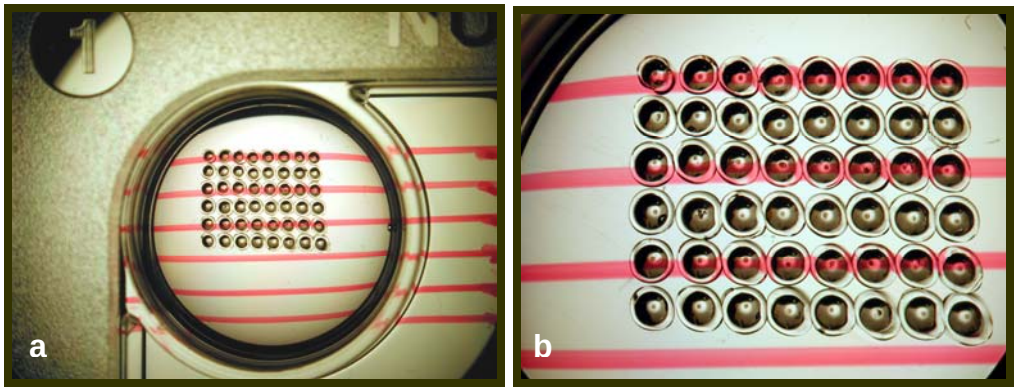

Fig. 2.2. Photograph of (a) WOW culture dish used for IVF and IVC of individual ova and embryos (b) and WOW culture dish harboring embryos taken with a NIKON SMZ1000 dissecting microscope.

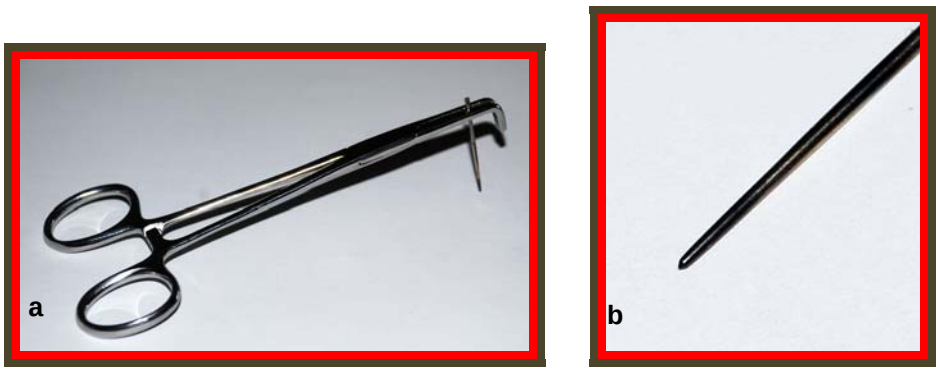

Fig. 2.3. Photograph of (a) hemostat-needle holding tool used to make mini-wells in WOW system, and (b) of #18 tapestry needle tip used to make mini-wells.

After 18 -20 hours post insemination, oocytes fluorescence labeled and imaged oocytes were subjected to IVF were washed free of remaining sperm in fresh TL Hepes at least two times, before transfer to G1/G2 version 3, embryo culture medium (VitroLife, Inc., Englewood, CO) and cultured according to manufacturer's recommendations via the WOW method described above (Fig. 2). Non-cleaving embryos were removed from culture at 24 hour intervals, fixed in 3.7% paraformaldehyde, stained with Hoechest 33342 (Sigma, St. Louis, MO) and observed under UV light (as described previously for bovine) to evaluate developmental status. On day 8 post insemination, the remaining embryos were fixed and stained accordingly to assess stage of development.

2.5 Analysis of oocyte images captured

For each oocyte image captured, specific measurements relating to oocyte morphology were recorded to include overall area of oocyte, diameter and shape factor. The shape factor is a dimensionless quantity used in image analysis and microscopy to numerically describe the shape of a particle, independent of its size. It is calculated from the measured dimensions of diameter, area and perimeter following hand-drawing of a continuous outline of the ooplasm using the "region tools" available in Metamorph software version 7.5.0 (MDS Analytical Technologies Inc., Mississauga, Ontario, CANADA). The shape factor often represents the degree of deviation from an ideal shape, such as a circle in the case of oocytes. The value of shape factor ranges from zero to

one. A shape factor equal to one usually represents an ideal case or maximum symmetry, such as a circle.

Average fluorescence intensity (AFI) or the ratio of fluorescence intensity for ratio-metric probes was evaluated using Metamorph software. For the probes rhodamine 123 and Fluo-4, AM, data collected with the Metamorph software were used to plot SF/AFI (defined as the ratio of SF to AFI against AFI in order to identify a specific relationship between the two parameters measured. For canine and bovine oocytes imaged using JC-1, analysis similar to that of rhodamine 123 was performed, with the exception of using fluorescence intensity (FI) of the ratio of green:red instead of AFI for analysis with Metamorph software in order to identify the specific relationship between SF/AFI and FI. The relationship between the two variables (SF/AFI) and AFI was found to be an exponential decay satisfying the following equation:

$$SF/AFI = A * \exp(-K*AFI) + B$$

The curve starts theoretically at A+B (Span) and decays to end at B (plateau) with a rate constant K. A, B and K are different for each probe tested.

Further for canine JC-1 analysis, another selection method was evaluated in an attempt to enhance the selection criteria for a good oocyte. Briefly, this method consisted of selecting retrospectively a reference oocyte. The reference oocyte was selected based on a compilation of the most common values for SF and FI for each oocyte as well as good fertilization. A maximum difference of 6

between the reference oocyte and the measured oocyte fluorescence intensity was determined as the cutoff limit for prediction.

2.6 Statistical analysis

Data comparing functional parameters based upon oocyte grade for both bovine and canine oocytes were compared statistically using ANOVA followed by Tukey's test (for all pairwise comparisons) or the Bonferroni procedure (for a subset of pairwise comparisons) multiple comparison tests at $P<0.05$.

Comparison of in vitro fertilization and embryo development based on the WOW IVF/IVC system were compared statistically using ANOVA followed by Tukey's test (for all pairwise comparisons) or the Bonferroni procedure (for a subset of pairwise comparisons) multiple comparison tests at $P<0.05$.

All statistical evaluations were analyzed using SPSS software version 15.0.

CHAPTER III

RESULTS

3.1 Evaluation of loading parameters

The loading of fluorescence probes of cellular function and evaluation of instrument parameters for the establishment of baseline imaging criteria were implemented in order to assess functional cellular homeostasis mechanisms. These criteria were further optimized to allow for comparisons across all grades of mature bovine oocytes. Fluorescent molecular probes that were used include rhodamine 123 and JC-1 for assessment of mitochondrial localization/distribution and membrane potential ($\Delta\psi m$), Fluo-4, AM for evaluation of free intracellular calcium ion (Ca^{2+}) levels, and monochlorobimane (mBCl) for assessment of glutathione (GSH) status. Redox fluorometry based on intrinsic fluorescence of reduced pyridine nucleotides NADH and NADPH was also attempted to examine cellular energy due to the intrinsic fluorescence of NADH and NADPH.

Experiments using the probes for mitochondrial localization and membrane potential, as well as intracellular Ca^{2+} concentration were determined as suitable for oocyte assessment and are reported individually below. In contrast, evaluation of GSH activity was determined to be unsuitable for oocyte assessment, as the mBCl probe irreversibly binds glutathione, thereby depleting the cell of cytosolic GSH necessary to combat oxidative stress resulting from generation of reactive oxygen species (ROS). While GSH status could be evaluated, the assessment could not be performed without compromising oocytes that were to be further analyzed. The evaluation of NADH and NADPH was also not successful due to the inability to reliably monitor the intrinsic fluorescence of these reduced pyridine nucleotides due to the high lipid concentration in both bovine and canine oocytes which limited detection sensitivity.

3.2 Experiment I - Characterization of the spatial distribution of mitochondria and mitochondrial activity and intracellular Ca^{2+} stores in relation to grade of in vitro matured bovine oocytes as they relate to morphology, and establishment of baseline criteria of functional parameters for oocyte selection

3.2.1 Characterization of the spatial distribution of mitochondria and mitochondrial activity in relation to grade of IVM bovine oocytes

In vitro matured bovine oocytes (n=200) denuded of cumulus cells were graded and sorted by morphology as previously described and labeled with the fluorescent dye, rhodamine 123. Images captured revealed patterns of mitochondrial distribution and activity that were not unique from each other according to morphological grade. Mitochondria were visualized as punctate areas of fluorescence and were distributed primarily in the peri-cortical and sub-cortical areas of the oocyte cytoplasm, with the most densely populated areas being peri-cortical. Comparison of morphological grading with fluorescence intensity also yielded similar trends between all grades of oocytes with no visually obvious, distinct or characteristic staining that would permit classification of each oocyte as a specific morphological grade (Fig. 3.1).

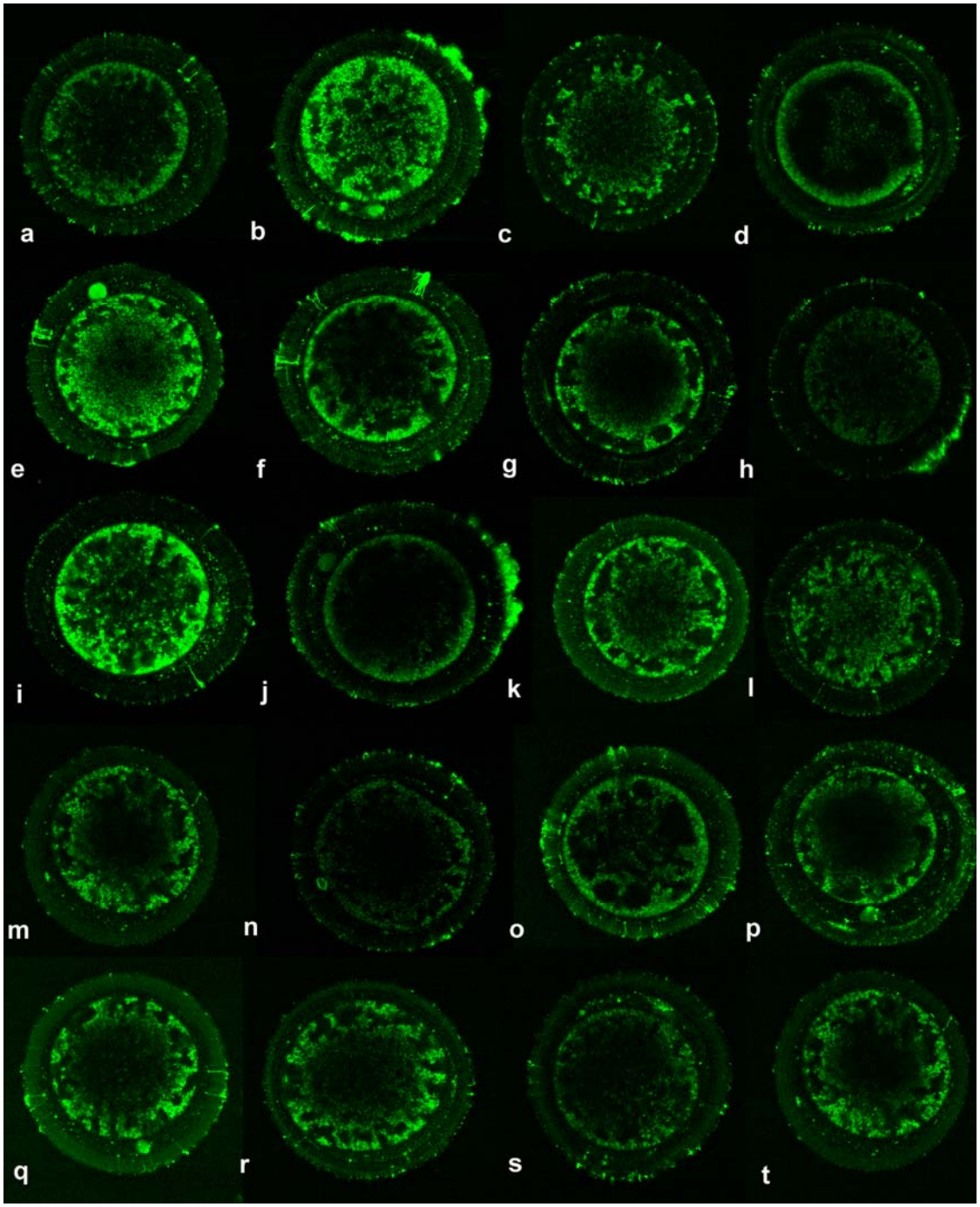

Fig. 3.1. Individually graded IVM bovine oocytes imaged using multiphoton microscopy with the mitochondrial probe, rhodamine 123. G1 **(a-d)**; G2 **(e-l)**; G3 **(m-t)**.

Average fluorescence intensity (AFI) was recorded for each oocyte imaged and plotted against a parameter that combines morphology and mitochondrial fluorescence which is the ratio of a shape factor to the average fluorescence intensity (SF/AFI) where the shape factor is a measure of the circularity of the oocyte (a shape factor of 1.0 represents perfect circularity of the oocyte in 2 dimensional images) (Fig. 3.2). Grade 2 oocytes were distributed throughout the curve and had AFI's ranging from 27.3-109.9, while the majority of G1 oocytes had an AFI between 40-60 (range 45.5-97.7), and G3 oocytes were distributed between 26.9-68.1. These data identified an inverse relationship between SF/AFI and AFI. The mean values for SF/AFI and AFI are listed in Table 3.1 and plotted in Fig. 3.3. Statistical analysis of SF/AFI and AFI values for each oocyte grade revealed significant differences between G1 and G2, as well as between G1 and G3 ($P<0.05$), respectively.

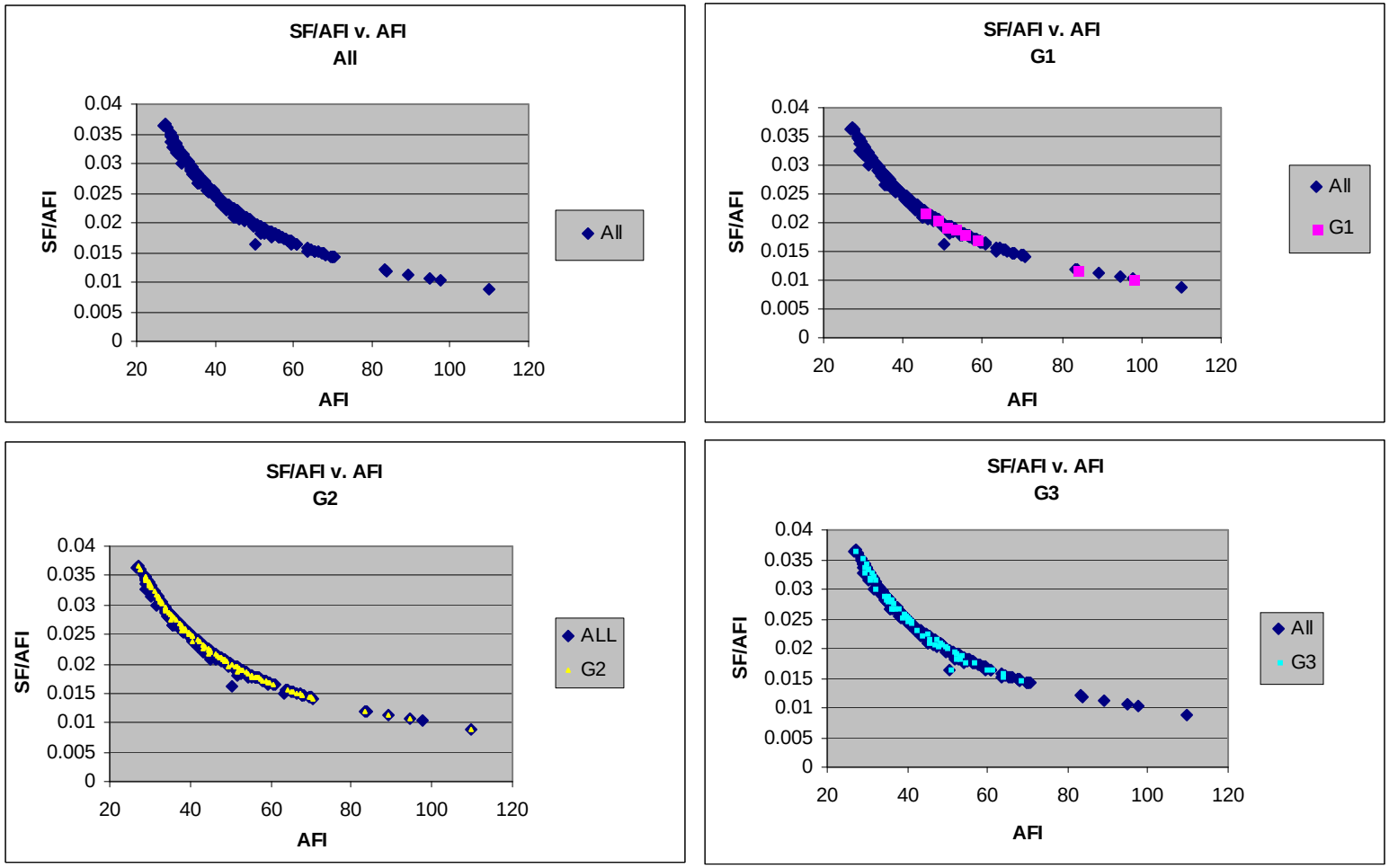

Fig. 3.2. Relationships between AFI and SF/AFI in G1, G2 & G3 bovine oocytes imaged using multiphoton microscopy with the mitochondrial probe, rhodamine 123.

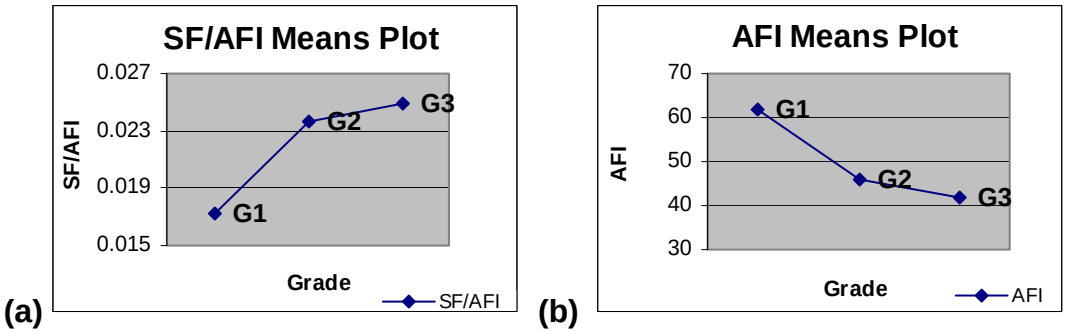

Fig. 3.3. Relationships between mean SF/AFI **(a)** and AFI **(b)** and oocyte grades in oocytes imaged using multiphoton microscopy with the mitochondrial probe, rhodamine 123.

Table 3.1. Mean Values and Range for SF/AF (a) and AFI (b) of Bovine Oocytes Imaged Using Multiphoton Microscopy with the Mitochondrial Probe Rhodamine 123.

a

Grade	(n)	(SF/AFI) Mean	(SF/AFI) Range
G1	8	0.172[a]	0.012-0.021
G2	125	0.024[b]	0.011-0.031
G3	67	0.025[b]	0.014-0.036
Total	**200**		

Lower case superscripts indicate significant differences in same column (P<0.05)

b

Grade	(n)	AFI Mean	AFI Range
G1	8	61.629[a]	45.5-97.705
G2	125	45.928[b]	27.320-109.875
G3	67	43.719[b]	26.914-68.118
Total	**200**		

Lower case superscripts indicate significant differences in same column (P<0.05)

In an effort to better define the spatial distribution of oocyte mitochondria and mitochondrial membrane potential ($\Delta\psi m$) as they relate to oocyte grade, 239 IVM bovine oocytes denuded of cumulus cells were labeled with JC-1 (5,5',6,6'-tetrachloro-1,1',3,3'-tetraethylbenzimidazolyl-carbocyanine iodide), a new generation, ratiometric fluorescent probe. JC-1 exists as a monomer at low concentrations and yields green fluorescence in the FITC channel and red fluorescence in the RITC channel due to the formation J-aggregates (an accumulation of higher concentrations of probe within the mitochondrial membrane), indicating hyperpolarization of the mitochondrial membrane (VanBlerkom *et al.* 2002).

Images captured in both the FITC and RITC channels revealed patterns of mitochondrial distribution and $\Delta\psi m$ that were similar to that of the rhodamine 123 probe, and again were not visually unique according to each grade (Fig. 3.4). Specifically, both green and red fluorescence (orange-yellow in merged image) appeared in the peri- and sub-cortical regions of the oocyte indicating a heterogeneous mitochondrial population. Further, when present in the field of view, the polar body fluoresced intensely in both FITC and RITC channels. However, a number of the G3 oocytes had much different patterns of fluorescence. Specifically, some exhibited fluorescence signal throughout the entire cytoplasm, showing vacuoles devoid of probe (Fig. 3.4q), while others had significantly more hyperpolarized mitochondria in the peri-cortical area with

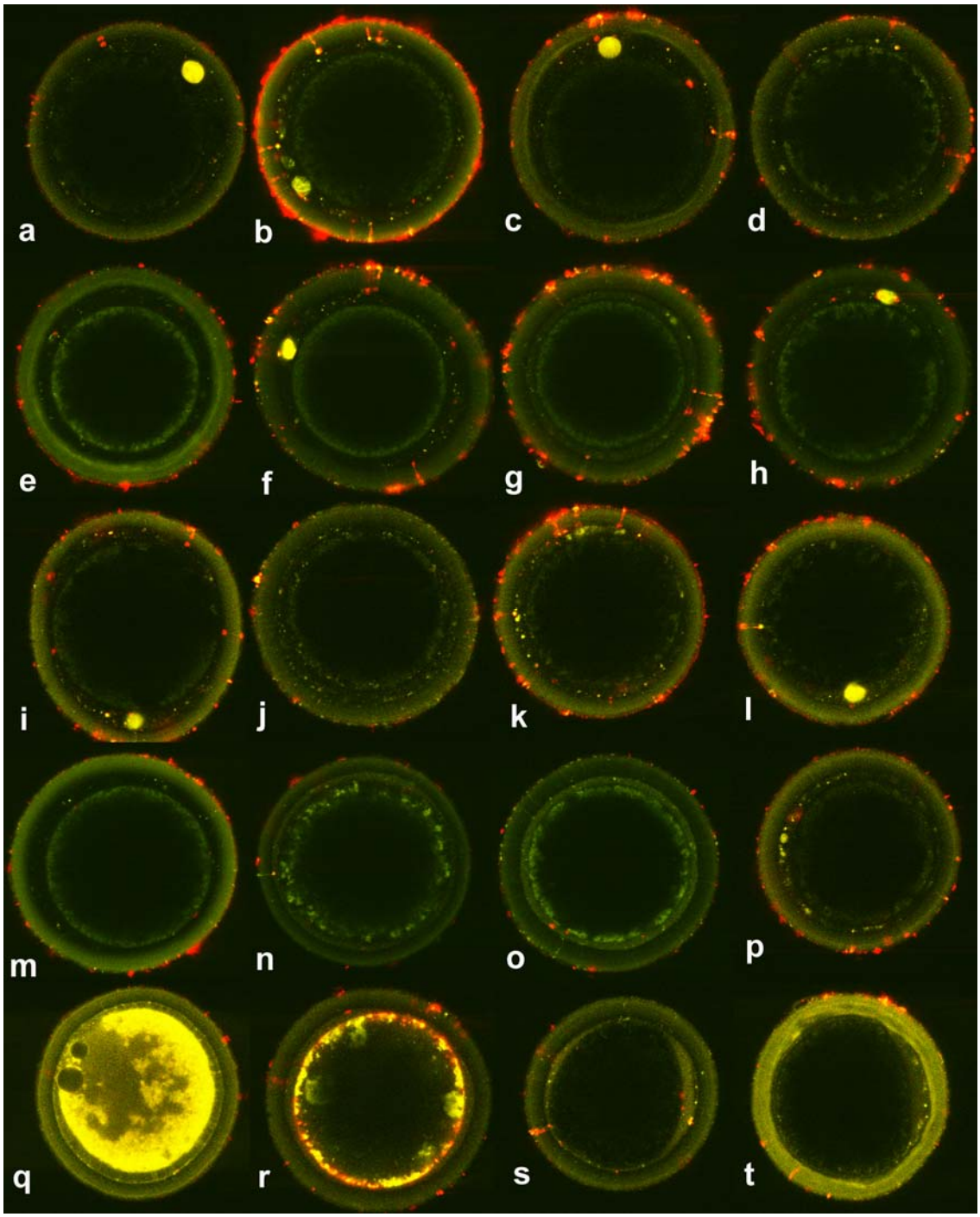

Fig. 3.4. Bovine oocytes classified as G1 **(a-d)**, G2 **(e-l)** & G3 **(m-t)** and imaged using multiphoton microscopy with the ratiometric mitochondrial probe, JC-1.

vacuoles that fluoresced (4r), as well as probe uptake by the zona pellucida, with little fluorescence in the cytoplasm (4t). When present, residual coronal and/or cumulus cells, along with their trans-zonal projections fluoresced red, indicating the presence of hyperpolarized mitochondria (Fig. 3.4b, 3.4g, & 3.4k).

A ratio of the green:red fluorescence was used to quantify the fluorescence intensity (FI) within each oocyte for this experiment. Fluorescent intensities and distribution of mitochondria recorded for all morphological grades yielded a similar trend to rhodamine 123, (i.e., there was an inverse relationship between SF/FI and FI (Fig. 3.5). Specifically, G2 oocytes were distributed throughout the curve (0.9-2.1), while G1 were distributed between 1.3-1.9. G3 oocytes were distributed between 0.9-2.0 (Fig. 3.5). There were no significant differences among SF/FI or FI between G1 and G2 ($P<0.05$). However, G2 and G3 oocytes were significantly different from each other ($P<0.05$) for both SF/FI and FI. The mean SF/FI and FI for each oocyte grade are shown in Table 3.2 and plotted in Fig. 3.6.

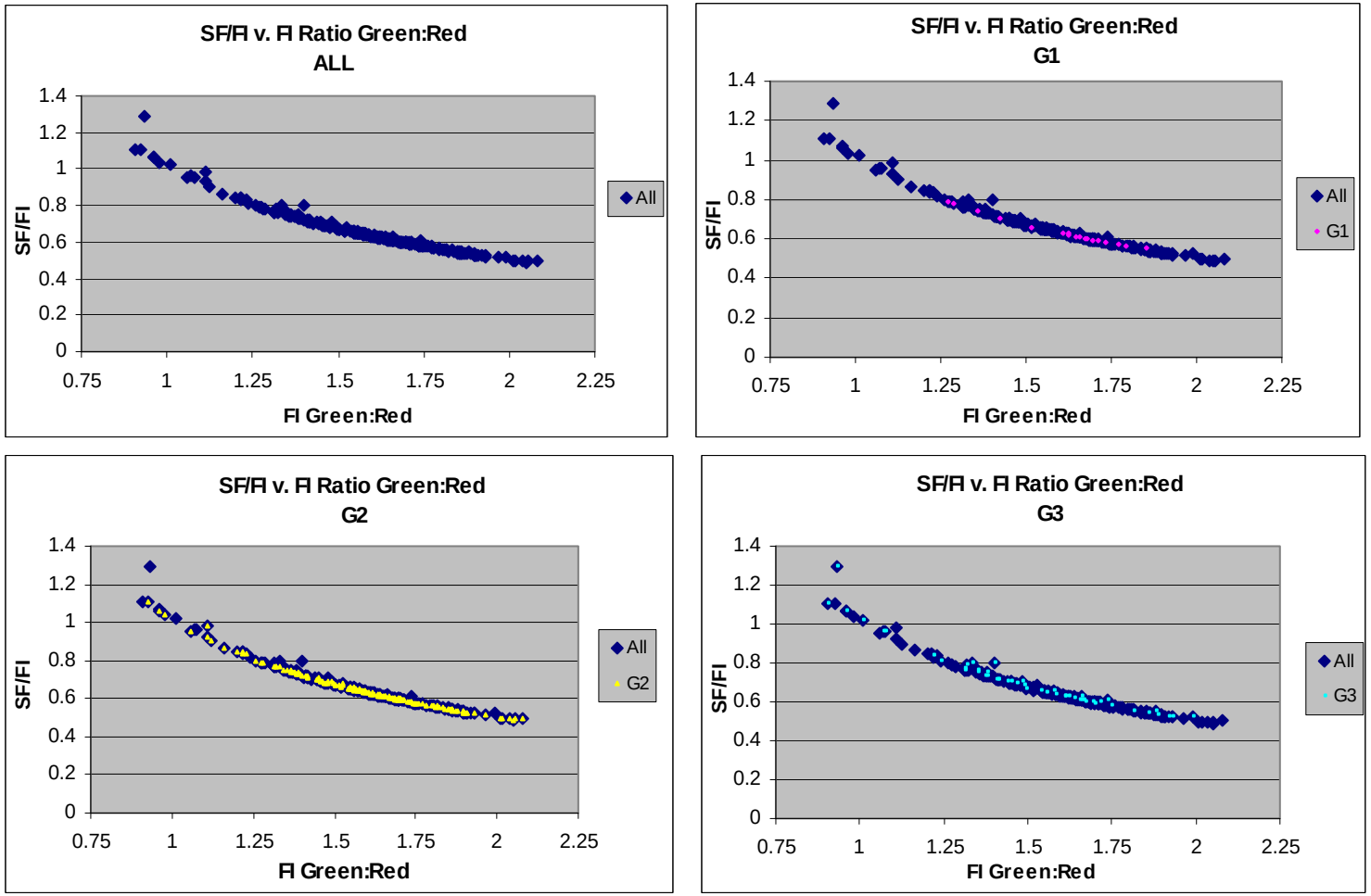

Fig. 3.5. Relationships between SF/FI and FI of G1, G2 & G3 bovine oocytes imaged using multiphoton microscopy with the ratiometric mitochondrial probe, JC-1.

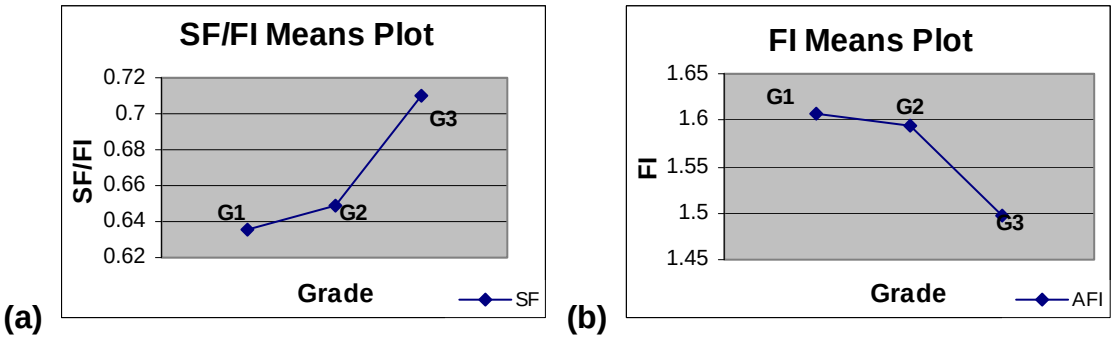

Fig. 3.6. Relationships between mean SF/FI **(a)** and FI **(b)** and oocyte grades in oocytes imaged using multiphoton microscopy with the ratiometric mitochondrial probe, JC-1.

Table 3.2. Mean Values and Ranges for the Ratio of SF/FI (a) and FI (b) of Bovine Oocytes Imaged Using Multiphoton Microscopy with the Ratiometric Mitochondrial Probe JC-1.

	Grade	(n)	SF Mean	SF Range
	G1	18	0.636^{ab}	0.553-0.792
	G2	170	0.649^{a}	0.490-1.107
	G3	51	0.710^{b}	0.522-1.291
a	**Total**	**239**		

Lower case superscripts indicate significant differences in same column (P<0.05)

	Grade	(n)	AFI Mean	AFI Range
	G1	18	1.607^{ab}	1.272-1.85
	G2	170	1.595^{a}	0.925-2.080
	G3	51	1.498^{b}	0.907-1.991
b	**Total**	**239**		

Lower case superscripts indicate significant differences in same column (P<0.05)

3.2.2 Characterization of the spatial distribution of free intracellular Ca^{2+} in relation to grade of IVM bovine oocytes

In vitro matured bovine oocytes (n=236) denuded of cumulus cells were sorted according to grade as previously described and incubated with the Ca^{2+}-sensitive fluorophore, Fluo-4, AM. Images were captured rapidly to avoid cell damage and revealed spatial patterns of intracellular Ca^{2+} that were generally not unique according to grade. Fluorescence intensity of the Fluo-4, AM within the oocyte cytoplasm was very low and areas of specific localization within the oocyte were either unremarkable, exhibited peri-cortical localized areas of fluorescence, or small aggregates of fluorescence indicative of localized elevations of intracellular Ca^{2+} levels. Punctate fluorescence was present in the peri-vitelline space (PVS) and the first polar body had a very intense Fluo-4, AM signal indicating high free Ca^{2+} levels within this structure (Fig. 3.7). Lastly when present, residual corona/cumulus cells, and trans-zonal projections showed evidence of intracellular Ca^{2+} activity within these structures as indicated by moderate fluorescence labeling as designated by the red arrows in Fig. 3.7. Comparison of morphological grading with fluorescence intensity yielded similar

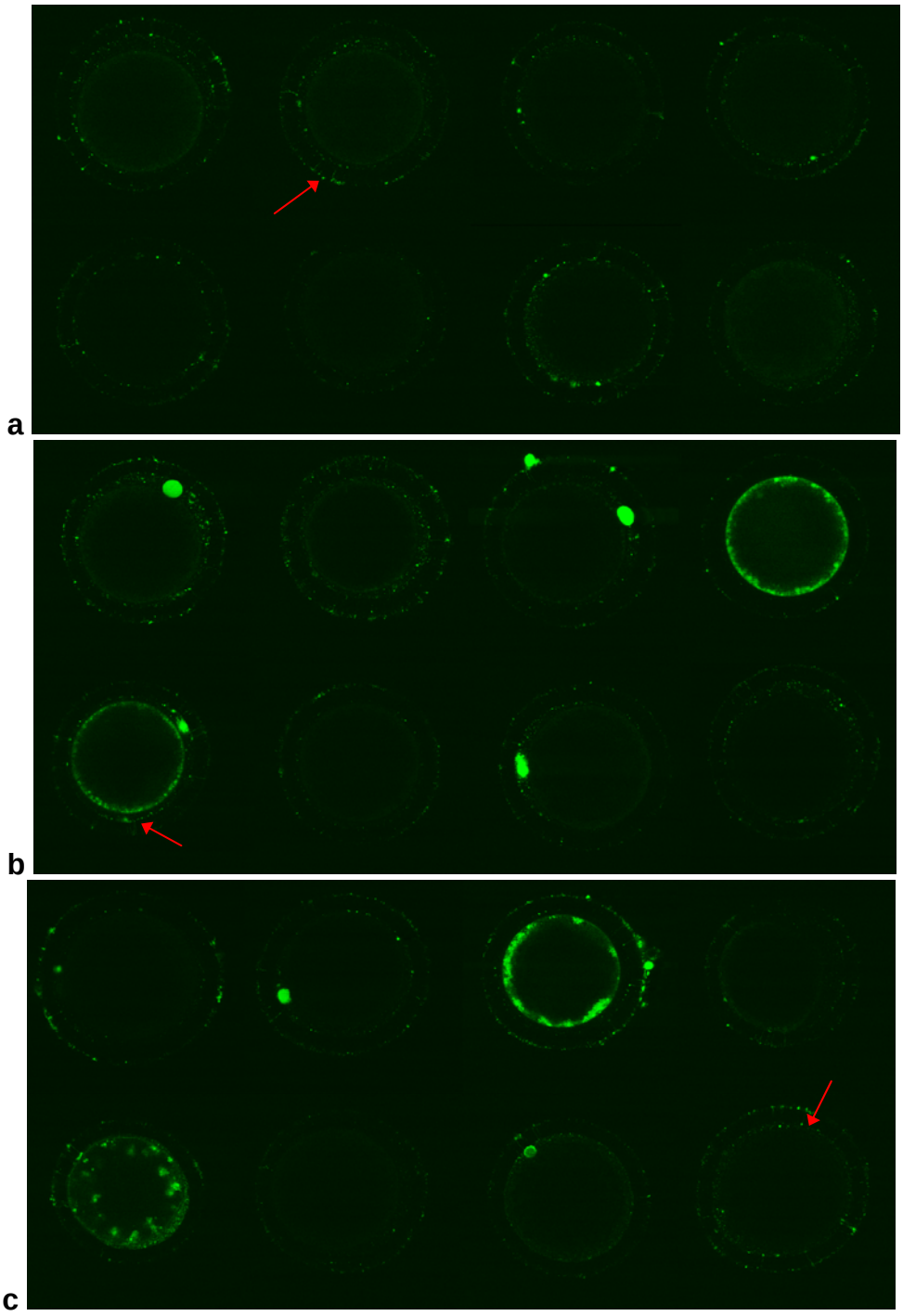

Fig. 3.7. Bovine G1 **(a)**, G2 **(b)**, and G3 **(c)** oocytes imaged using multiphoton microscopy with the Ca^{2+}-sensitive fluorophore, Fluo-4, AM. Red arrows indicate Ca^{2+} activity within residual corona/cumulus cells and trans-zonal projections.

trends between all grades of oocytes with no visually obvious, distinct characteristic Fluo-4, AM signal that that would allow identification of each oocyte as belonging to a specific morphological grade. However, Grade 3 oocytes showed more intense Fluo-4, AM fluorescence that was predominantly located in the peri-coritical region of the oocyte (Fig. 3.7). When plotted together, the SF/AFI and AFI of imaged oocytes generated a curve that confirmed an inverse relationship between SF/AFI and AFI (Fig. 3.8). The mean values for both SF/AFI and AFI are reported in Table 3.3 and plotted in Fig. 3.9. Specifically, G2 and G3 oocytes had AFI's distributed throughout the curve with ranges of 20.245-51.790 and 21.604-53.297, respectively, with the majority of oocytes for both grades having AFI's between 21-26. G1 oocytes were distributed in the 20.303-26.130 range of lower Fluo-4, AM fluorescence intensity. Statistical analysis of both SF/AFI and AFI revealed that G2 was significantly different from G3 ($P<0.05$), respectively (Table 3.3).

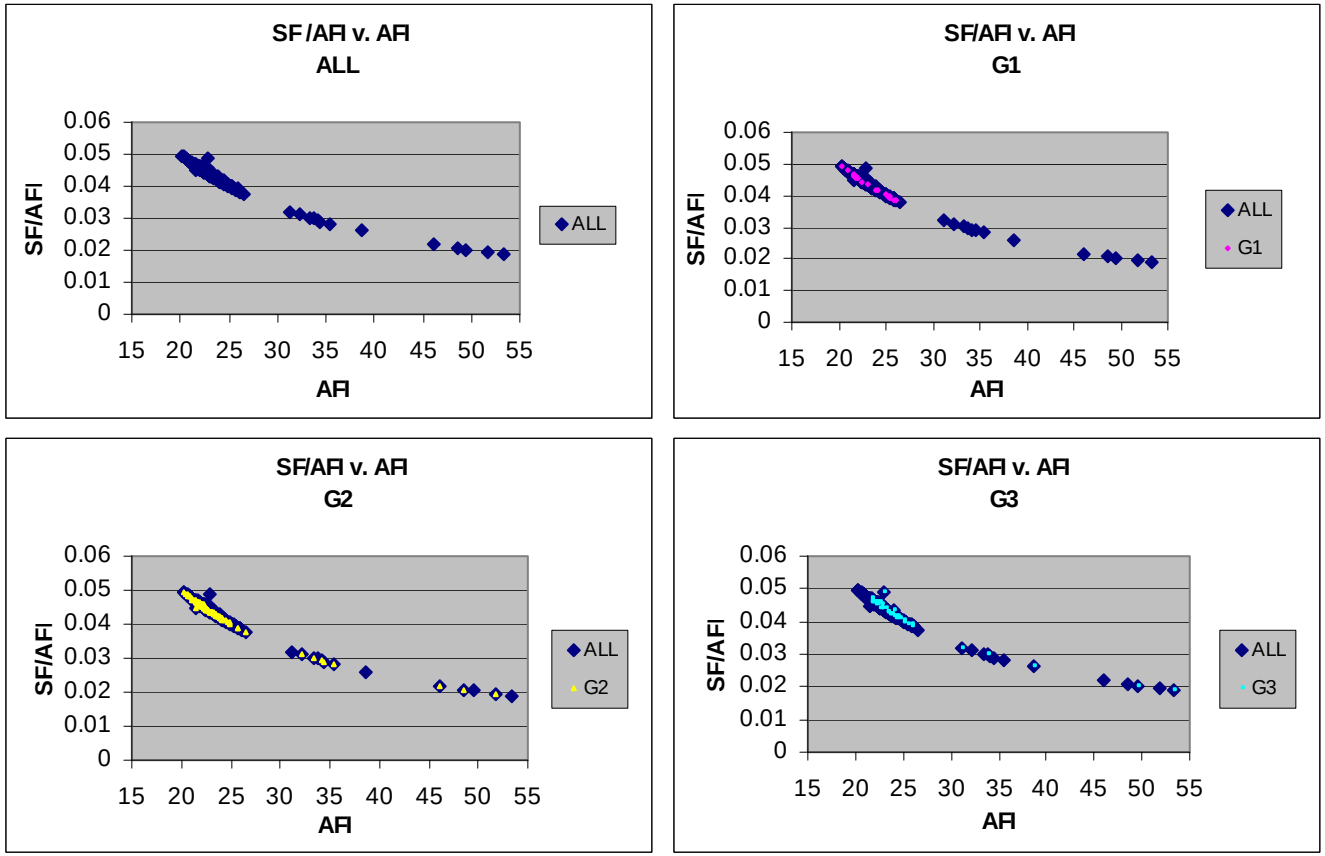

Fig. 3.8. Relationships between SF/AFI vs. AFI (as an index of intracellular Ca^{2+}) in G1, G2 & G3 bovine oocytes imaged using multiphoton microscopy with the Ca^{2+}-sensitive fluorophore, Fluo-4, AM.

Table 3.3. Mean Values and Ranges for the Ratio of SF/AFI (a) and AFI (b) of Bovine Oocytes Imaged Using Multiphoton Microscopy with the Ca^{2+}-sensitive Probe, Fluo-4.

Grade	(n)	SF Mean	SF Range
G1	20	0.043^{ab}	0.038-0.049
G2	170	0.044^{a}	0.019-0.049
G3	46	0.041^{b}	0.019-0.049
Total	**236**		

a

Lower case superscripts indicate significant differences in same column (P<0.05)

Grade	(n)	AFI Mean	AFI Range
G1	20	23.504^{ab}	20.303-26.130
G2	170	23.300^{a}	20.245-51.790
G3	46	25.281^{b}	21.604-53.3
Total	**236**		

b

Lower case superscripts indicate significant differences in same column (P<0.05)

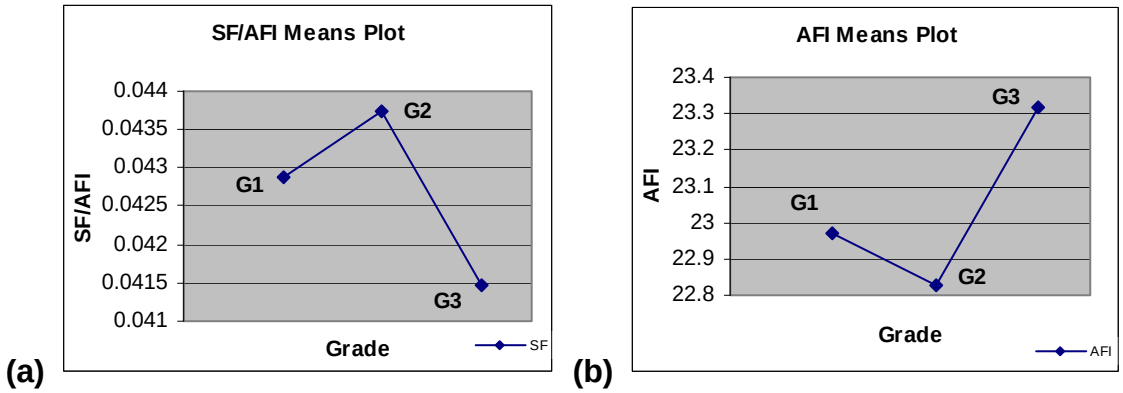

(a) **(b)**

Fig. 3.9. Relationships between mean SF/AFI **(a)** and AFI **(b)** and oocyte grades in oocytes imaged using multiphoton microscopy with the Ca^{2+}-sensitive fluorophore, Fluo-4, AM

3.2.3 Evaluation of embryonic developmental potential of bovine oocytes imaged by multiphoton microscopy and subsequently fertilized in vitro

Using the WOW method as previously described (Vajta *et al.,* 2000), bovine oocytes examined in experiments II & III were fertilized in vitro following fluorescence probe loading and imaging in order to assess embryonic developmental potential to the blastocyst stage (Fig. 3.10). There were no visually obvious morphological differences between imaged and non-imaged in vitro derived hatched blastocysts (Fig. 3.11). The identity of each oocyte imaged was maintained throughout the entire study, from the grading step, through probe loading and imaging followed by the IVF process and embryo culture. Oocytes and embryos were maintained in their respective wells within the WOW system containing 10 µl of medium/oocyte during the course of the culture period. Embryonic development of imaged and non-imaged oocytes in the WOW culture system were also compared to a similar number of non-imaged oocytes cultured in larger groups using the same total amount of culture medium/oocyte (i.e., 50 oocytes in 500 µl of culture medium). Oocytes in the bulk cultures were .prepared as cumulus-oocyte complexes (COC), oocytes denuded of cumulus cells (DO), or denuded oocytes supplemented with cumulus cells (DO + CU).

For bovine oocytes labeled with rhodamine 123 and imaged, the percentage of oocytes fertilized were 37.5, 75.2, and 53.7 for G1, G2, and G3 oocytes, respectively. The percentages of embryos undergoing cleavage were 12.5, 28.0, and 23.9 for G1, G2 and G3 oocytes, respectively; and percentages of development to blastocyst were 12.5, 3.2, and 1.5 for G1, G2 and G3 oocytes,

A

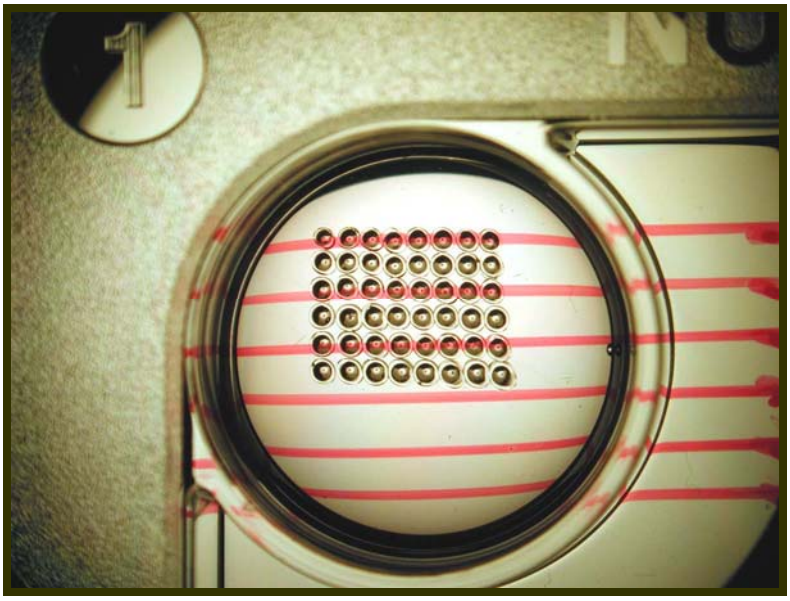

B

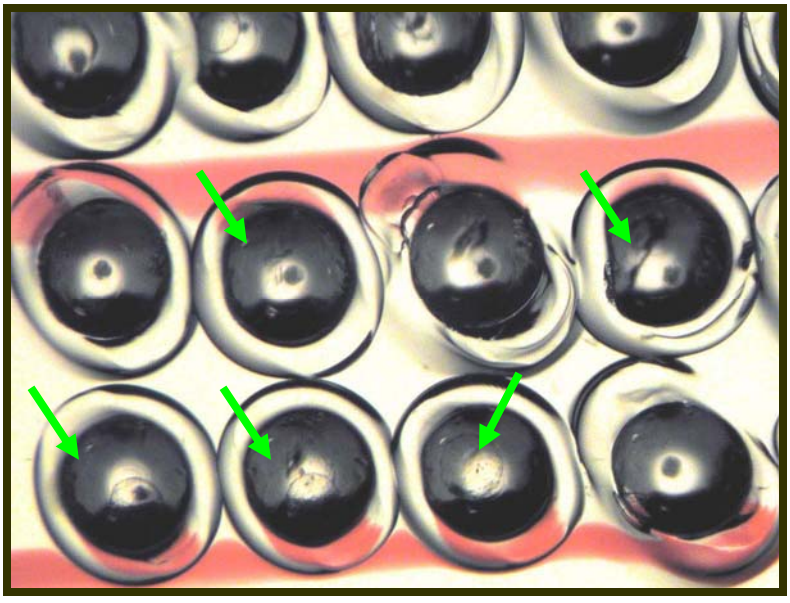

Fig. 3.10. Photograph of the WOW culture system. A: each well contains 48 mini-wells for oocyte/embryo culture; B: higher magnification of individual wells that harbor cleaving/blastocyst stage embryos, several of which are shown (arrowheads).

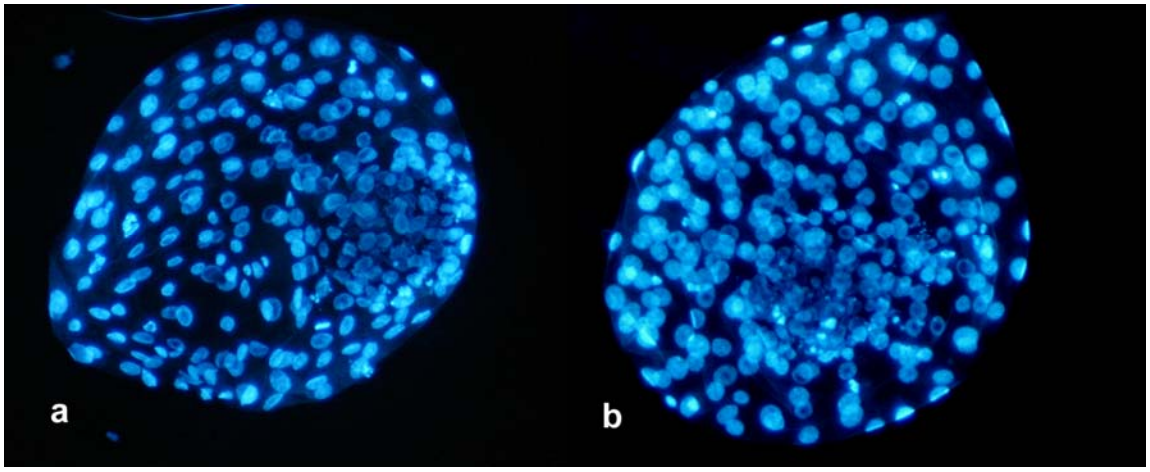

Fig. 3.11. Fluorescence microscopy of fixed, hatched in vitro derived bovine blastocysts labeled with the DNA stain Hoechst 33342 comparing **A:** multiphoton microscopy imaged and **B:** non-multiphoton microscopy imaged embryos using the WOW system.

respectively (Table 3.4, Fig. 3.12). There were no significant differences among grades of imaged oocytes. For the non-imaged control oocytes, percentages of oocytes fertilized were 88.9, 86.5, and 75.5 for G1, G2 and G3 oocytes, respectively; percentages of cleaved embryos were 55.6, 65.2, and 32.7 for G1, G2 and G3 oocytes respectively; and percentages of development to blastocyst were 0.0, 20.6, and 8.2 for G1, G2 and G3 oocytes, respectively (Table 3.4, Fig. 3.12). There were no significant differences in fertilization, cleavage or blastocyst embryo development between oocyte grades in the non-imaged control group. For the bulk culture control groups, percentages of fertilization for the COC and DO groups were 68.1 and 64.2, respectively; embryo cleavage percentages were 44.9 and 11.3, respectively, and percentages of development to blastocyst were 18.8 and 0.0, respectively (Table 3.4, Fig. 3.12). There were

no significant differences in fertilization, cleavage or blastocyst development among the bulk cultured control groups. Lastly, statistical analysis of the imaged vs. non-imaged vs. bulk cultured groups revealed significant differences between the imaged G1 and non-imaged G1 groups ($P>0.05$). This part of the experiment included the initial trials using the WOW methods, thus embryo development for bovine oocytes labeled with rhodamine 123 and imaged were lower than that reported for subsequent experiments. Further, there was not a DO+CU bulk culture group in the rhodamine 123 bovine imaging experiment.

For bovine oocytes labeled with the ratiometric mitochondrial probe, JC-1 and imaged using multiphoton microscopy, the percentages of oocytes fertilized were 93.8, 90.9, and 53.8 for G1, G2, and G3 oocytes, respectively; percentages of embryo cleavage were 93.8, 76.8 and 28.8 for G1, G2 and G3 oocytes, respectively; and development to blastocyst stage were 37.5, 19.5 and 1.9 for G1, G2 and G3 oocytes, respectively (Table 3.5, Fig. 3.13). Statistical analysis revealed significant differences in the percentages of fertilization, embryo cleavage, and blastocyst development between JC-1 imaged G1 and G3 oocytes ($P<0.05$). For the non-imaged control oocytes, percentages undergoing fertilization were 84.2, 87.7, and 88.4 for G1, G2 and G3 oocytes, respectively; embryo cleavage percentages were 78.9, 74.9, and 65.1 for G1, G2 and G3 oocytes respectively; and development to blastocyst stage were 36.8, 26.9 and 16.3 for G1, G2 and G3 oocytes, respectively (Table 3.5, Fig. 3.13).

Table 3.4. Embryo Development in Non-imaged and Multiphoton Microscopy Imaged Bovine Oocytes Labeled with Rhodamine 123 and Maintained in the WOW System Compared with Bulk Cultures of Untreated Oocytes.

Imaged	Grade	n	# Fertilized (%)	# Cleaved (%)	# Blast (%)
	G1	8	3/8[A] (37.5)	1/8 (12.5)	1/8 (12.5)
	G2	125	94/125 (75.2)	35/125 (28)	4/125 (3.2)
	G3	67	36/67 (53.7)	16/67 (23.9)	1/67 (1.5)
	Total	**200**	**133/200 (66.5)**	**52/200 (26.0)**	**6/200 (3.0)**
Non-Imaged	**Grade**	**n**	**# Fertilized (%)**	**# Cleaved (%)**	**# Blast (%)**
	G1	9	8/9[B] (88.9)	5/9 (55.6)	0/9 (0.0)
	G2	141	122/141 (86.5)	92/141 (65.2)	29/141 (20.6)
	G3	49	37/49 (75.5)	16/49 (32.7)	4/49 (8.2)
	Total	**199**	**167/199 (83.9)**	**113/199 (56.8)**	**33/199 (16.6)**
Bulk	**Grade**	**n**	**# Fert (%)**	**# Cleaved (%)**	**# Blast (%)**
	COC	69	47/69 (68.1)	31/69 (44.9)	13/69 (18.8)
	DO	53	34/53 (64.2)	6/53 (11.3)	0/53 (0.0)
	Total	**122**	**81/122 (66.4)**	**37/122 (30.3)**	**13/122 (10.7)**

Lower case superscripts indicate significant differences in same column (P<0.05)
Upper case superscripts indicate significant differences between groups (P<0.05)

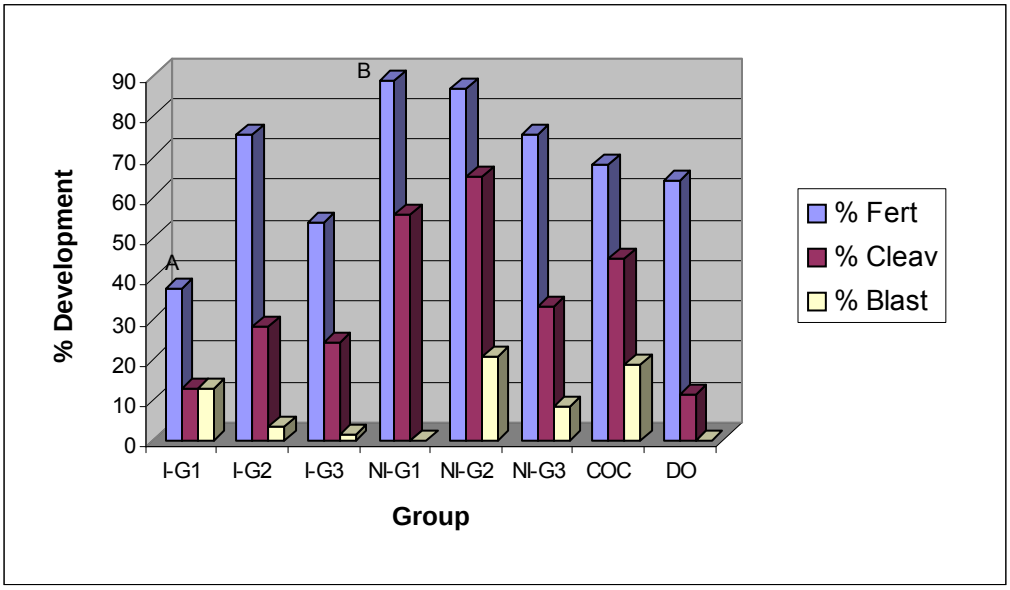

Fig. 3.12. Comparisons of fertilization and embryo development of cultured bovine oocytes labeled with rhodamine 123 and multiphoton microscopy imaged (I), with non-imaged (NI) oocytes using the WOW system, or bulk (COC, DO) cultured bovine oocytes.

There were no significant differences in fertilization, cleavage or blastocyst embryo development between oocyte grades in the non-imaged control group. For the bulk culture control groups, fertilization percentages for the COC, DO & DO+CU were 85.2, 70.8 and 81.6, respectively; embryo cleavage percentages were 70.4, 44.1, and 66.7, respectively, and percentages of development to blastocyst were 25.9, 9.4, and 19.3, respectively (Table 3.5, Fig. 3.13). There were no significant differences in fertilization, cleavage or blastocyst development among the bulk cultured control groups. Further, there were no significant differences in embryo development among each grade for imaged vs. non-imaged oocytes. Lastly, there were no distinct differences in morphology or

Table 3.5. Embryo Development in Non-imaged and Multiphoton Microscopy Imaged Bovine Oocytes Labeled with JC-1 and Maintained in the WOW System Compared with Bulk Cultures of Untreated Oocytes.

Imaged	Grade	n	# Fertilized (%)	# Cleaved (%)	# Blast (%)
	G1	16	15/16 [a] (93.8)	15/16[a] (93.8)	6/16[b] (37.5)
	G2	164	149/164 [ab] (90.9)	126/164[ab] (76.8)	32/164[ab] (19.5)
	G3	52	28/52 [b] (53.8)	15/52[b] (28.8)	1/52[b] (1.9)
	Total	**232**	**192 (82.8)**	**156 (67.2)**	**39 (16.8)**
Non-Imaged	**Grade**	**n**	**# Fert (%)**	**# Cleaved (%)**	**# Blast (%)**
	G1	19	16/19 (84.2)	15/19 (78.9)	7/19 (36.8)
	G2	171	150/171 (87.7)	128/171 (74.9)	46/171 (26.9)
	G3	43	38/110 (88.4)	28/43 (65.1)	7/43 (16.3)
	Total	**233**	**204/233 (87.6)**	**171/233 (73.4)**	**60/233 (16.3)**
Bulk	**Grade**	**n**	**# Fert (%)**	**# Cleaved (%)**	**# Blast (%)**
	COC	216	184/216 (85.2)	152/216 (70.4)	56/216 (25.9)
	DO	202	143/202 (70.8)	89/202 (44.1)	(19/202) (9.4)
	DO+CU	207	169/207 (81.6)	138/207 (66.7)	40/207 (19.3)
	Total	**625**	**496/625 (79.4)**	**241/625 (38.6)**	**75/625 (12)**

Lower case superscripts indicate significant differences in same column (P<0.05)

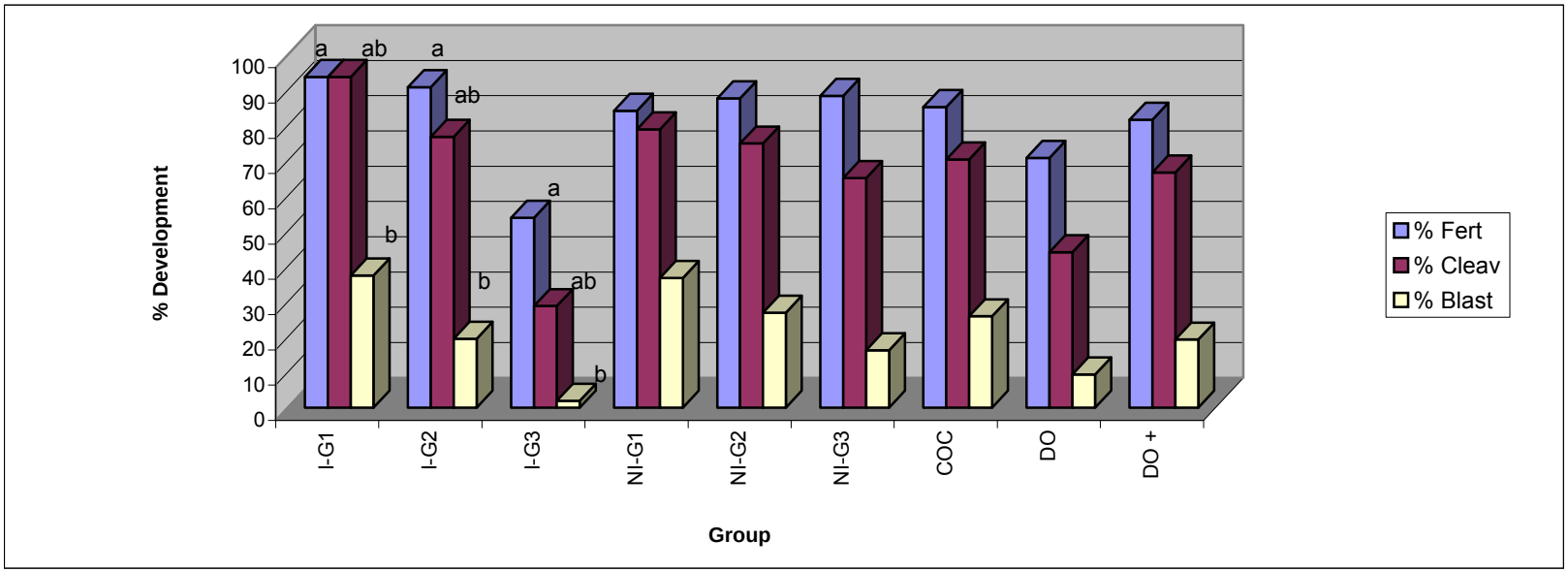

Lower case superscripts indicate significant differences in same column (P<0.05

Fig. 3.13. Comparisons of fertilization and embryo development of cultured bovine oocytes labeled with JC-1 and multiphoton microscopy-imaged (I), with non-imaged (NI) oocytes using the WOW system, or bulk (COC, DO, & DO+CU) cultured bovine oocytes.

patterns of fluorescence between oocytes that developed to blastocyst when compared with those that did not (Fig. 3.4 & 3.14).

For bovine oocytes labeled with Fluo-4, AM and imaged, percentages of oocytes fertilized were 89.5, 91.0, and 81.3 for G1, G2, and G3 oocytes, respectively; embryo cleavage percentages were 78.9, 76.9 and 64.1 for G1, G2 and G3 oocytes, respectively; and percentages of development to blastocyst stage were 15.8, 18.6 and 6.3 for G1, G2 and G3 oocytes, respectively (Table 3.6, Fig. 3.15). For the non-imaged control oocytes, fertilization percentages were 88.2, 92.2, and 87.3 for G1, G2 and G3 oocytes, respectively; embryo cleavage percentages were 88.2, 80.7, and 73 for G1, G2 and G3 oocytes respectively; and percentages of development to blastocyst stages were 23.5, 11.4 and 9.5 for G1, G2 and G3 oocytes, respectively (Table 3.6, Fig. 3.15). For bulk culture control groups COC, DO, and DO+CU, fertilization percentages were 86.0, 74.0, and 83.6, respectively; embryo cleavage percentages were 70.6, 52.7, and 64.2, respectively; and percentages of embryo development to blastocyst stage were 16.9, 6.9, and 17.9, respectively (Table 3.6, Fig. 3.15). Percentages of embryo development from this experiment showed no significant differences between grades in fertilization, cleavage or blastocyst development for imaged, non-imaged or bulk control groups, nor were there any significant differences among imaged vs. non-imaged oocytes for each grade. Further, there were no distinct differences in morphology or patterns of fluorescence between oocytes that developed to blastocyst when compared with those that did not (Fig. 3.7 & 3.16).

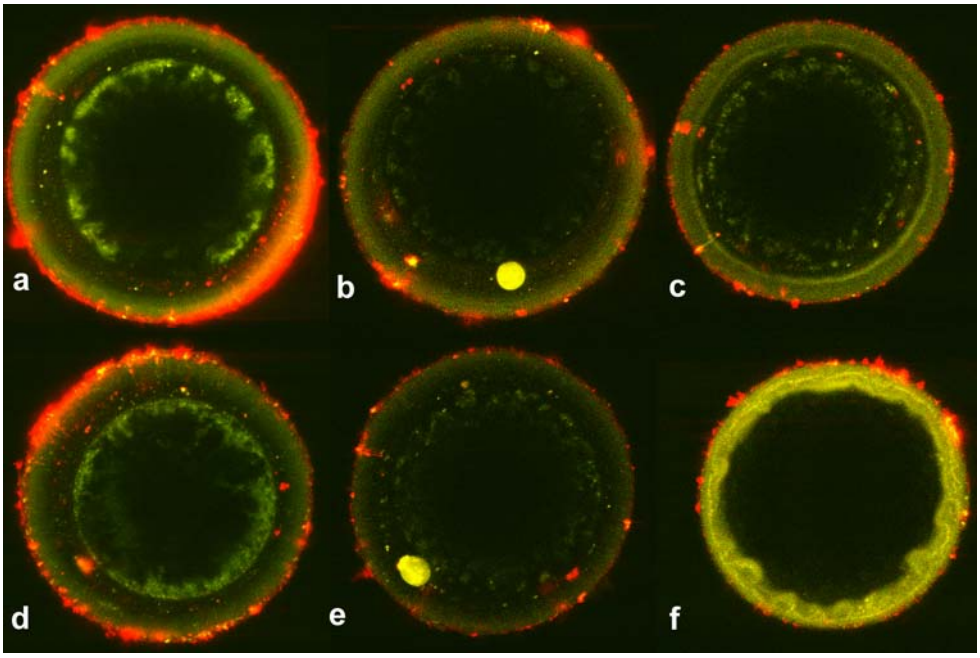

Fig. 3.14. Examples of bovine G1 **(a, d)**, G2 **(b, e)**, & G3 **(c, f)** imaged by multiphoton microscopy with the ratiometric mitochondrial probe, JC-1 that developed to blastocyst stage.

When plotted with SF/AFI vs. AFI, the rhodamine 123, JC-1 and Fluo-4, AM imaged oocytes that developed to blastocyst had AFI's that ranged from 35.0 – 89.2, 1.1 - 2.1 and 20.8 - 35.5, respectively (Table 3.7 and Fig. 3.17, 3.18 & 3.19). Therefore, we report that 28% (144/200), 5.2% (220/233), and 11.9% (208/237) of bovine oocytes were selected using this form of image analysis by sorting oocytes that have been labeled with rhodamine 123 with an AFI that falls within the 30-100 range, labeled with JC-1 with an FI between 1.25-2.25, or labeled with Fluo-4, AM with an AFI that lies between 20-30. Moreover, the achievement of embryo development to the blastocyst stage using this method of image analysis was 16.8% (37/220) and 15.9% (33/208) for JC-1 and Fluo-4, AM, respectively when sorting oocytes within these parameters.

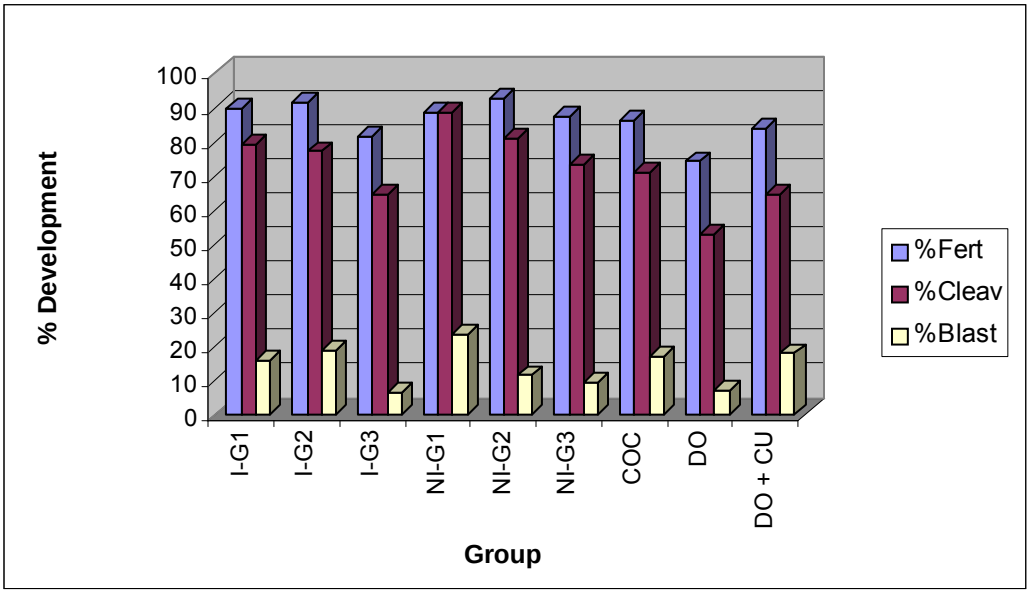

Fig. 3.15. Comparisons of fertilization and embryo development of cultured bovine oocytes labeled with Fluo-4 and multiphoton microscopy-imaged (I), with non-imaged (NI) oocytes using the WOW system, or bulk (COC, DO, & DO+CU) cultured bovine oocytes.

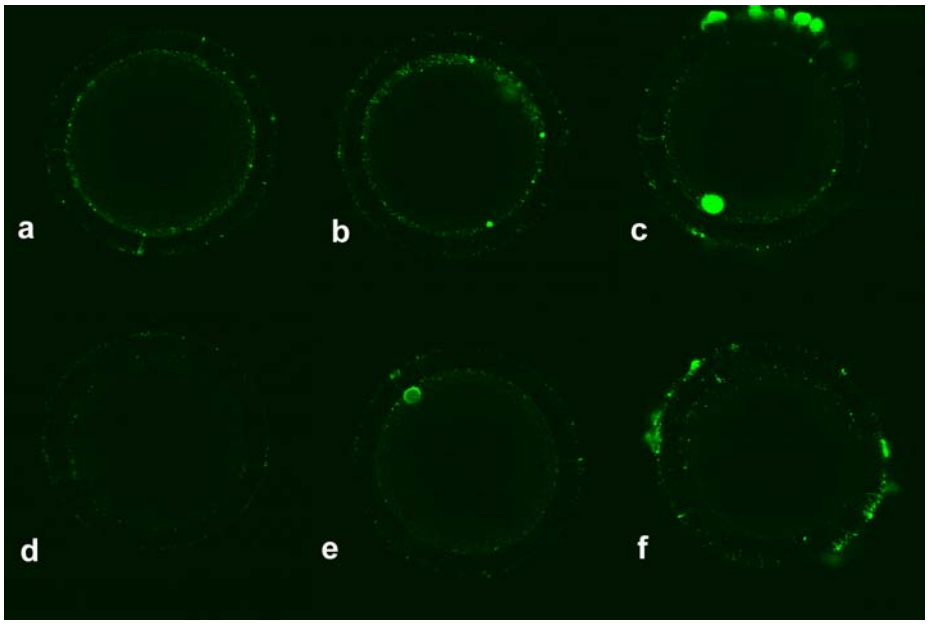

Fig. 3.16. Examples of bovine G1 **(a, d)**, G2 **(b, e)**, & G3 **(c, f)** imaged by multiphoton microscopy with the Ca^{2+}-sensitive fluorophore that developed to blastocyst stage.

Table 3.6. Embryo Development in Non-imaged and Multiphoton Microscopy Imaged Bovine Oocytes Labeled with Fluo-4 and Maintained in the WOW System Compared with Bulk Cultures of Untreated Oocytes.

Imaged	Grade	n	# Fertilized (%)	# Cleaved (%)	# Blast (%)
	G1	19	17/19 (89.5)	15/19 (78.9)	3/19 (15.8)
	G2	156	142/156 (91.0)	120/156 (76.9)	29/156 (18.6)
	G3	64	58/70 (81.3)	41/64 (64.1)	4/64 (6.3)
	Total	**239**	**211/239 (88.3)**	**176/239 (73.6)**	**36/239 (15.1)**
Non-Imaged	**Grade**				
	G1	17	15/17 (88.2)	15/17 (88.2)	4/17 (23.5)
	G2	166	153/166 (92.2)	134/166 (80.7)	19/166 (11.4)
	G3	63	55/63 (87.3)	46/63 (73)	6/63 (9.5)
	Total	**246**	**223/246 (90.7)**	**195/246 (29.0)**	**29/246 (11.8)**
Bulk	**Grade**				
	COC	136	117/136 (86.0)	96/136 (70.6)	23/136 (16.9)
	DO	131	97/131 (74.0)	69/131 (52.7)	9/131 (6.9)
	DO+CU	134	112/134 (83.6)	86/134 (64.2)	24/134 (17.9)
	Total	**401**	**326/401 (81.3)**	**251/401 (62.6)**	**56/401 (14)**

Table 3.7. Blastocyst Development of Bovine Oocytes Imaged Using Multiphoton Microscopy with Rhodamine 123 (a,b), JC-1 (c,d), or Fluo4 (e,f) Based upon Parameters Used in Tables 3.1-3.3.

(a)

Grade	n	SF/AFI Mean	Range
G1 Blast	1	0.021	0.021
G2 Blast	4	0.019	0.011-0.029
G3 Blast	1	0.019	0.019
Total	**6**		

(b)

Grade	n	AFI Mean	Range
G1 Blast	1	48.660	48.660
G2 Blast	4	59.807	35.034-89.222
G3 Blast	1	52.0	52.0
Total	**6**		

(c)

Grade	n	SF/FI Mean	Range
G1 Blast	6	0.653	0.594-0.742
G2 Blast	31	0.620	0.493-0.928
G3 Blast	1	0.798	0.798
Total	**38**		

(d)

Grade	n	FI Ratio Mean	Range
G1 Blast	6	1.560	1.38-1.712
G2 Blast	31	1.593	1.110-2.08
G3 Blast	1	1.401	1.401
Total	**38**		

(e)

Grade	n	SF/AFI Mean	Range
G1 Blast	2	0.043	0.041-0.046
G2 Blast	31	0.044	0.028-0.048
G3 Blast	4	0.041	0.042-0.046
Total	**37**		

(f)

Grade	n	AFI Mean	Range
G1 Blast	2	22.973	21.725-24.222
G2 Blast	31	23.828	20.845-35.488
G3 Blast	4	23.312	22.444-24.073
Total	**37**		

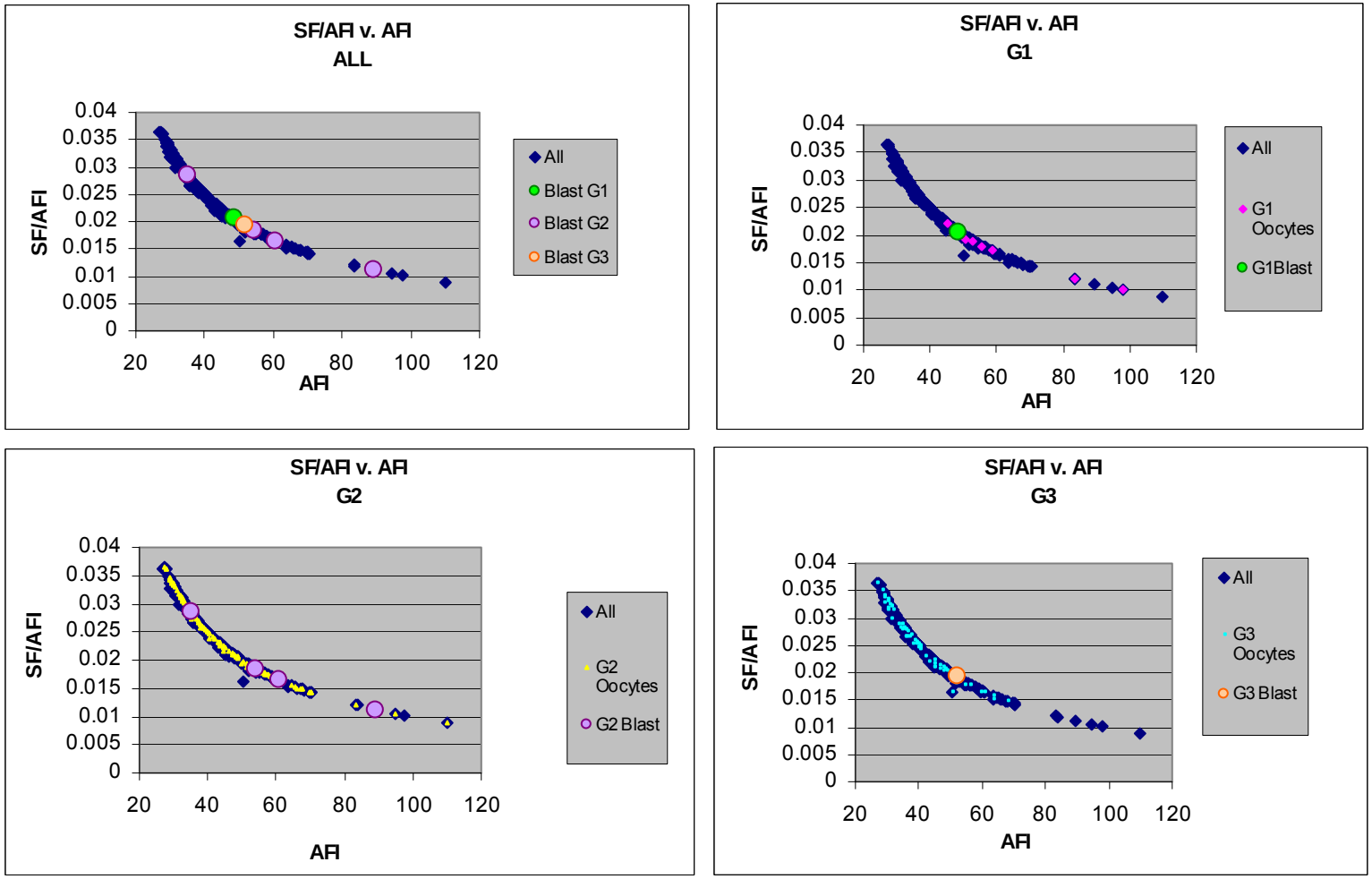

Fig. 3.17. Relationships between SF/AFI and AFI in bovine oocytes that developed to the blastocyst stage following imaging by multiphoton microscopy with the mitochondrial probe, rhodamine 123.

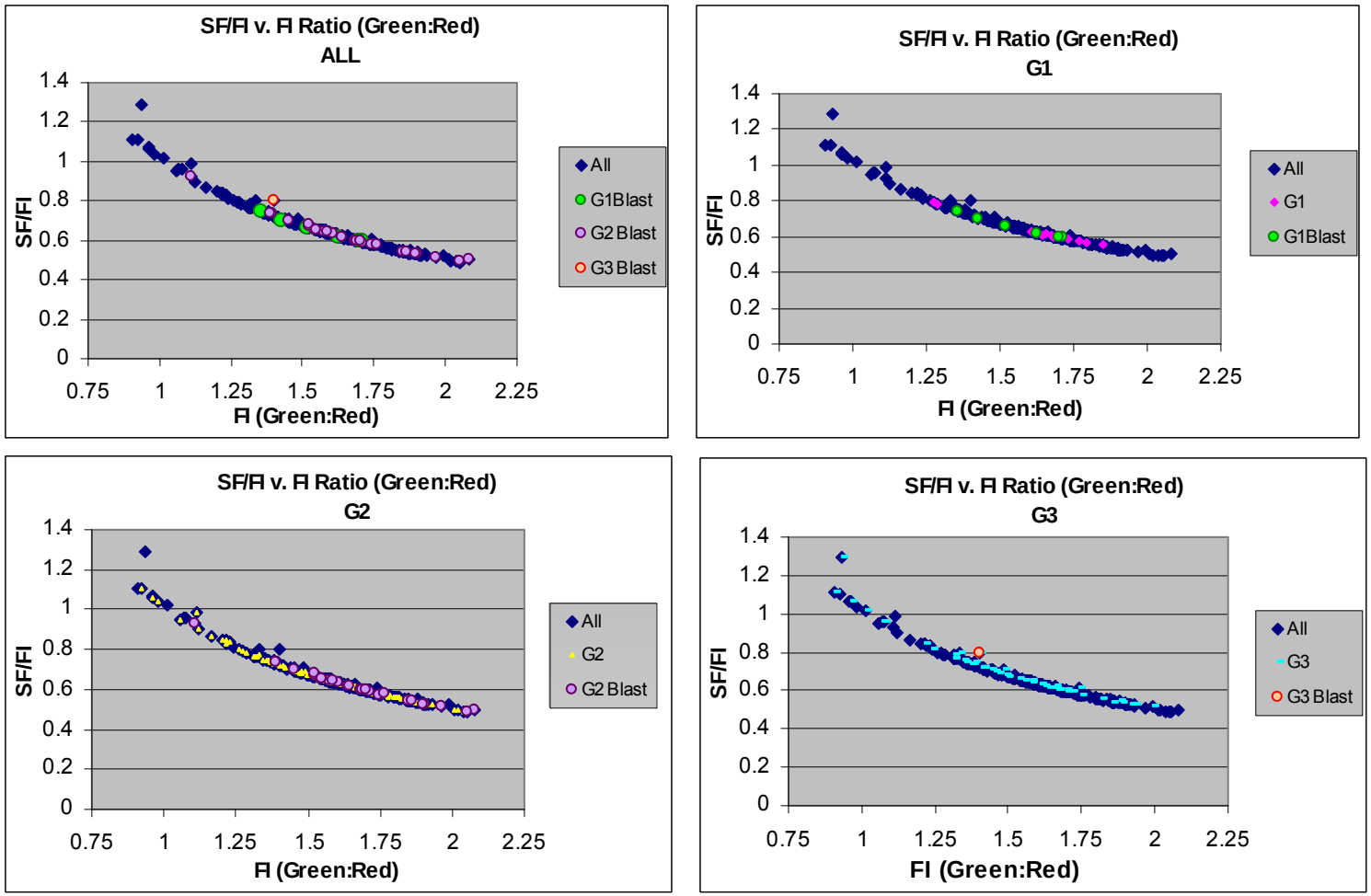

Fig. 3.18. Relationships between SF/AFI and AFI in bovine oocytes that developed to the blastocyst stage following imaging by multiphoton microscopy with the ratiometric mitochondrial probe, JC-1.

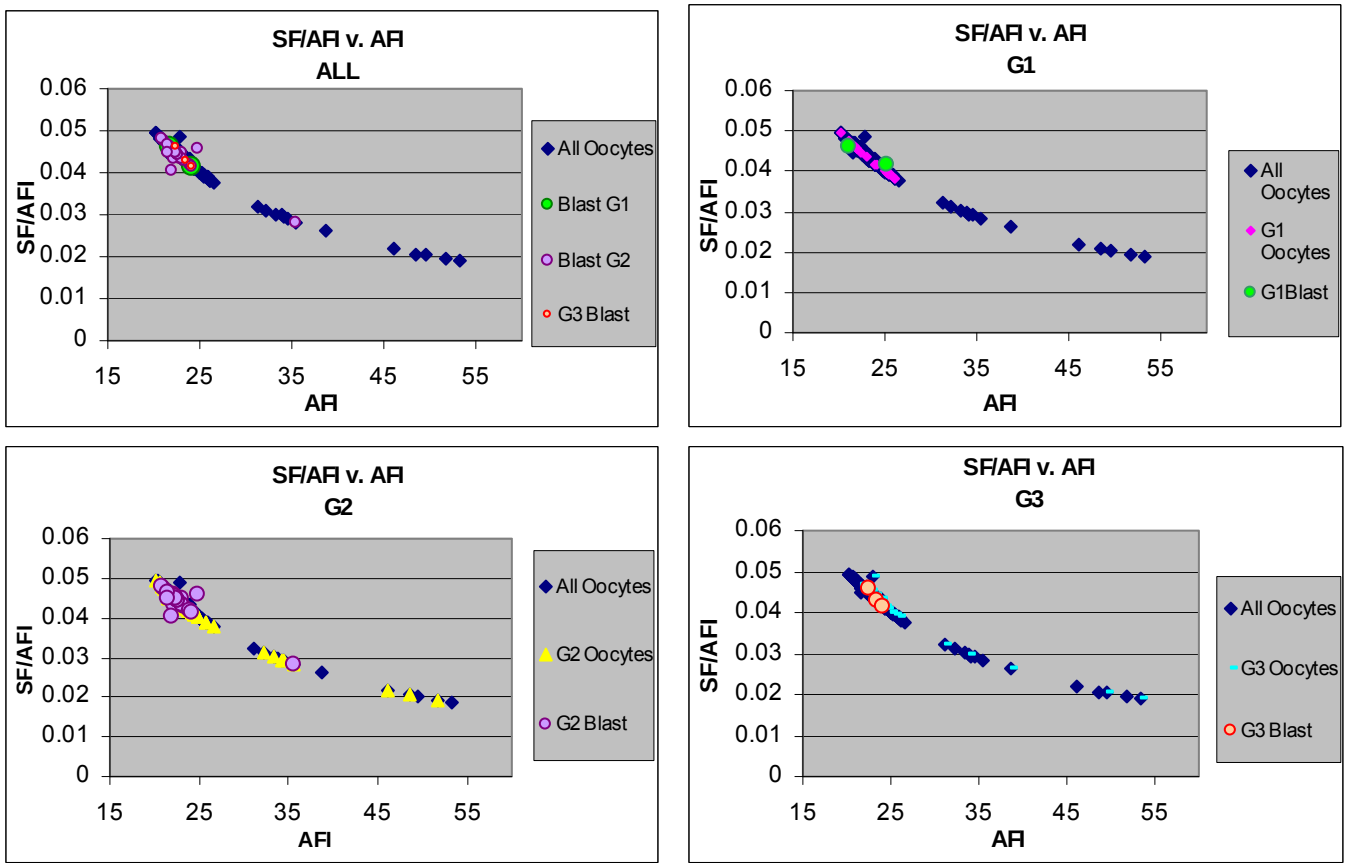

Fig. 3.19. Relationships between SF/AFI vs. AFI (as an index of intracellular Ca^{2+}) in bovine oocytes that developed to the blastocyst stage following imaging using multiphoton microscopy with the Ca^{2+}-sensitive fluorophore, Fluo-4, AM .

3.3 Experiment II – Characterization of the spatial distribution of mitochondria, mitochondrial membrane potential ($\Delta\psi m$), and intracellular Ca^{2+} stores in relation to morphology of IVM canine oocytes using criteria from Experiment 1 that could potentially be used to evaluate developmental competence in this species

3.3.1 *Characterization of the spatial distribution of mitochondria and mitochondrial activity in relation to grade of IVM canine oocytes using the fluorescent probe rhodamine 123*

Given that canine oocytes harvested from excised ovaries for in vitro studies are at the GV stage of meiosis and have poor, inconsistent IVM to MII stage (unlike commercially available bovine oocytes for similar studies), they were not sorted into grades as previously described for the bovine prior to imaging and subsequent IVF. After IVM, canine oocytes were labeled with fluorescent dye and imaged with the identity of each oocyte maintained using the WOW method as previously described. These data were then organized according to meiotic stage and statistically analyzed for SF/AFI and AFI for each oocyte in all experiments, again maintaining the identity of the oocyte throughout the evaluation.

Canine oocytes were evaluated for mitochondrial localization and membrane potential using rhodamine 123 (n=84) and JC-1 (n=157) in the same manner as previously described for bovine oocytes. Similar to the bovine oocyte, the localization pattern and mitochondrial fluorescence with rhodamine

123 (Fig. 3.20) was not different from that of oocytes labeled with JC-1 (Fig. 3.21). Canine oocyte mitochondria appeared as punctate areas of fluorescence and were primarily localized to the pericortical regions, with lighter punctate staining throughout the ooplasm.

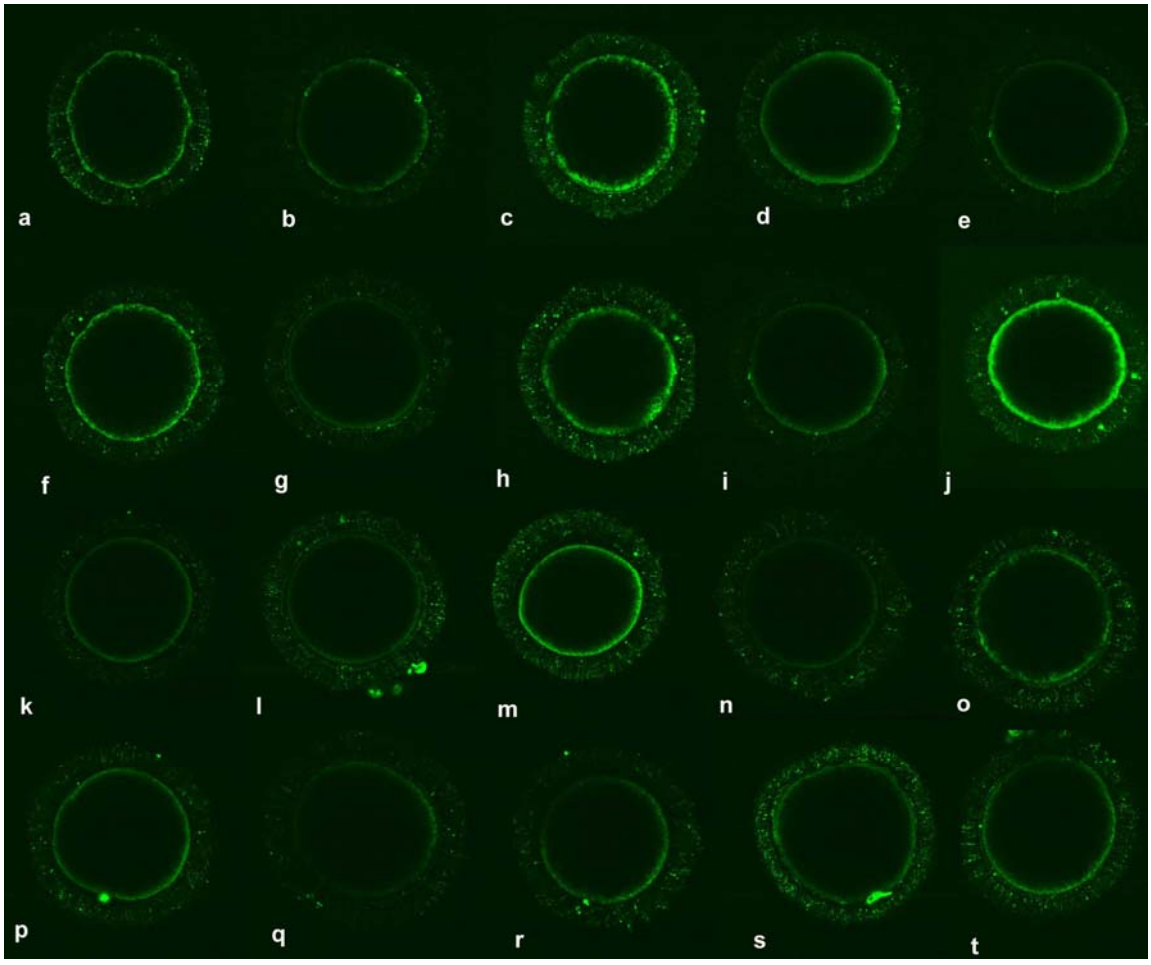

Fig. 3.20. Canine oocytes classified as DEG **(a-e)**, GV-GVBD **(f-j)**, MI **(k-o)**, MII **(p-t)** and imaged using multiphoton microscopy with the mitochondrial probe, rhodamine 123.

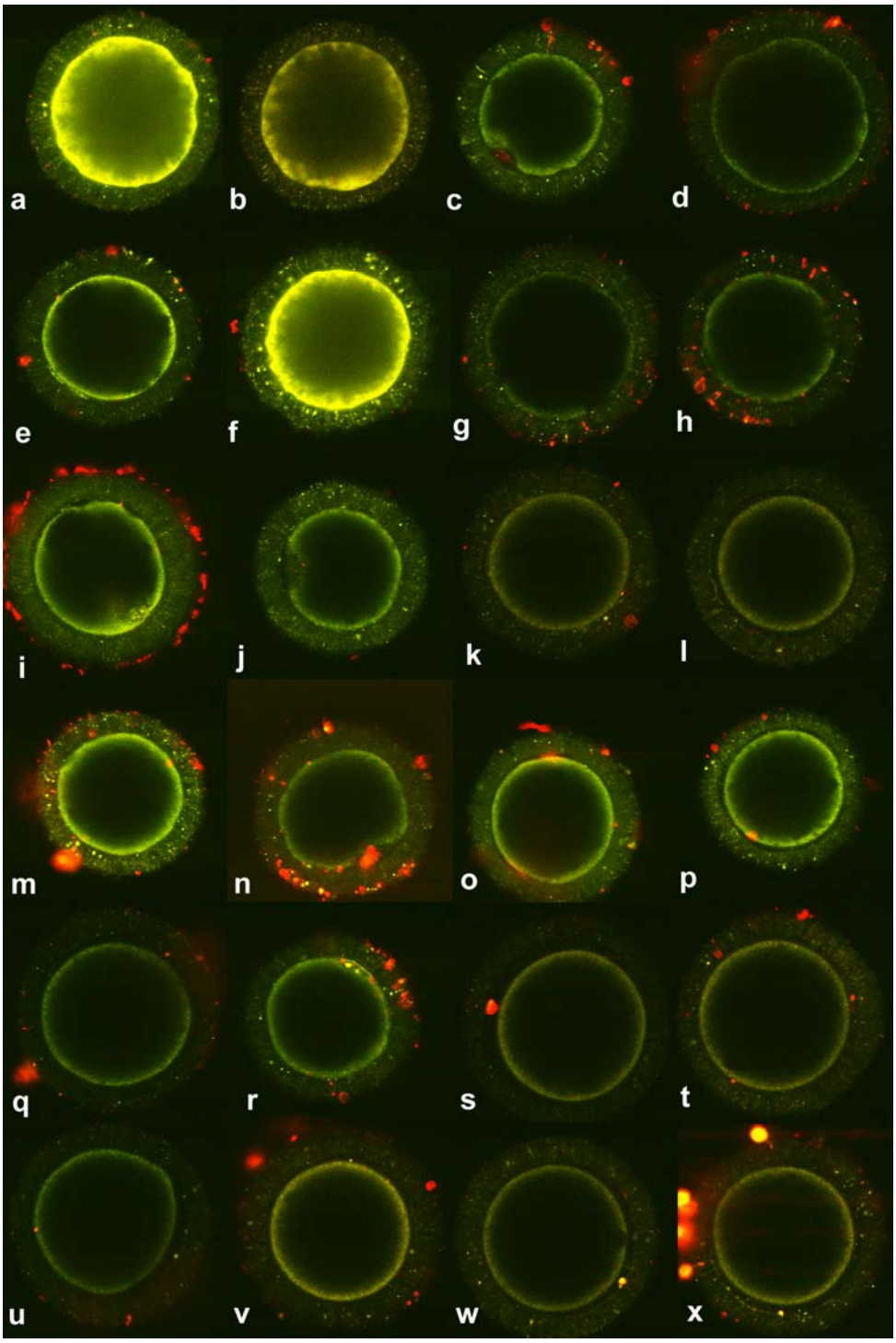

Fig. 3.21. Canine oocytes classified as DEG **(a,b)**, DEG-IMP **(c,d)**, GV-GVBD **(e,f)**, GV-GVBD-IMP **(g,h)**, MI **(i,j)**, MI-IMP **(k,l)**, MII **(m-o)**, MII-IMP **(p-t)** 1-CELL-IMP **(u-w)**, CLEAVED **(x)** and imaged using multiphoton microscopy with JC-1.

Percentages of IVM oocytes labeled with rhodamine 123 and imaged versus non-imaged oocytes are presented in Table 3.8 and Fig. 3.22. There were no significant differences in percentages of maturation for any meiotic stage within or between the imaged versus non-imaged groups, thus indicating no influence of rhodamine 123 or imaging on meiotic stage or progression in canine oocytes.

Statistical analysis of SF/AFI for oocytes labeled with rhodamine 123 and imaged revealed significant differences between DEG and MI stage oocytes. There were no significant differences in AFI between meiotic stages. Further, the means and ranges for SF/AFI and AFI for each meiotic stage are shown in Table 3.9 and plotted in Fig. 3.23. When SF/AFI was plotted against AFI, the curve generated revealed an inverse relationship for all meiotic stages of canine oocytes labeled with rhodamine 123 and imaged as previously reported for the bovine (Fig. 3.24).

Both DEG and GV-GVBD oocytes had AFI's that were distributed throughout the curve (25.6 to 52.9), while MI and MII oocytes had AFI's that ranged from 23.2 and 23.5 to 43.2 and 46.3, respectively, with 13/15 (87.0%) of MI and 11/14 (79%) MII oocytes having AFI's between 20-35. Therefore, we report that 28.6% (60/84) of canine oocytes were selected using this form of image analysis by selecting oocytes that have AFI's that lie between 20-35 when imaged by multiphoton microscopy with rhodamine 123, thus excluding the remaining oocyte population from further experimentation.

Table 3.8. In vitro Maturation of Non-imaged and Multiphoton Microscopy Imaged Canine Oocytes Labeled with Rhodamine 123 Compared with Bulk Cultures of Untreated Oocytes.

Stage	Imaged n (%)	Non-Imaged n (%)
DEG	19 (22.6)	43 (38.4)
GV-GVBD	36 (42.9)	46 (41.1)
MI	15 (17.9)	13 (11.6)
MII	14 (16.7)	10 (8.9)
TOTAL	**84**	**112**

Table 3.9. Mean Values and Range for SF/AFI (a) and AFI (b) of Canine Oocytes Imaged Using Multiphoton Microscopy with the Mitochondrial Probe Rhodamine 123.

Stage	n	SF/AFI Mean	SF/AFI Range	AFI Mean	AFI Range
DEG	19	0.029^{a}	0.02-0.04	33.29	25.61-48.57
GV-GVBD	36	0.030^{a}	0.018-0.041	32.80	24.02-52.95
MI	15	0.035^{b}	0.022-0.043	29.24	23.25-43.21
MII	14	0.031^{ab}	0.021-0.041	34.06	23.52-46.35
TOTAL	**84**				

Lower case superscripts indicate significant differences in same column ($P<0.05$)

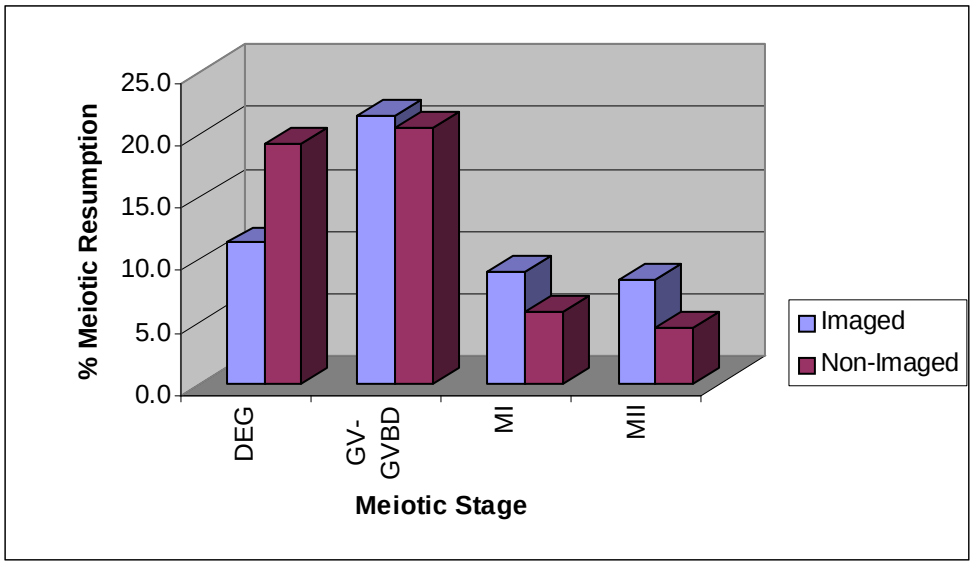

Fig. 3.22. In vitro maturation of canine oocytes imaged using multiphoton microscopy with rhodamine 123 compared with non-imaged oocytes.

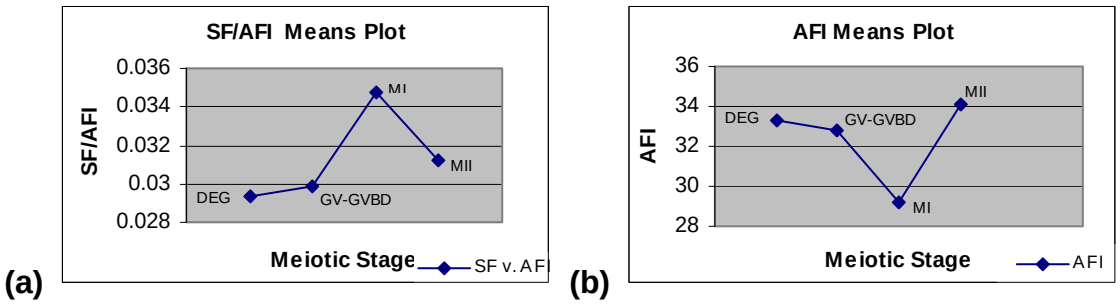

Fig. 3.23. Relationships between SF/AFI **(a)** and AFI **(b)** in canine oocytes imaged using multiphoton microscopy with rhodamine 123.

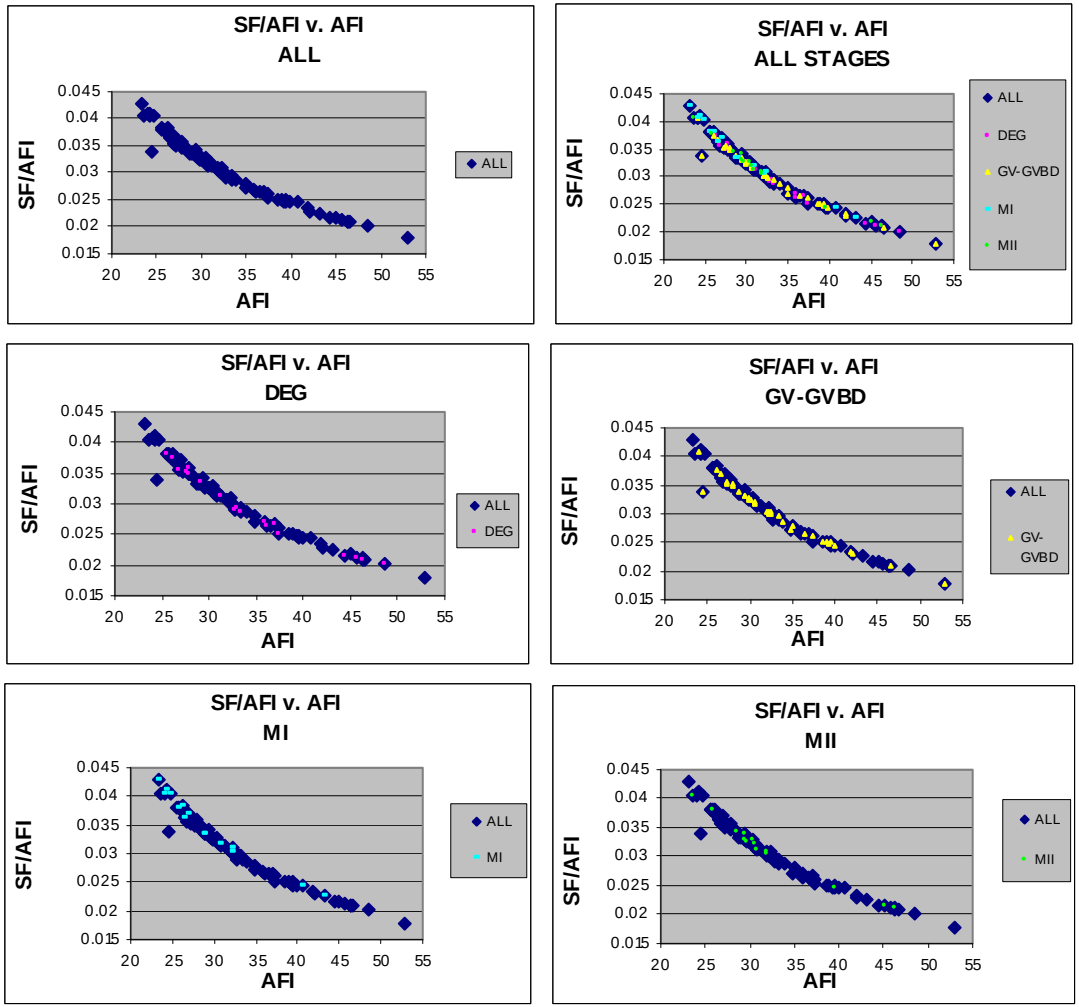

Fig. 3.24. Relationships between SF/AFI vs. AFI in canine oocytes imaged using multiphoton microscopy with rhodamine 123.

3.3.2 Characterization of the spatial distribution of free intracellular Ca^{2+} in relation to grade of IVM canine oocytes

For canine oocytes labeled with Fluo-4, AM, images revealed spatial patterns of free intracellular Ca^{2+} that were not unique according to each meiotic stage. Like the bovine, Fluo-4, AM fluorescence within the oocyte cytoplasm was, as expected, either very low with unremarkable areas of specific localization, or showed the same pattern of localization that was previously described for the Grade 3 bovine oocytes labeled with Fluo-4, AM, wherein higher intracellular Ca^{2+} levels were localized to the peri-cortical regions of the ooplasm (Fig. 3.25).

Percentages of in vitro maturation of oocytes labeled with Fluo-4, AM and imaged versus non-imaged versus labeled only oocytes are presented in Table 3.10 and Fig. 3.26. There were no significant differences in percentages of maturation for any meiotic stage within the imaged versus non-imaged groups. Within the labeled only group, there were significant differences between GV-GVBD and both MI and MII stage oocytes ($P<0.05$). Between group analysis revealed no significant differences between groups of thesame meiotic stage ($P<0.05$). Further, there were no significant differences in meiotic progression to MI or MII between the imaged, non-imaged or labeled only cultured groups.

The mean values for SF/AFI and AFI of Fluo-4, AM labeled and imaged canine oocytes are listed in Table 3.11 and plotted in Fig. 3.27, indicating an inverse relationship between SF/AFI and AFI. The SF/AFI was plotted against AFI and also showed an inverse relationship between the two measurements

(Fig. 3.28). Statistical analysis of AFI revealed significant differences between the degenerating oocytes (DEG) and oocytes in the GV-GVBD, MI, and MII stages of meiosis, respectively ($P<0.05$). For SF/AFI, statistical analysis indicated that DEG oocytes were significantly different from GVBD and MI, but not from MII oocytes, respectively ($P<0.05$).

Both DEG and GV-GVBD oocytes had AFI's that were distributed throughout the curve (21.6 to 39.2), while MI and MII oocytes had AFI's that ranged from 21.8 to 36.9 and 21.3 to 29.7, respectively. Therefore, we report that 48.8% of canine oocytes were selected by sorting oocytes that have an AFI that falls within the 20-25.5 (59/121) range and thus eliminating 48.7% of the oocyte population. Further, 90.1 (10/11) MII and 90% (9/10) MI and MII stage oocytes had an AFI within this range. Lastly, the loading of fluorescent probe to bulk cultured, non-imaged oocytes appears to have no effect on IVM of canine oocytes.

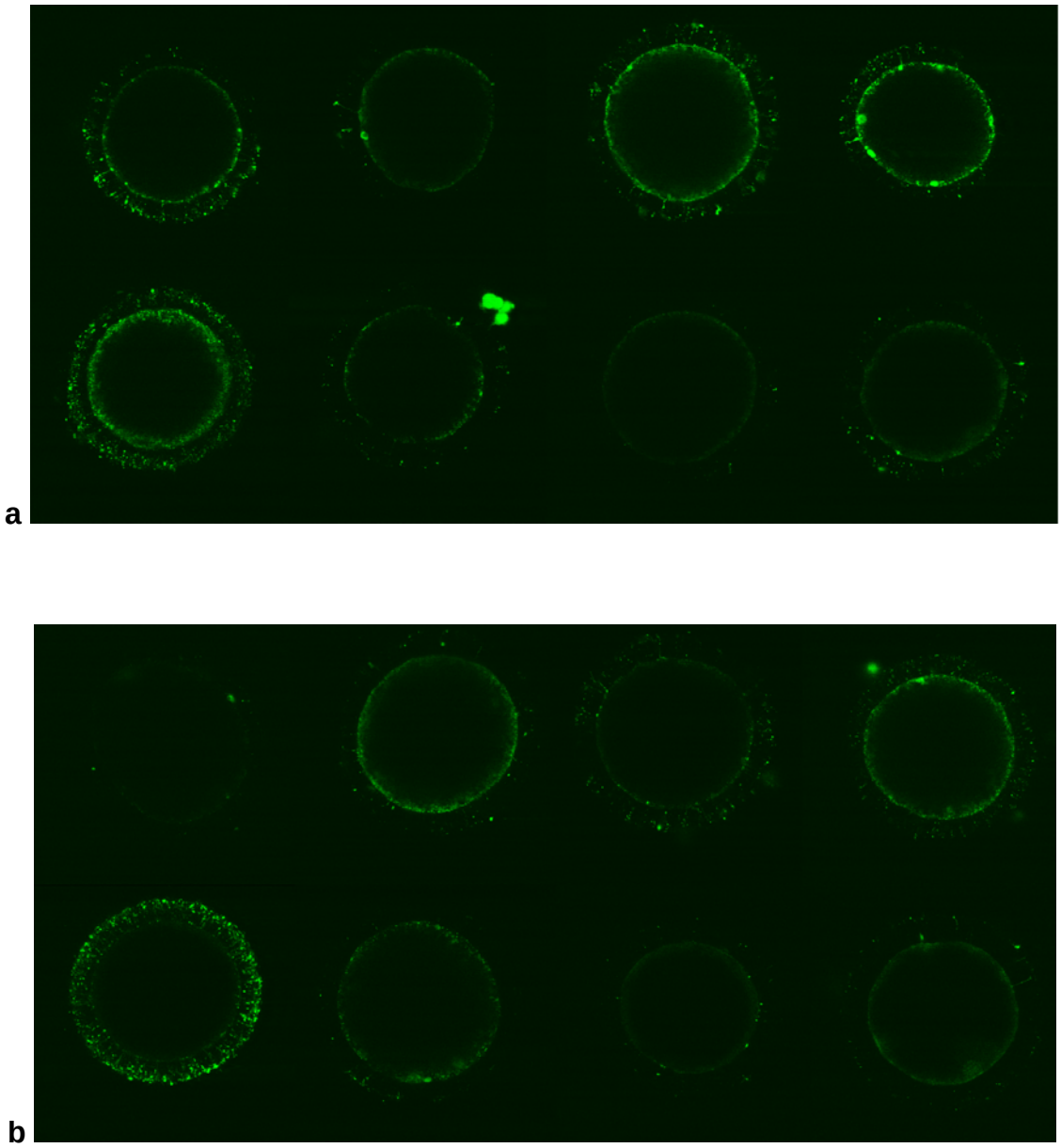

Fig. 3.25. Canine oocytes classified as DEG **(a)**, GV-GVBD **(b)**, MI **(c)**, MII **(d)** and imaged using multiphoton microscopy with Fluo4.

c

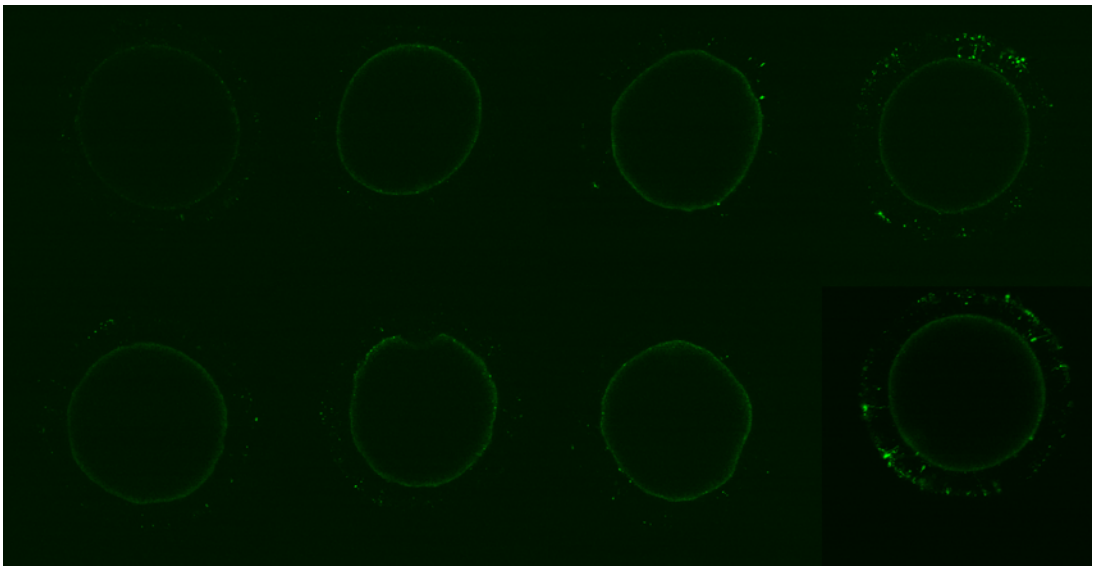

d

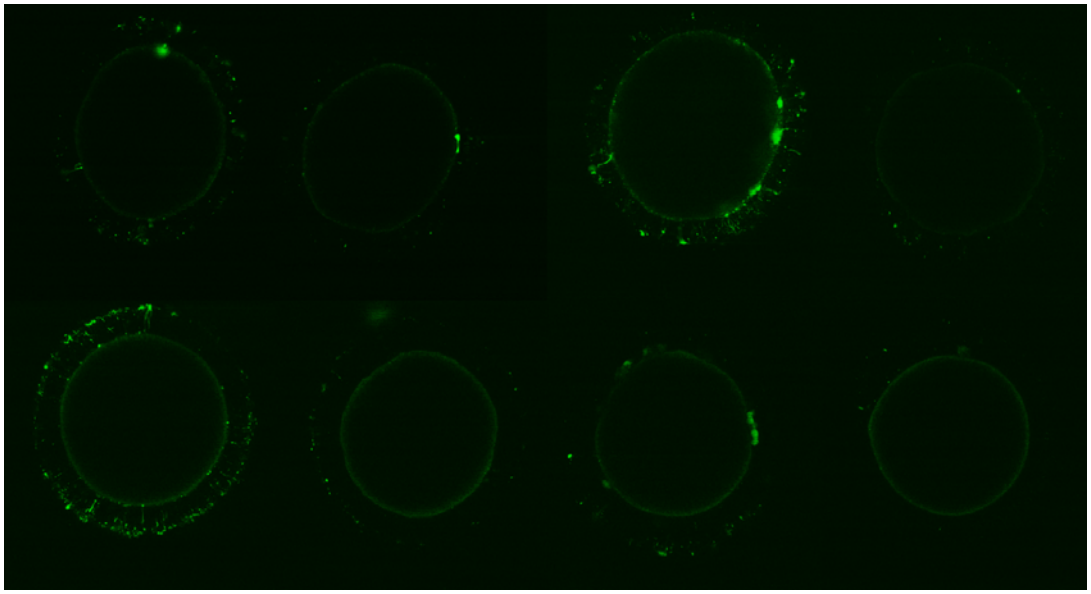

Fig. 3.25 (cont).

Table 3.10. In vitro Maturation of Non-imaged and Multiphoton Microscopy Imaged Canine Oocytes Labeled with Fluo-4, AM Compared with Bulk Cultures of Untreated Oocytes.

Stage	Imaged n (%)	Non-Imaged n (%)	Bulk n (%)
DEG	42/119 (35.3)	49/113 (43.4)	41/97[ab] (42.2)
GV-GVBD	56/119 (47.1)	40/113 (35.4)	52/97[a] (53.6)
MI	11/119 (9.2)	16/113 (14.2)	2/97[b] (2.1)
MII	10/119 (8.4)	8/113 (7.1)	2/97[b] (2.1)
Total	**119**	**113**	**97**

Lower- case superscripts indicate significant differences in same column;

upper-case superscripts indicate significant differences between columns (P<0.05)

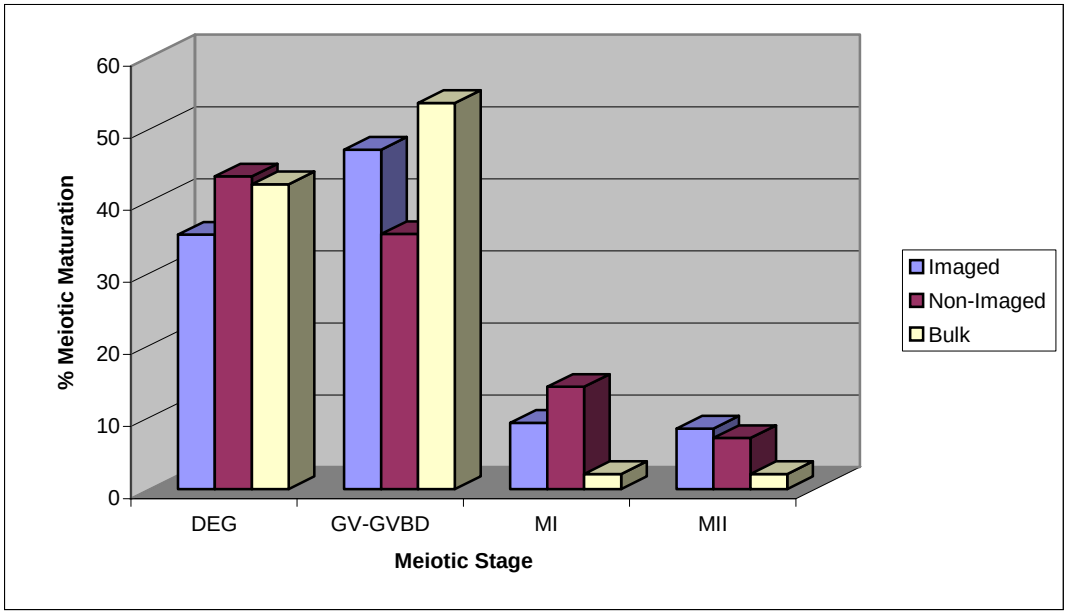

Fig. 3.26. In vitro maturation of canine oocytes imaged using multiphoton microscopy with Fluo-4 compared with non-imaged control oocytes.

Table 3.11. Mean Values and Range for SF/AFI (a) and AFI (b) of Canine Oocytes Imaged Using Multiphoton Microscopy with the Ca^{2+}-sensitive Probe, Fluo-4, AM.

	Grade	(n)	SF/AFI Mean	SF/AFI Range
	DEG	43	0.036^{a}	0.014 - 0.046
	GV-GVBD	57	0.039^{b}	0.021-0.047
	MI	11	0.041^{b}	0.027-0.046
	MII	10	0.043^{ab}	0.023-0.047
a	**TOTAL**	**121**		

Lower case superscripts indicate significant differences in same column (P<0.05)

	Grade	(n)	AFI Mean	AFI Range
	DEG	43	28.489^{b}	22.019-39.197
	GV-GVBD	57	26.099^{a}	21.645-35.640
	MI	11	24.821^{a}	21.808-36.908
	MII	10	23.657^{a}	21.343-29.703
b	**TOTAL**	**121**		

Lower case superscripts indicate significant differences in same column (P<0.05)

(a)

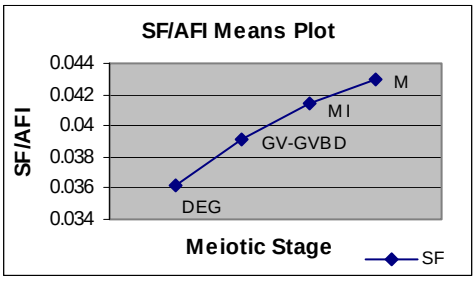

(b)

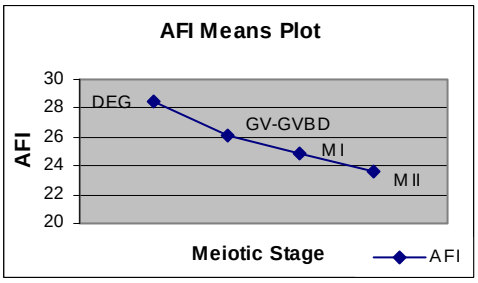

Fig 3.27. Relationships between means of SF/AFI **(a)** and AFI **(b)** (as an index of intracellular Ca^{2+}) in canine oocytes imaged using multiphoton microscopy with Fluo-4.

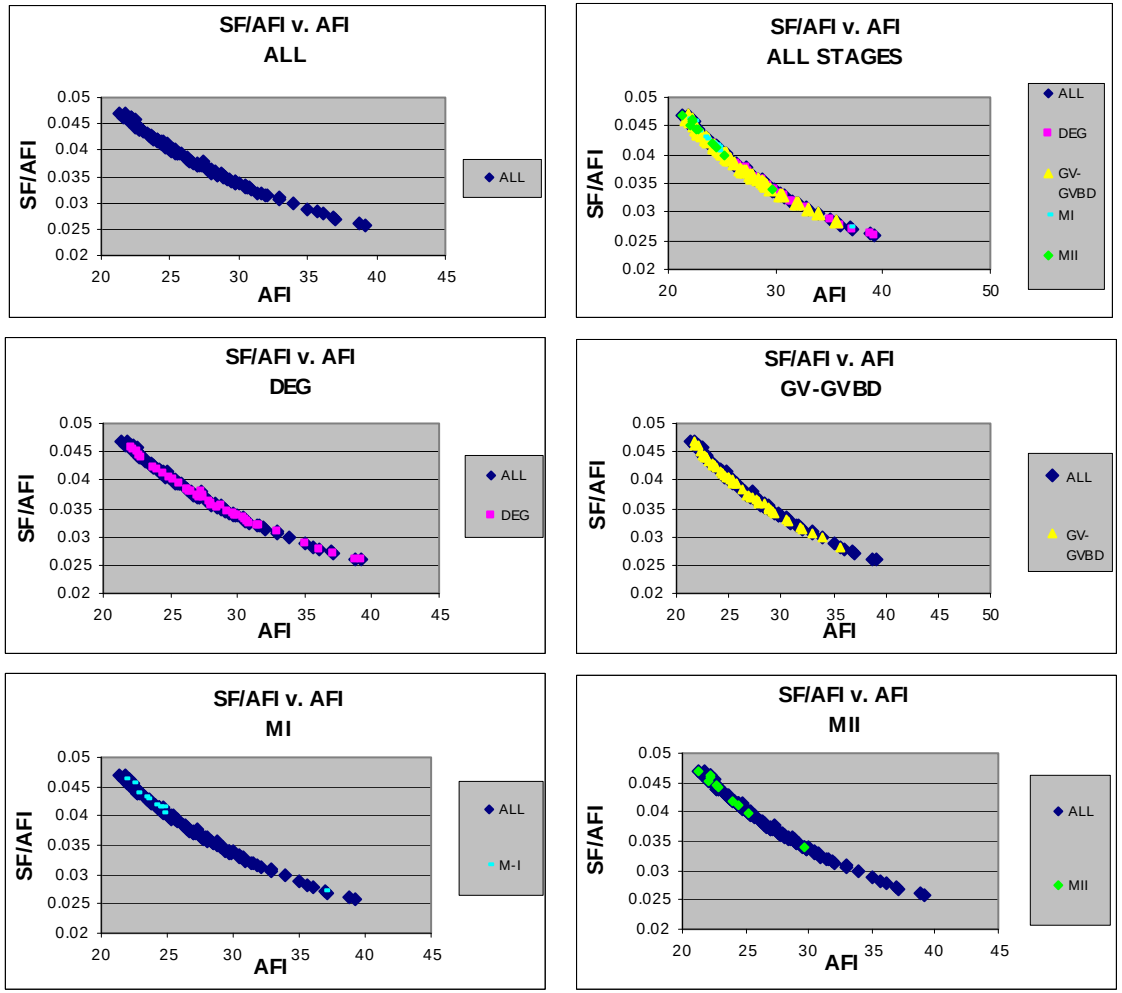

Fig. 3.28. Relationships between SF/AFI vs. AFI (as an index of intracellular Ca^{2+}) of all meiotic stages of canine oocytes imaged by multiphoton microscopy with Fluo-4.

3.3.3 Characterization of the spatial distribution of mitochondria and mitochondrial activity in relation to grade of IVM canine oocytes using the ratiometric fluorescent probe JC-1

Initial survey of the JC-1 probe in the canine was evaluated by methods as previously reported for bovine and generated fluorescent localization of mitochondrial heterogeneity similar to that seen in the bovine for IVM MII oocytes. Interestingly, the polar body in canines fluoresced primarily in the RITC channel, with very minimal fluorescence (if any) in the FITC channel, indicating a high degree of mitochondrial concentration and hyperpolarization, unlike that reported for mouse and human, or as observed in the bovine from this study.

Analysis of the ratiometric JC-1 fluorescence generated the same inverse relationship between SF/FI and fluorescence intensity (FI; green:red) as observed for bovine (Fig. 3.29). GV-GVBD oocytes had FI's that were distributed throughout the curve (1.0-2.1), while MI and MII oocytes had FI's that ranged from 1.6-1.8 and 0.1-2.9, respectively, with 33.3% (3/9) of MI and 66.7% (6/9) MII oocytes in the range of 0.5-2.0 (29/32), respectively (Fig. 3.30 and Table 3.12).

Further analysis of mitochondrial fluorescence using JC-1 in canine oocytes was investigated retrospectively and involved the use of an enhanced method of evaluating each oocyte for selection. Briefly, this method consisted of selecting a reference oocyte based on a compilation of the most common values for SF and FI for each oocyte as well as good fertilization. A maximum difference of 6 between the reference oocyte (a value of 0) was determined as the cutoff limit for prediction. The average values for each oocyte are plotted in Fig. 3.30, 3.32, 3.33 & 3.34 to illustrate the intensity with respect to other oocytes within the same meiotic grade for both the unfertilized and fertilized oocytes. While this study characterized mitochondrial localization and $\Delta\psi m$ in the canine oocyte using an improved method of image analysis, each fertilization repetition utilized a different sperm source (frozen v. fresh) as outlined in the Materials & Methods section and are reported independently herein as informative data. Only the percentages of embryo development are reported for each sperm source, hence no statistical evaluation was made accordingly.

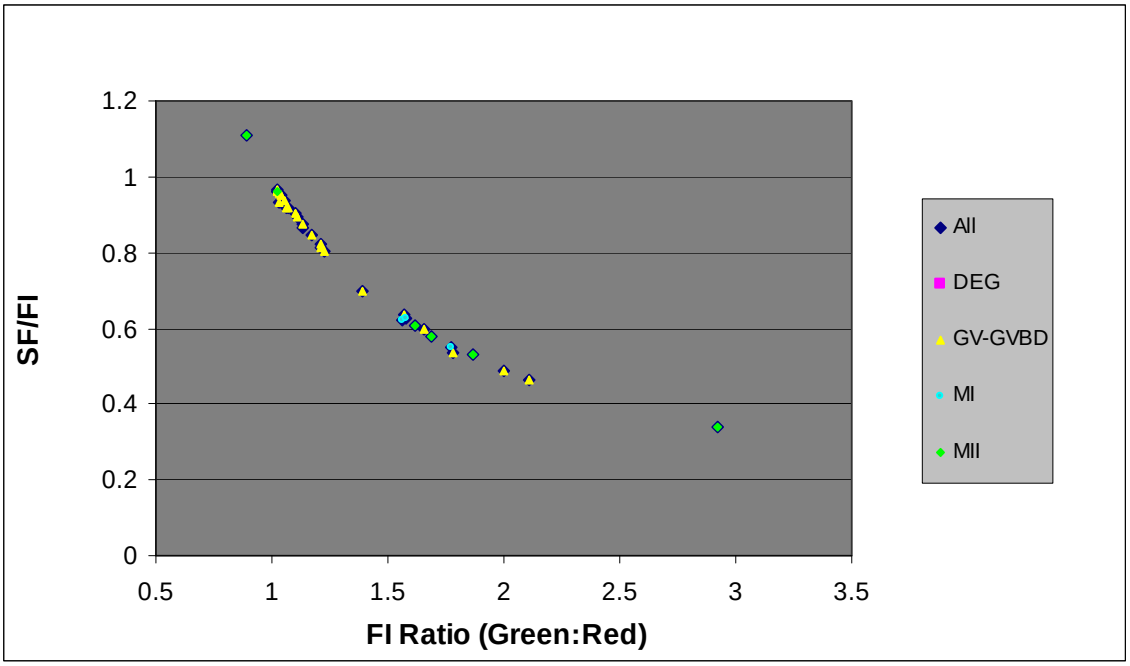

Fig. 3.29. Relationship between SF/AFI vs. FI (ratio of green:red fluorescence intensity) in canine oocytes imaged by multiphoton microscopy with the ratiometric mitochondrial probe, JC-1.

The mean values of the FI for each oocyte grade in the unfertilized group (repetition 1) were 43.4, 30.4, 6.4, and 19.6 for DEG, GV-GVBD, MI and MII, respectively and the ranges were 43.4, 1.5-50.2, 4.5-7.6, and 0-58.0 for DEG, GV-GVBD, MI and MII, respectively (Table 3.12). For the fertilized oocytes, values for each repetition are reported individually and defined as 1) repetition 2

(n=47) using frozen semen fertilized at $2X10^6$, 2) repetition 3 (n=46) using frozen semen fertilized at $5x10^6$ and 3) repetition 4 (n=39) using fresh collected, extended semen fertilized at $5X10^6$. The average fluorescence values and ranges for each repetition are reported in Table 3.13 and Fig. 3.32, 3.33, & 3.34.

As previously described, a maximum difference of 6 was determined as the FI cutoff for selection of oocytes in our initial assessment using the new method of evaluation. From these parameters, 9/32 29/47, 23/46 and 23/39 oocytes from the unfertilized and fertilized groups (repetitions 2, 3 & 4), respectively were predicted competent, thus excluding 71.9, 38, 50, and 41% of the oocytes from both unfertilized and fertilized groups (repetitions 2, 3 & 4), respectively as non-competent based on the fluorescence intensity of mitochondria localization and activity. Of the unfertilized oocytes, 4/9 (44.4%) were at MII using the improved selection method vs. 6/32 (18.8%) that were at MII from the total oocyte population evaluated (Table 3.14 and Fig. 3.30). The mean fluorescence values for the unfertilized group are graphed to exemplify fluorescent differences within the population (Fig. 3.31).

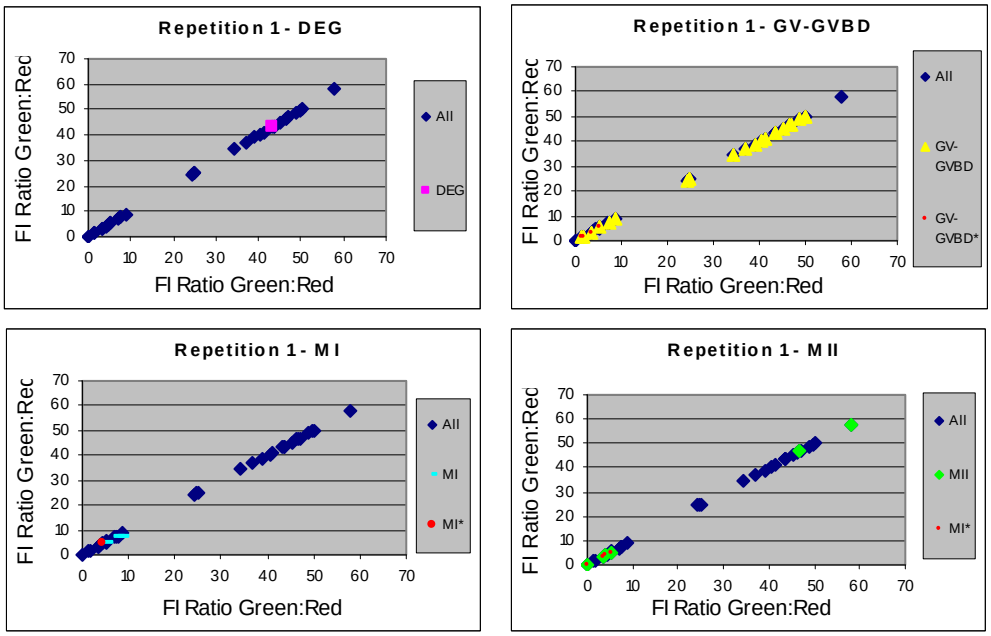

*Denotes oocytes selected using improved method

Fig. 3.30. Relationships between FI and meiotic stages of *unfertilized* canine oocytes imaged using multiphoton microscopy with JC-1.

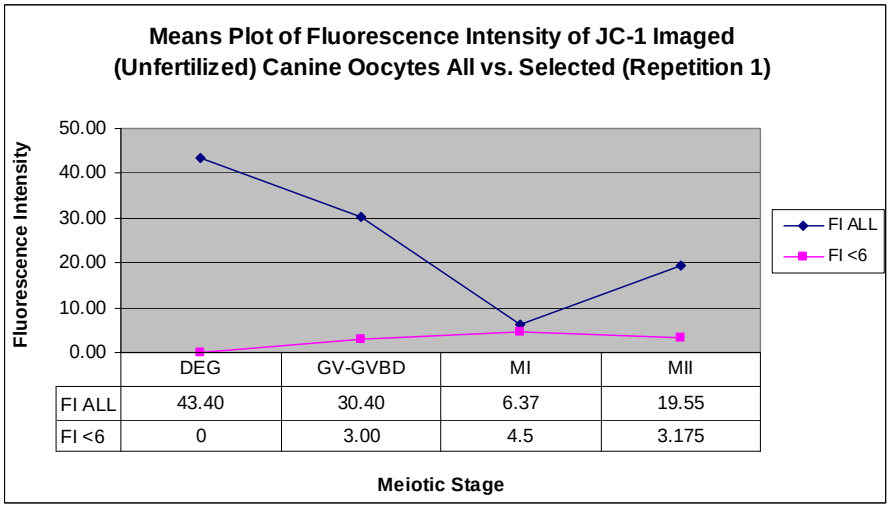

	DEG	GV-GVBD	MI	MII
FI ALL	43.40	30.40	6.37	19.55
FI <6	0	3.00	4.5	3.175

Fig. 3.31. FI means for canine oocytes imaged using multiphoton microscopy with JC-1 (unfertilized).

.

Table 3.12. Average Fluorescence Values for Canine Oocytes Imaged Using Multiphoton Microscopy with the Ratiometric Mitochondria Probe, JC-1 (Unfertilized, Rep. 1).

Grade	(n)	(n) FI ≤ 6 (% of Total/ % of Grade)	Avg. Value (All)	Avg. Value (n≤6)	Range (All)
DEG	1	0 (0.0)	43.4	0	43.4
GV-GVBD	22	4 (44.4/18.2)	30.4	3.0	1.5-50.2
MI	3	1 (11.1/33.3)	6.4	4.5	4.5-7.6
MII	6	4 (44.4/66.7)	19.6	3.2	0.0-58.0
Total	**32**	**9 (28.1)**			

Table 3.13. Average Fluorescence Values for Canine Oocytes Imaged Using Multiphoton Microscopy with the Ratiometric Mitochondria Probe, JC-1. and Fertilized In vitro Using Frozen Canine Semen Concentrated at 2 X 10^6 (Repetition 2), Frozen Canine Semen Concentrated at 5 X 10^6 (Repetition 3), Fresh Collected, Extended Canine Semen Concentrated at 5 X 10^6 (Repetition 4).

	Repetition 2					Repetition 3				
Grade	**(n) % Total**	**(n) Fl ≤ 6 (% of Total/ % of Grade)**	**Avg. Fluor. Value (All)**	**Avg. Fluor. Value (n≤6)**	**Range (All)**	**(n)**	**(n) Fl ≤ 6 (% of Total/ % of Grade)**	**Avg. Fluor. Value (All)**	**Avg. Fluor. Value (n≤6)**	**Range (All)**
DEG	8 (17.0)	3 (10.3/37.5)	36.8	4.8	2.8-63.9	15 (32.6)	3 (13.0/20.0)	32.4	3	0.8-46.2
GV-GVBD	23 (48.9)	17 (58.6/73.9)	5.6	4.7	2.5-12.5	21 (45.7)	11 (48-52.)	17.5	11	1.1-41.2
MI	5 (10.6)	4 (13.8/80)	5.3	4.8	4.0-7.0	2 (4.3)	1 (4.4/50)	16	1	3.9-28.1
MII	11 (23.4)	5 (17.2/45.5)	7.0	3.3	0.0-13.4	7 (15.2)	7 (30/100)	2.7	7	0.0-5.8
Fert.	0 (0.0)	0 (0/0)	0	0	0	1 (2.2)	1 (4.3/100)	2.3	1	2.3
Cleav.	0 (0.0)	0 (0.0/0.0)	0	0	0	0 (0.0)	0 (0.0/0.0)	0.0	0	0
Total	**47**	**29 (61.7)**				**46**	**23 (50.0)**			

Table 3.13 (cont.).

Repetition 4					
Grade	**(n)**	**(n) FI ≤ 6 (% of Total/ % of Grade)**	**Avg. Fluor. Value (All)**	**Avg. Fluor. Value (n≤6)**	**Range (All)**
DEG	10 (25.6)	1 (4.3/10)	23.5	4	4.0-34.2
GV-GVBD	13 (33.3)	7 (30.4/53.9)	9.1	2.5	1.1-24.8
MI	2 (5.1)	2 (8.7/100)	3.0	3	2.8-3.2
MII	8 (20.5)	8 (34.8/100)	2.8	2.8	1.4-5.1
Fertilized	5 (12.8)	5 (21.8/100)	3.0	3	1.9-4.7
Cleaved	1 (2.6)	0 (0.0/0.0)	6.3	0	6.3
Total	**39**	**23 (50.0)**			

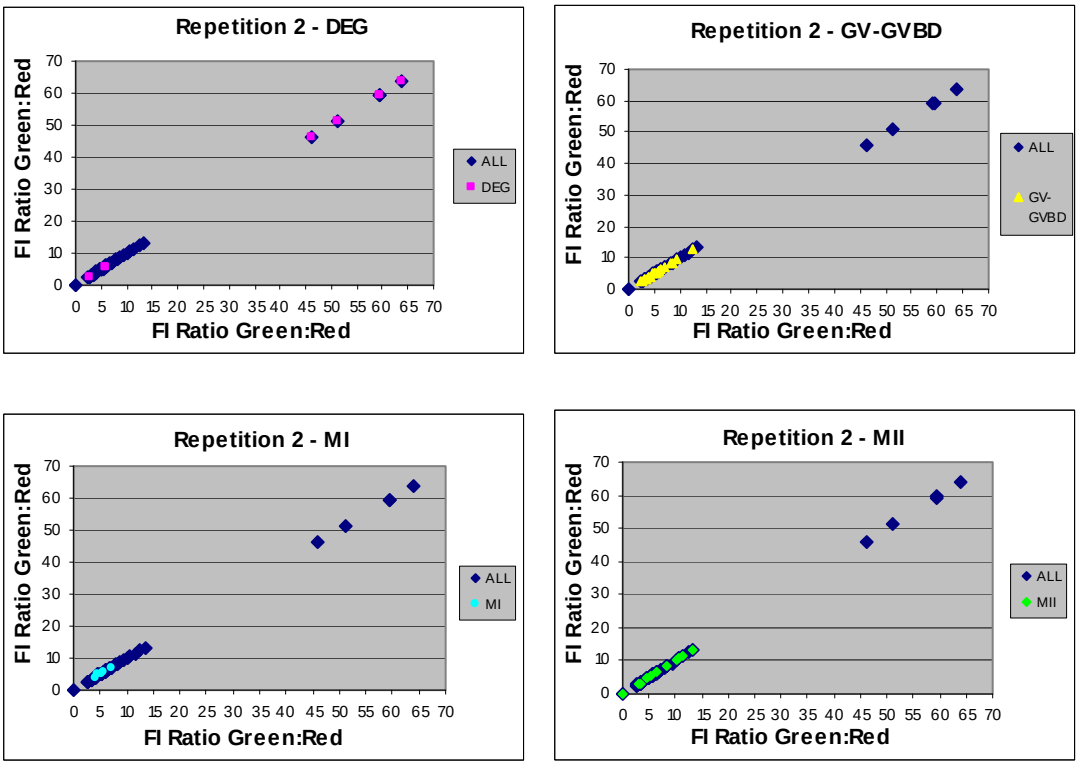

Fig. 3.32. Relationships between FI and meiotic stages of canine oocytes imaged using multiphoton microscopy with JC-1 and fertilized with frozen semen at $2x10^6$/ml (repetition 2).

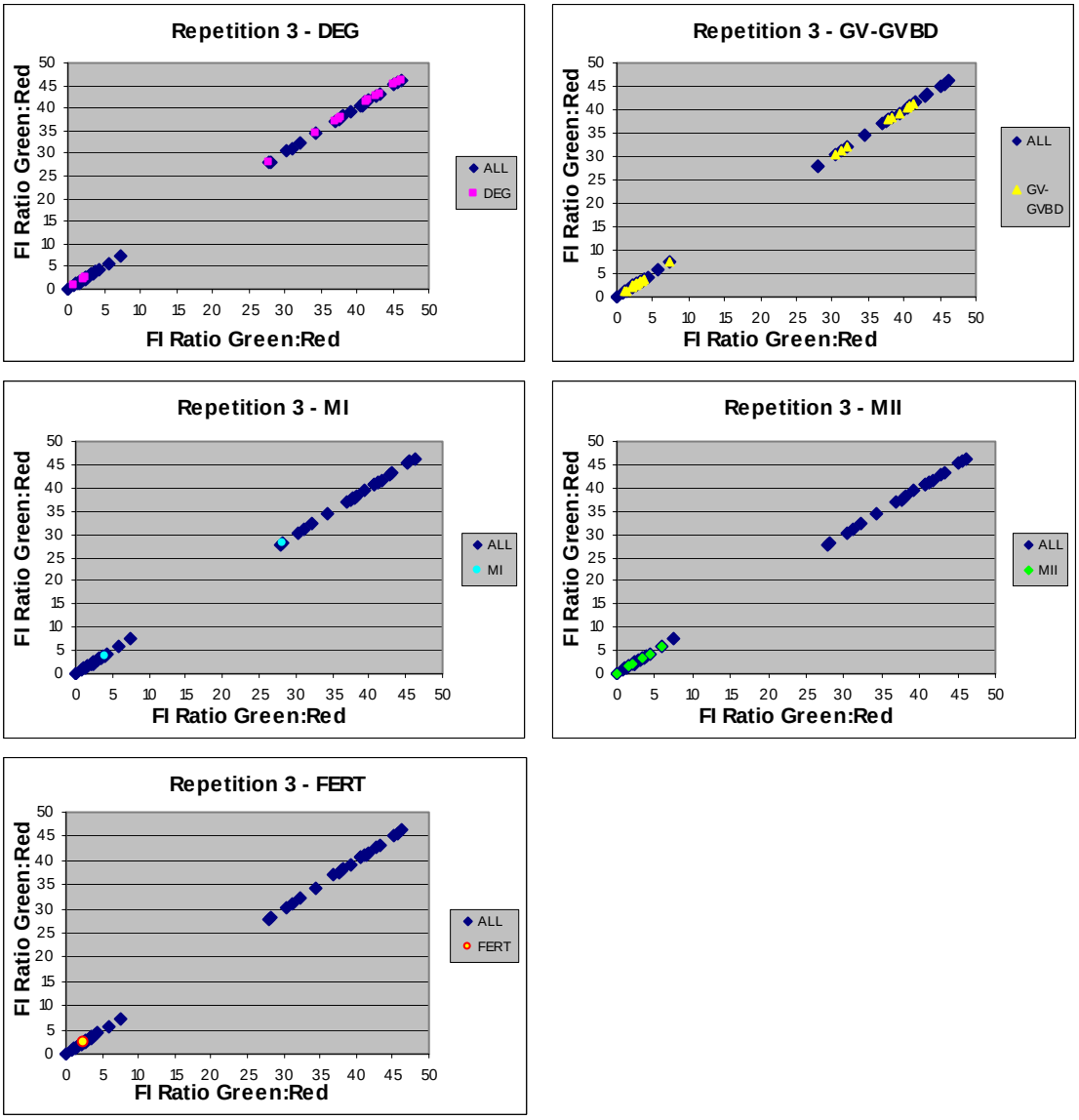

Fig. 3.33. Relationships between FI and meiotic stages of canine oocytes imaged using multiphoton microscopy with JC-1 and fertilized with frozen semen at $5x10^6$/ml (repetition 3).

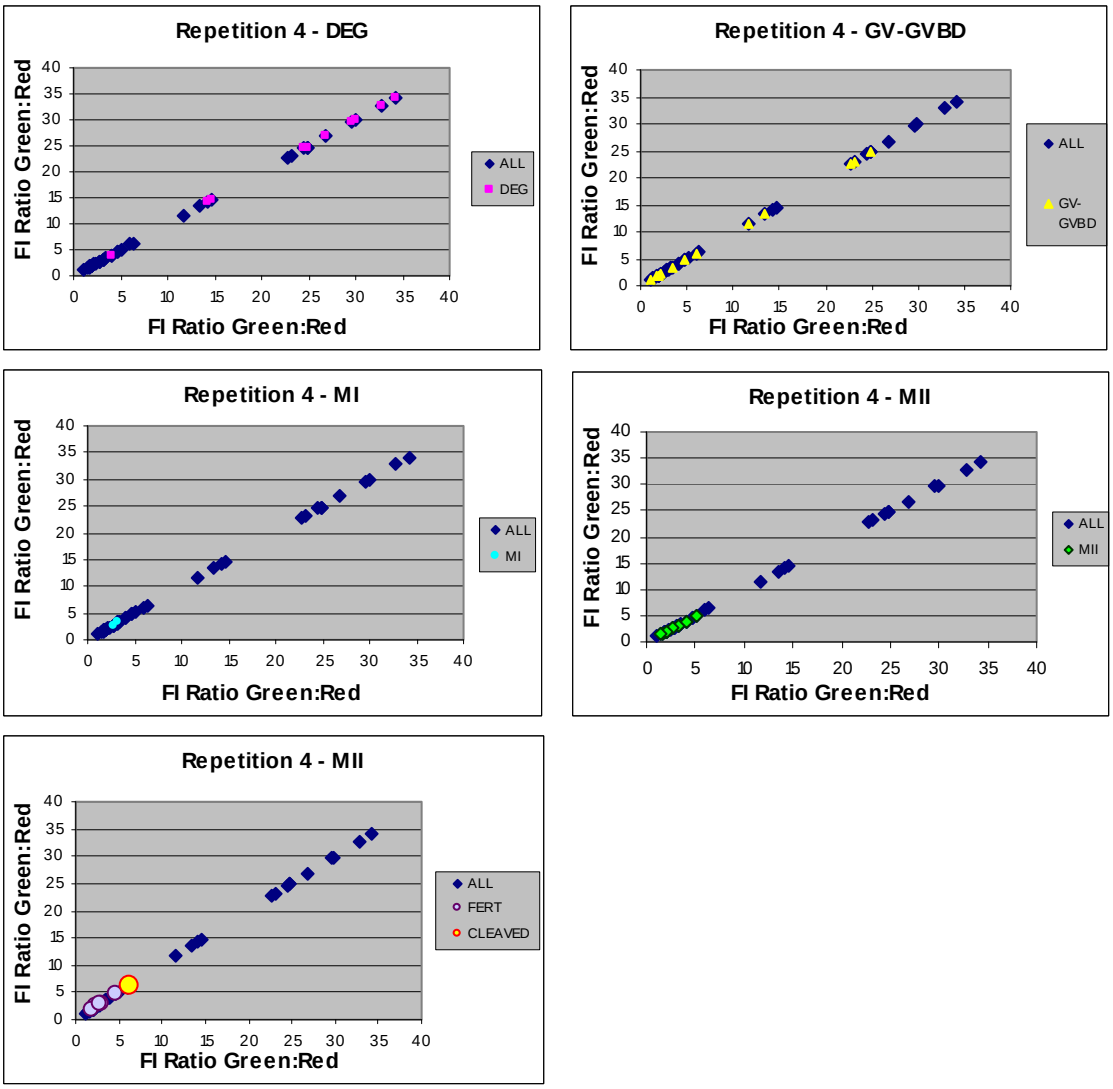

Fig. 3.34. Relationships between FI and meiotic stages of canine oocytes imaged using multiphoton microscopy with JC-1 and fertilized with fresh, extended semen at $5x10^6$/ml (repetition 4).

Using the same method of selection followed by fertilization, 29/47 (62%), 23/46 (57%) and 23/39 (59%) oocytes were pre-selected using the improved method and of these, 5/29 (17%), 7/23 (30%) and 8/23 (35%) were at MII vs. 11/47 (23%), 7/46 (15%) and 8/39 (21%) that were at MII from the total population evaluated and not pre-selected from repetitions 2, 3 and 4, respectively (Tables 3.15, 3.16 & 3.17). In addition, 1/23 (4.0%) and 5/23 (21.7%) oocytes with average fluorescent values $\leq$6 fertilized from repetitions 3 and 4, respectively, (Fig. 3.35a) and one cleaved to 4-cell stage (FI = 6.3) (repetition 4), although the DNA of the cleaved embryo appeared to be degenerating at the time of removal from culture (Fig. 3.35b). Thus, the pre-selection of canine MII oocytes, has the potential to improve the overall efficiency of predicted competency from 15.2-23% (MII/total population) to 17-44.4% (MII/total pre-selected population) and subsequently improving the selection of MII oocytes, including those competent to undergo fertilization.

From these combined, informative data, a potential improvement in the overall efficiency of canine oocyte selection of 51.2% (84/164; pre-selected/total) using the improved method of oocyte selection is possible when labeled with JC-1 and imaged using multiphoton microscopy. Moreover, a potential improvement in the efficiency of canine MII oocyte selection (including oocytes competent to undergo fertilization and/or cleavage) of 18.8% (23/32; improved/total of MII FERT & CLEAVED, respectively) is possible using the improved method. Furthermore, we report a collective reduction in the number

of oocytes needed for experimentation by 43.2% using this improved method of image analysis. Lastly, in both the unfertilized and fertilized groups, a distinct pattern in fluorescence intensity of the population was revealed whereby an absence of oocytes existed with FI's ranging from 0.0-8.8 then 24.0-58.0 for the unfertilized group and 0.0-14.6 to 22.7-63.9 for the fertilized groups (Fig. 3.30, 3.32, 3.33 & 3.34). The portion of oocytes with FI >24 were either degenerating (DEG) or in the GV- GVBD stage, with exception of one MI stage canine oocyte that had an FI of 28.1.

In vitro maturation and fertilization percentages of JC-1 labeled and imaged versus non-imaged versus labeled only oocytes are presented in Tables 3.14, 3.15, 3.16 & 3.17 and Fig. 3.36, 3.37, 3.38 & 3.39. Lastly, the loading of fluorescent probe to the labeled only group appears to have no effect on the meiotic status in canines.

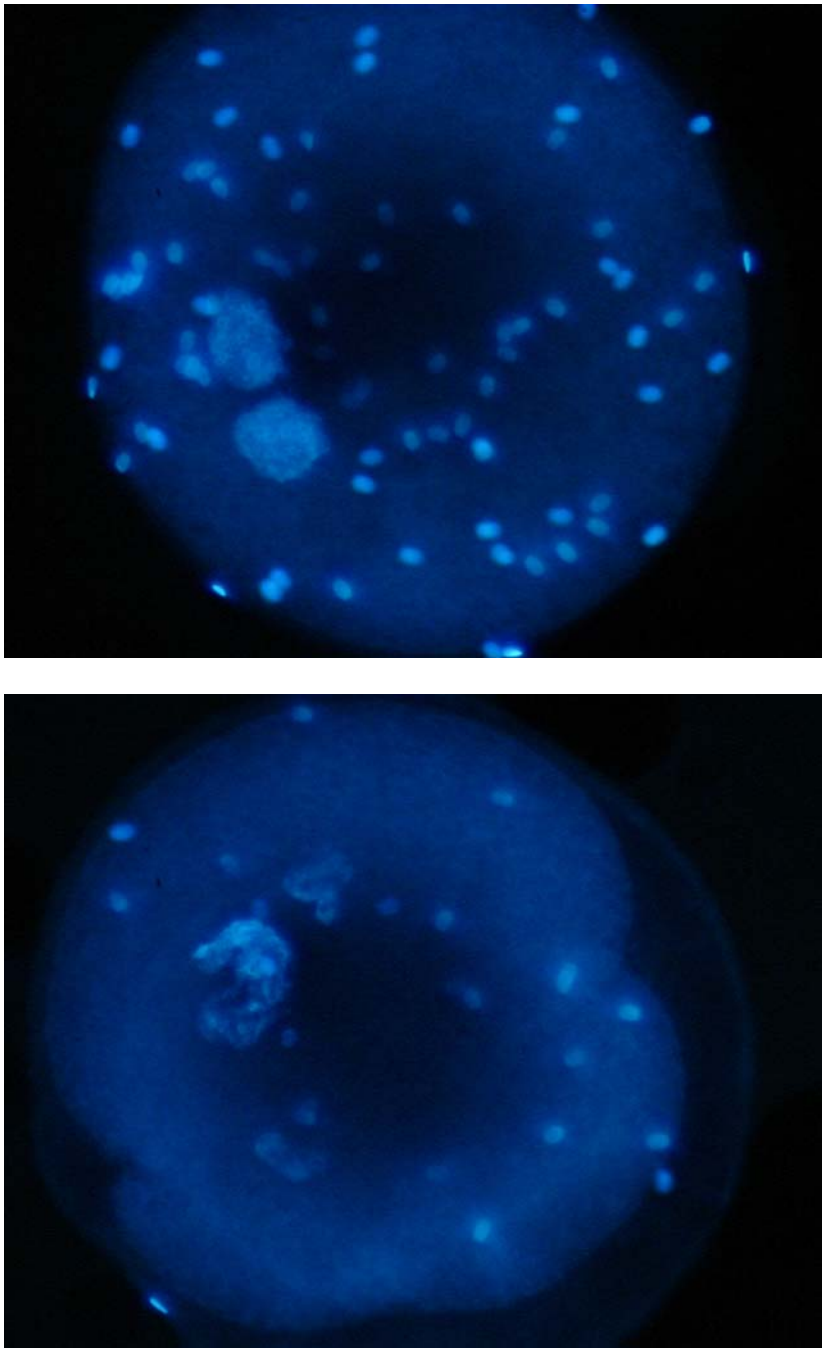

Fig. 3.35. Canine fertilized oocyte (a) and 4-cell embryo (b) fixed and stained with Hoeschst 33342 following imaging using multiphoton microscopy with JC-1.

Table 3.14. In vitro Maturation of Non-imaged and Multiphoton Microscopy Imaged Canine Oocytes Labeled with the Ratio Metric Probe JC-1 Compared with Labeled Only Cultures of Untreated Oocytes (Unfertilized, Rep. 1).

Stage	Imaged n (%)	Non-Imaged n (%)	Labeled Only n (%)
DEG	1 (3.1)	2 (7.1)	3 (9.7)
GV-GVBD	22 (68.8)	18 (64.3)	18 (58.1)
MI	3 (9.4)	4 (14.3)	7 (22.6)
MII	6 (18.8)	4 (14.3)	3 (9.7)
Total	**32**	**28**	**31**

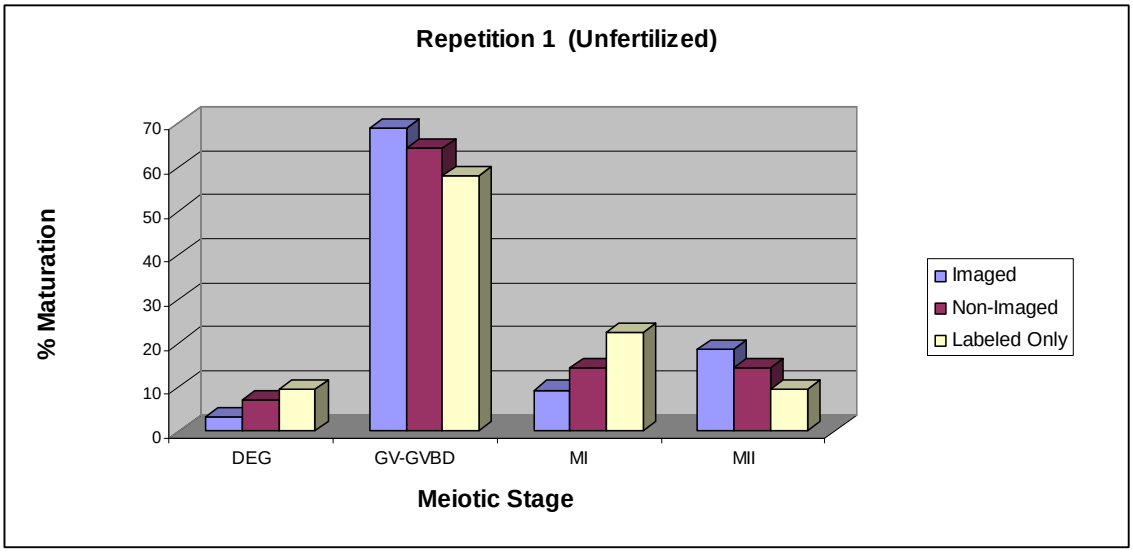

Fig. 3.36. In vitro maturation of canine oocytes imaged using multiphoton microscopy with JC-1 compared with non-imaged and bulk cultured oocytes (unfertilized, Rep. 1).

Table 3.15. In vitro Maturation of Non-imaged and Multiphoton Microscopy Imaged Canine Oocytes Labeled with the Ratio Metric Probe JC-1 Compared with Labeled Only Cultures of Untreated Oocytes (Fertilized, Rep. 2).

Stage	Imaged n (%)	Non-Imaged n (%)	Labeled Only n (%)
DEG	8 (17.0)	22 (45.6)	9 (23.7)
GV-GVBD	23 (48.9)	18 (37.5)	19 (50)
MI	5 (10.6)	3 (6.3)	5 (13.2)
MII	11 (23.4)	5 (10.42)	5 (13.2)
Fertilized	0 (0)	0 (0.0)	0 (0.0)
Cleaved	0 (0.0)	0 (0.0)	0 (0.0)
Total	**47**	**48**	**38**

Lower- case superscripts indicate significant differences in same column;
Upper-case superscripts indicate significant differences between columns (P<0.05)

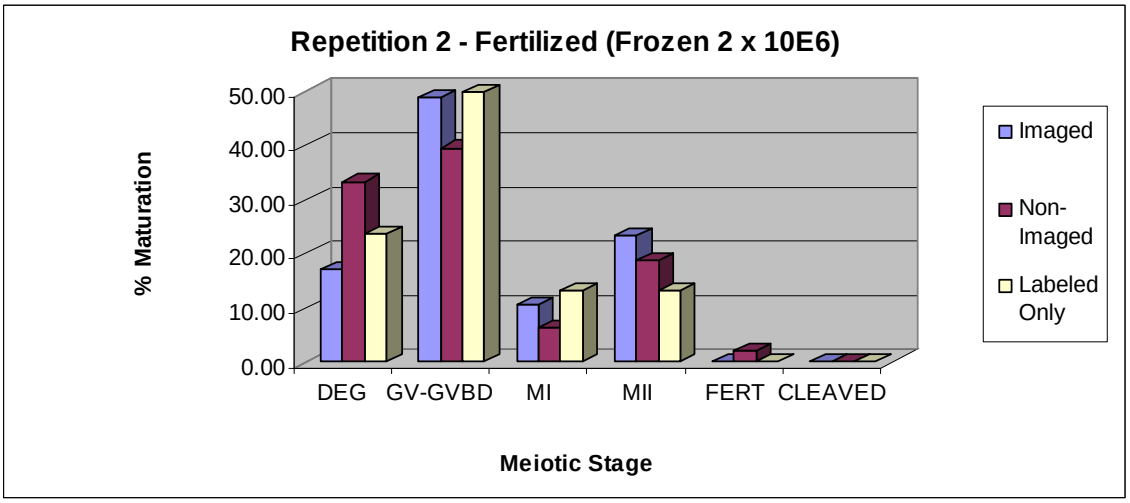

Fig. 3.37. In vitro maturation of canine oocytes imaged using multiphoton microscopy with JC-1 compared with non-imaged and labeled only cultured oocytes followed by IVF using frozen semen at 2 x 10^6/ml (Rep. 2).

Table 3.16. In vitro Maturation of Non-imaged and Multiphoton Microscopy Imaged Canine Oocytes Labeled with the Ratio Metric Probe JC-1 Compared with Labeled Only Cultures of Untreated Oocytes (Fertilized, Rep. 3).

Stage	Imaged n (%)	Non-Imaged n (%)	Labeled Only n (%)
DEG	22 (45.8)	22 (45.6)	15 (40.5)
GV-GVBD	18 (37.5)	18 (37.5)	14 (37.8)
MI	3 (6.3)	3 (6.3)	2 (5.4)
MII	5 (10.4)	5 (10.42)	5 (13.5)
Fertilized	0 (0)	0 (0.0)	1 (2.7)
Cleaved	0 (0.0)	0 (0.0)	0 (0.0)
Total	**48**	**48**	**38**

Lower- case superscripts indicate significant differences in same column;
Upper-case superscripts indicate significant differences between columns (P<0.05)

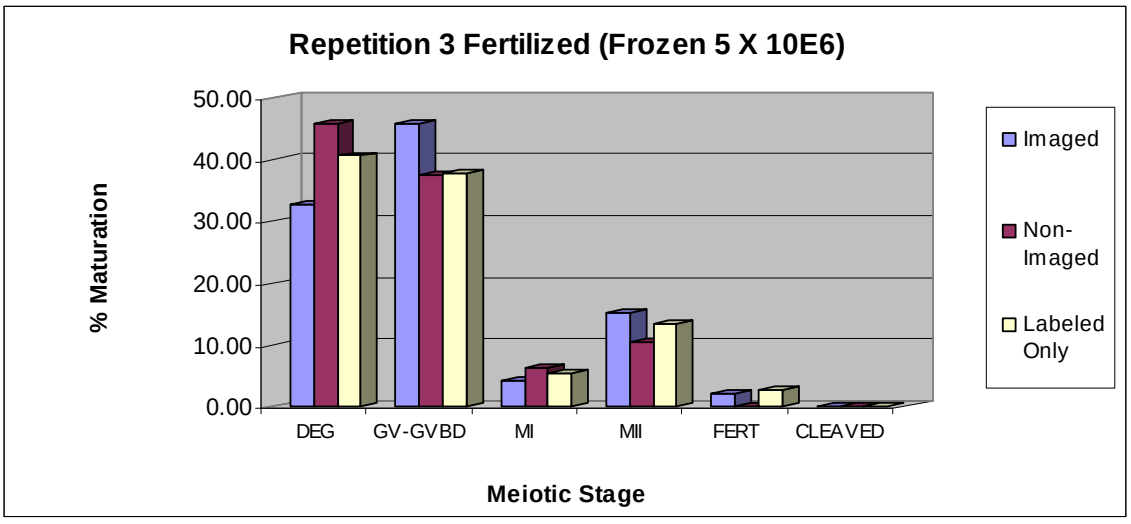

Fig. 3.38. In vitro maturation of canine oocytes imaged using multiphoton microscopy with JC-1 compared with non-imaged and bulk cultured oocytes followed by IVF using frozen semen at 5 x 10^6/ml (Rep. 3).

Table 3.17. In vitro Maturation of Non-imaged and Multiphoton Microscopy Imaged Canine Oocytes Labeled with the Ratio Metric Probe JC-1 Compared with Labeled Only Cultures of Untreated Oocytes (Fertilized, Rep. 4).

Stage	Imaged n (%)	Non-Imaged n (%)	Labeled Only n (%)
DEG	10 (25.6)	12 (30.0)	13 (32.5)
GV-GVBD	13 (33.3)	13 (32.5)	12 (30)
MI	2 (5.13)	2 (5.0)	3 (7.5)
MII	8 (20.5)	10 (25.0)	9 (13.2)
Fertilized	5 (12.8)	3 (7.5)	3 (7.5)
Cleaved	1 (2.6)	0 (0.0)	0 (0.0)
Total	**39**	**40**	**40**

Lower- case superscripts indicate significant differences in same column;
Upper-case superscripts indicate significant differences between columns (P<0.05)

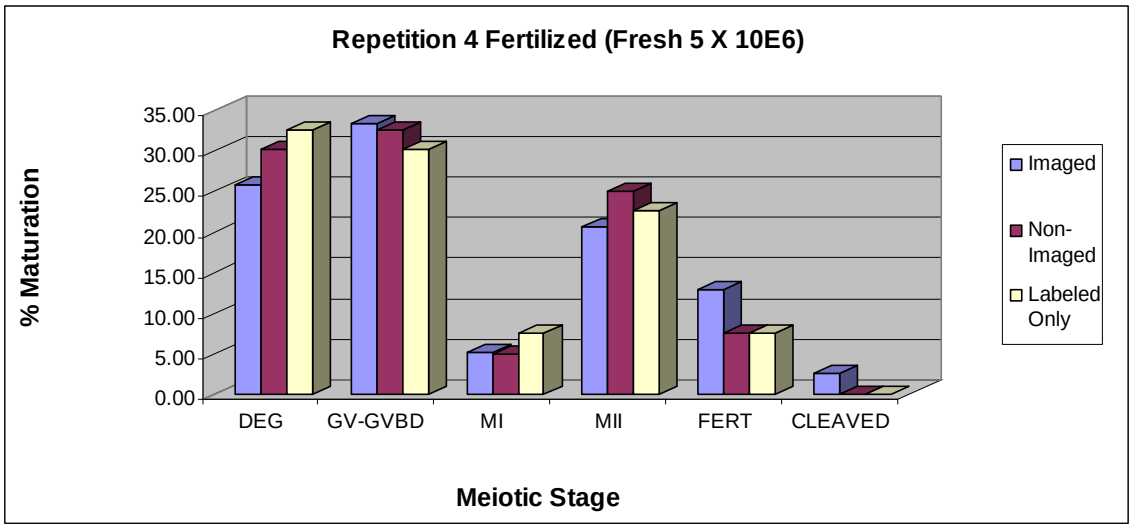

Fig. 3.39. In vitro maturation of canine oocytes imaged using multiphoton microscopy with JC-1 compared with non-imaged and bulk cultured oocytes followed by IVF using fresh-collected semen at 5 x 10^6/ml (Rep. 4).

CHAPTER IV

DISCUSSION AND SUMMARY

Traditionally, the prediction of oocyte competency for in vitro studies and/or ART has been defined by morphological parameters using light microscopy (Wurth and Kruip, 1992; Gandolfi *et al.,* 1997). While these guidelines are useful for sorting, the efficiency of selecting oocytes that have achieved successful cytoplasmic, nuclear, and molecular maturation, and are competent to undergo successful fertilization, ultimately producing live, healthy offspring is inefficient. This deficit is complicated by the unknown parameters surrounding oocyte competency that cannot be identified from a morphological assessment, as well as the highly variable interpretation of the grading criteria by each scientist. The overall aim of this study was to non-invasively identify specific molecular markers within the oocyte that correspond to the achievement of embryonic development to the blastocyst stage using fluorescent molecular probes known to be “cell friendly,” or natural, inherent fluorescence, combined with advanced imaging technology and analysis wherein the bovine was used as a model system for the development of techniques for application to canine oocytes. To our knowledge, this is the first report of implementing an image analysis system and multiphoton microscopy to evaluate mammalian oocytes for the potential prediction of competency.

4.1 Experiment I - Characterization of the spatial distribution of mitochondria and mitochondrial activity and intracellular Ca^{2+} stores in relation to grade of in vitro matured bovine oocytes as they relate to morphology, and establishment of baseline criteria of functional parameters for oocyte selection

4.1.1 Characterization of the spatial distribution of mitochondria and mitochondrial activity in relation to grade of IVM bovine oocytes

Mitochondrial metabolic activity and function within mammalian oocytes and embryos has only recently been investigated, specifically for the mouse and human (Squirrell *et al.,* 1999; Van Blerkom *et al.,* 2002; 2003; Van Blerkom 2006, 2008). Previous investigations of oocyte mitochondria have been limited to the various structural aspects of this dynamic organelle during oocyte and embryo development (Batten *et al.,* 1987; Hyttel et al, 1990; Van Blerkom 1991; Van Blerkom *et al.,* 1995; Hyttel *et al.,* 1997). However, studies in the last decade have determined that mitochondria have a complex central function that exceeds the historical dogma of this organelle as simply being the “power house” of the cell. Research has shown that mitochondria also contribute to redox and intracellular Ca^{2+} homeostasis, provide intermediary metabolites and store proapoptotic factors (Reviewed by Dummolard *et al.,* 2007). As specifically related to the oocyte, studies conducted in the mouse, human and cattle have defined particular attributes of mitochondria that include cytoplasmic

localization and membrane potential, heterogeneity of mitochondria membrane potential, [ATP], polarity of mitochondria, mtDNA complement number and Ca^{2+}-induced Ca^{2+}-release (CICR) from mitochondria of oocytes and embryos, all of which have been related to oocyte competency (Bavister and Squirrell, 2000; Van Blerkom, 2008). Thus, the organization of mitochondria into specialized areas of metabolic need (i.e., “microzones”) in a transient fashion to meet the direct demands of cytoplasmic orderliness and regulation are likely more significantly related to oocyte competency than simply the production of ATP (Dumollard *et al.,* 2007; VanBlerkom, 2008).

Localization of mitochondria within the mammalian oocyte is stage specific with respect to the meiotic cell cycle; mitochondria undergo cytoplasmic remodeling by translocating to cytoplasmic areas with changes in energy demands or a required alteration in density (VanBlerkom, 2002). In the human, mouse, and pig, mitochondria are more densely populated around the nucleus during the GV stage and gradually translocate to the cortical and peri-cortical regions of the cytoplasm as the oocyte resumes meiosis and progresses to the MII stage (Van Blerkom *et al.,* 2002; Van Blerkom, 2008). This study focused on the localization and activity of mitochondria within MII stage bovine and canine oocytes and no attempt to quantify $\Delta\psi m$ or relate this parameter to developmental competence was performed. However, results obtained are consistent with other studies reported for mouse, human and pig with respect to the localization of mitochondria and the heterogeneity of depolarized and

hyperpolarized mitochondria that are primarily localized to the cortical and peri-cortical regions of the ooplasm in MII stage bovine IVM oocytes (VanBlerkom *et al.,* 2002).

Research by Van Blerkom *et al.,* (2002) first reported the presence of a heterogeneous population of depolarizing and hyperpolarized mitochondria within mouse and human oocytes and proposed that the presence of hyperpolarized mitochondria in the peri-cortical region of the ooplasm may be related to the acquisition of oocyte competence as well as the regulation of early developmental processes. More specifically, the compartmentalization of mitochondria into microzones could represent a functional aspect of the specific spatial ATP requirements of the oocyte and early embryo as indicated by the fertilization and cortical granule exocytosis being restricted to regions of the plasma membrane that correspond with highly polarized mitochondria in the mouse (VanBlerkom and Davis, 2007). Further, it has been hypothesized that mitochondrial compartmentalization may also participate in the regulation of free Ca^{2+} concentration within the cytoplasm due to the ability of mitochondria to release Ca^{2+} in response to external ionic Ca^{2+} influxes (CICR*)* and electrical signals associated with the molecular events surrounding fertilization (Gunter *et al.,* 2004; Boni *et al.,* 2007; VanBlerkom, 2008).

Further, studies described here attempted to identify relationships between oocyte morphology (as defined by SF/AFI or FI) using light microscopy, and mitochondrial localization and function via multiphoton microscopy.

Evaluation of two different molecular probes for mitochondrial localization and function (rhodamine 123 and JC-1) did not identify any obvious, distinct fluorescent patterns that would help to classify any particular oocyte as belonging to a specific morphological grade for either species. To the contrary, several bovine G3 oocytes and canine DEG oocytes had a higher ratio of green:red fluorescence intensity using JC-1 wherein the mitochondria exhibited very concentrated areas of labeling and appeared in a more diffuse localized pattern as compared to oocytes from other grades. Historically, JC-1 has also been used to evaluate apoptosis in living cells wherein a higher ratio of green:red fluorescence is indicative of low $\Delta\psi$m levels of depolarization within dying cells (Troiano *et al.,* 2007). Although, this study did not investigate the use of JC-1 to evaluate apoptosis within the bovine oocyte, this pattern of intense fluorescence within the poor-quality oocytes is likely to be indicative of early stages of apoptotic or necrotic cell death pathways.

Evaluation of the fluorescence intensity of both mitochondrial probes revealed relationships between the morphological characteristics (SF) of the bovine oocyte and mitochondrial activity using multiphoton microscopy. For both probes, G2 and G3 oocytes were distributed throughout the curve (Fig. 3.2 & 3.5), while G1 oocytes were concentrated in a more narrow range that was consistent with optimal embryo development as discussed below. Lastly, through these experiments it was possible to non-invasively establish baseline

criteria of functional parameters reflective of mitochondrial activity in bovine oocytes.

4.1.2 Characterization of the spatial distribution of free intracellular Ca^{2+} in relation to grade of IVM bovine oocytes

The role of intracellular Ca^{2+} has been well characterized with respect to both oocyte maturation and fertilization in mammals and lower vertebrates (reviewed by Ducibella, 2008). In the oocyte, Ca^{2+} is an essential cation involved in gap junction-mediated intercellular communication between the cumulus cells and the oocyte, which is essential during the resumption of meiosis in the cow and pig (Tosti *et al.,* 2000; Boni *et al.,* 2007). This mode of intercellular communication also allows for the transport of second messengers generated by the cumulus cells that act on the oocyte to trigger Ca^{2+} release from the ER of the oocyte. Ultrastructural studies have established that organelles such as mitochondria, ER and cortical granules, among others, are very concentrated at the cortical regions of MII stage oocytes of mouse, human, cow, and dog, presumably for the Ca^{2+} release at fertilization necessary to induce oocyte activation (Hyttel *et al.,* 1990; Hyttel *et al.,* 1997; reviewed by Van Blerkom 2008; Viaris De Lesegno *et al.,* 2008; and Viaris De Lesegno *et al.,* 2008b). This sperm-oocyte interaction triggers a sharp Ca^{2+} release response and subsequent oscillations, thereby changing the resting potential of the plasma membrane and also increasing the steady-state levels of intracellular

Ca^{2+} within the oocyte. In contrast, sustained elevated levels of intracellular Ca^{2+} have been linked to apoptosis in both mature oocytes and in individual embryo cells (Sergeev and Norman, 2003). Moreover, regulation of intracellular Ca^{2+} levels also involves mitochondria, as this organelle is capable of releasing and sequestering intracellular Ca^{2+} to maintain cellular homeostasis (Tosti *et al.,* 2000; Gunter *et al.,* 2004; Boni *et al.,* 2007).

The implementation of optical microscopy methods for analysis of intracellular Ca^{2+} localization and responses in oocytes and embryos has been primarily limited to laser scanning confocal microscopy, and only recently using more advanced optical systems such as multiphoton laser scanning microscopy in lower order vertibrates (Lee *et al.,* 2004; Fein and Terasaki, 2005; Zhou and Jin, 2007). While the goals of these experiments and others were to better characterize or define a specific functional role for intracellular Ca^{2+}, the aim of the current study was to characterize the spatial distribution of intracellular Ca^{2+} as it relates to morphological grades of bovine oocytes using image analysis and multiphoton microscopy technologies. No attempt was made in these studies to quantify the levels of intracellular Ca^{2+} within the oocyte.

The fluorescence intensity of Ca^{2+}-sensitive probes was either unremarkable or very low and localized to the peri-cortical region of the oocyte as expected considering the localization of ER in the MII stage oocyte and the low levels of free intracellular Ca^{2+} in healthy oocytes. In a few cases, especially in G3 oocytes, small aggregates of fluorescence were observed which are

indicative of concentrated, localized areas of intracellular Ca^{2+}. The observation of minimal fluorescence are consistent with the maintenance of low levels of free intracellular Ca^{2+} in MII stage oocytes prior to fertilization. Higher levels of Fluo-4, AM fluorescence were likely to be associated with unhealthy oocytes which were probably in the early stages of apoptosis. Fluorescence observed in the PVS is likely to reflect the presence of free Ca^{2+} that had escaped the oolema via Ca^{2+} channels or as a result of damage to the plasma membrane.

Further, through experiments using Fluo-4, AM as a Ca^{2+}-sensitive fluorophore, we were able to identify a relationship between oocyte morphology (as defined by SF/AFI) and Fluo-4 fluorescence intensity. Specifically, G2 and G3 oocytes were distributed throughout the curve (Fig. 3.8) whereas G1 oocytes were localized to a particular area of the curve (AFI 20-30) that corresponded with optimal embryo development as discussed below. Lastly, through these experiments we were able to non-invasively establish baseline criteria of functional parameters related to Ca^{2+} homeostasis in bovine oocytes.

4.1.3 Evaluation of embryonic developmental potential of IVM bovine oocytes imaged by multiphoton microscopy and subsequently fertilized in vitro

In order to accomplish the ultimate goal of this project, *to non-invasively identify specific, functional molecular markers as they relate to oocyte competency*, the embryonic developmental potential of each imaged oocyte using the WOW method was evaluated (Vajta *et al.,* 2000). For all three

fluorescent probes (rhodamine 123, JC-1, and Fluo-4, AM), ranges of oocyte fluorescence intensity that were compatible with blastocyst production after IVF were identified which was used to narrow the range of oocytes that were considered competent from the initial populations, regardless of morphological grading criteria. Further, there were no visually obvious differences or patterns in fluorescence intensities among any of the probes used that would characterize any of the oocytes as belonging to a particular grade. Therefore, these data are consistent with others wherein oocyte competency cannot be determined based solely on morphological parameters, nor by patterns of fluorescence intensity characterized by oocyte grade as investigated in the current study.

Moreover, the percentages of embryo development to blastocyst stage were lower than that currently reported in the literature of (~40%) (Longeran and Fair, 2008). We attribute this difference in part to the effects of cumulus cell removal in all oocytes prior to IVF (except the COC Bulk control group). Several studies have shown that removal of cumulus cells prior to IVF decreases embryo development, however, this step was necessary in the current study in order to obtain oocyte-specific information derived from fluorescence probes of cellular function (Fatehi *et al.,* 2002; Luciano *et al.,* 2005; Wongsrikeao *et al.,* 2005; Ge *et al.,* 2008). In contrast, differences in the percentages of embryo development to blastocyst were not statistically significant between any of the WOW cultured groups and the COC Bulk cultured control group. These percentage differences

would suggest that the WOW method for IVF and IVC is an effective method for the production of in vitro derived embryos. Another possible explanation for the decreased development to blastocyst in all groups may be related to the timing of the IVF procedure. All groups were fertilized at the same time, i.e., at the conclusion of our imaging experiments, generally ~2-3 hours post the 24 hour maturation time. Therefore, the delay in the timing of fertilization may be a factor in the overall decline in embryo development. Finally, while this system proved efficient for supporting IVF (not previously reported in the literature), and IVC for bovine embryos, more research is needed to optimize its efficiency in an attempt to improve embryo development.

For oocytes imaged with rhodamine 123, an AFI ranging from 35.0-89.2 was consistent with a combined G1, G2 & G3 blastocyst production to only 4% (6/144). There were no statistically significant differences in blastocyst development between morphological grades. While experiments with rhodamine 123 produced a very low percentage of embryo development, they are representative of initial trials using the WOW method for IVF and IVC and were likely affected by the initial trials using this system for embryo culture versus a traditional micro-drop IVC system in order maintain the individuality of each imaged oocyte. Also, these initial investigations did not implement the use of a co-culture system with cumulus cells as outlined in later experiments. Lastly, there were no differences between the imaged and non-imaged group,

indicating that the exposure of bovine oocytes to rhodamine 123, followed by multiphoton microscopy had no adverse effect on embryo development.

JC-1 imaged bovine oocytes having fluorescence ratios of green:red ranging from 1.25 to 2.25 showed a combined embryo blastocyst development of 16.8% (37/220). In these experiments a relationship between factors linking oocyte morphology (as defined by SF/FI) and mitochondrial fluorescence intensity were identified that defined parameters conducive to optimal embryo development. Although this potential improved efficiency may be interpreted as nominal, further experimentation utilizing these techniques would add value to these data, and are expected to further improve the efficiency of bovine oocyte selection.

For oocytes labeled with Fluo-4, AM and imaged, fluorescence intensities in the range of 20 to 30 were indicative of combined blastocyst development to 15.9% (33/208) among all oocyte grades. A relationship between oocyte morphology (as defined by SF/AFI) and Fluo-4 fluorescence intensity levels was identified by combining image analysis and multiphoton microscopy.

Again, while the potential improved efficiency for bovine oocyte selection may be interpreted as modest for both JC-1 and Fluo-4, AM, further experimentation utilizing these techniques should add value to these data, and is likely to improve the efficiency of bovine oocyte selection, and should also be applicable to the selection of other mammalian oocytes. These experiments and

findings identify a novel method for the evaluation of oocyte competency in the bovine using non-invasive techniques.

4.2 Experiment II – Characterization of the spatial distribution of mitochondria and mitochondrial activity, and intracellular Ca^{2+} stores in relation to morphology of in vitro matured canine oocytes using criteria from Experiment I that could potentially be used to evaluate developmental competence in this species

4.2.1 Characterization of the spatial distribution of mitochondria and mitochondrial activity in relation to meiotic status of IVM canine oocytes

To our knowledge, this is the first report using image analysis and multiphoton microscopy technologies on canine oocytes to study possible connections between oocyte function and morphology on living cells. Historically, efforts at unraveling the mysteries of canine oocyte biology have largely been limited to supplementation of IVM media, and structural studies using both electron microscopy and epifluorescence (Szabo, 1967; Mahi and Yanagimachi, 1976; Hyttel *et al.,* 1990;Yamada *et al.,* 1992; Yamada *et al.,* 1993, Nickson *et al.,* 1993, Hewitt, 1997; Metcalfe, 1999, Otoi *et al.,* 1999, 2000 and 2002; Songsasen *et al.,* 2002; Bolamba *et al.,* 2002; Willingham-Rocky *et al.,* 2002; Rodrigues and Rodrigues, 2003; Songsasen *et al.,* 2003; Willingham-Rocky *et al.,* 2003; Kim *et al.,* 2004; Saint-Dizier M *et al.,* 2004; Viaris De

Lesegno *et al.,* 2008a; Viaris De Lesegno *et al.,* 2008b). However, no significant advances have been made toward improving in vitro maturation to the MII stage. An aim of this investigtion was to apply the knowledge developed from the multiphoton fluorescence imaging of bovine oocytes to canine oocytes in order to conduct similar characterization of functional endpoints including the spatial distribution of mitochondria, $\Delta\psi m$, and intracellular Ca^{2+} in oocytes and to use this information to establish criteria for oocyte selection.

Localization of mitochondria in the MII canine oocyte revealed a similar pattern to that reported for other mammalian species indicating active mitochondrial localized to the peri- and sub-cortical regions of the oocyte. For rhodamine 123, labeling was primarily in the peri-cortical area, closest to the oolema of the canine oocyte, whereas for bovine, mitochondria appeared to have a more dispersed localization throughout the ooplasm, with more concentrated areas at the peri-and sub-cortical regions. When labeled with JC-1, canine MI and MII oocytes fluoresced in a similar pattern as bovine MII stage oocytes, indicating concentrated areas of mitochondrial activity in the peri-cortical regions of the oocyte. DEG and GV-GVBD oocytes labeled with JC-1 had higher ratios of green:red fluorescence which is indicative of early oocyte apoptosis. While labeling for both mitochondrial probes revealed similar areas of localized fluorescence compared to that of bovine, the fluorescence intensity was not as distinctly visualized in the non-cortical regions of the oocyte. According to ultrastructural studies in the IVM canine oocyte as described below,

mitochondria are distributed throughout the cytoplasm and more are concentrated in the peri- and sub-cortical regions. Therefore, it is not possible to rule out the prospect that the abundant and concentrated lipid stores in the canine oocyte may potentially mask the ability to detect the total mitochondrial fluorescence signal within oocytes of this species.

Of particular interest in the current study was the unusual level of hyperpolarized mitochondria within the 1PB of the canine MII oocyte, as compared to those reported for the mouse and human, as well as in this investigation of bovine oocytes. For canine oocytes, mitochondria in the 1PB fluoresced primarily in the RITC channel, with very minimal fluorescence (if any) in the FITC channel, indicating mitochondrial hyperpolarization, unlike that reported for mouse and human, or as observed in the bovine from this study. Moreover, the integrity of the 1PB (when in the field of view) was often compromised or appeared fragmented and/or irregularly shaped as compared to that observed for bovine oocytes. While the significance of these findings is unclear, the morphological integrity of the 1PB may be related to a combination of compromising factors such as oocyte source (estrous cycle stage, age of bitch, and general health/nutrition, etc.), handling (poorly defined ovary transport and oocyte collection protocols, etc.) and/or a poorly defined IVM protocol for this species.

The spatial distribution of hyperpolarized mitochondria function to provide ATP within the oocyte in areas of high metabolic need, however, little is known

about mitochondrial function in the polar body. Furthermore, aside from its morphology, ultrastructural organization, utility for preimplantation genetic diagnosis and potential cloning applications, the 1PB in general has received negligible attention (Gitlin, 2003). Moreover, the relationship between 1PB morphology and embryo development is controversial but is believed to be an indicator of both postovulatory age of the oocyte and synchrony between nuclear and cytoplasmic maturation (Ciotti *et al.,* 2004).

Recent ultrastructurel studies of canine in vivo matured oocytes reported that after the LH surge, mitochondria undergo massive replication, and after ovulation, they remain quite numerous and homogenously distributed (Viaris De Lesegno *et al.,* 2008a). After meiotic resumption and achievement of MII stage, the cytoplasm of the oocyte is primarily composed of mitochondria and smooth endoplasmic reticulum (SER) that are homogenously distributed between lipid droplets. Therefore, in the canine oocyte at final maturation in vivo, the association of SER/mitochondria and SER/lipid droplet is much more organized than has been observed in oocytes of other mammals. Further, cytoplasmic maturation of the canine oocyte involves very extensive reconstruction at final maturation as compared to late follicle stages suggesting that canine oocytes obtained from late follicle stages may be more immature than that reported for other species which may account for the difficulty in achieving successful maturation in vitro (Viaris De Lesegno *et al.,* 2008a). Ultrastructural studies of in vitro matured canine oocytes performed by the same investigators revealed an

accumulation of mitochondria in the cytoplasm beginning at the MI stage that were primarily localized to the cortical regions of the ooplasm. This pattern remained consistent through the progression to MII, with more intense accumulation of mitochondria localized to the cortical region (Viaris De Lesegno *et al.,* 2008b).

Consequently, considering the extensive accumulation of mitochondria during final maturation, the concentrated cortical localization of mitochondria during MII of IVM, and the highly concentrated lipid content in the canine oocyte, the metabolic demands of mitochondrial function and ATP synthesis may be greater in the canine than in other species in preparation for fertilization. Furthermore, the observation of hyperpolarized mitochondria in the 1PB may be a consequence of the metabolic demands related to the extrusion of the 1PB since it is generated from the same spatial location, or may be a consequence of the abundance of hyperpolarized mitochondria just beneath the oolema. However, future studies are required to confirm this hypothesis.

As a consequence of the investigations performed in this dissertation, it was possible to implement the use of a novel selection method for canine oocytes using the JC-1 mitochondrial probe that further narrowed the parameters necessary for efficiently selecting oocytes that were deemed competent to achieve fertilization and cleavage. From these combined data, a potential improvement in the overall efficiency of canine oocyte selection by 63.6% (84/132; pre-selected/total) was obtained using the improved method of

oocyte selection. Moreover, it was possible to predict a potential improvement in the efficiency of canine MI and MII oocyte selection (including oocytes competent to undergo fertilization and/or cleavage) by 31% (29/42; improved/total of MI, MII, FERT & CLEAVED, respectively) using these improved methods. Furthermore, a collective reduction in the number of oocytes needed for experimentation by 43.2% was obtained using this improved method combining image analysis and multiphoton microscopy of JC-1-labeled canine oocytes.

4.2.2 Characterization of the spatial distribution of free intracellular Ca^{2+} in relation to grade of IVM canine oocytes

Analysis of intracellular Ca^{2+} in canine oocytes provided similar results to that reported for bovine oocytes in this investigation. Again, a relationship was identified between oocyte morphology (as defined by SF/AFI) and Fluo-4 fluorescence intensity that indicates a range for MI and MII canine oocyte selection of 20-25.5. With these data, the efficiency of selection of MI and MII canine oocytes can potentially be improved by 32.2%, while also potentially

eliminating almost 50% of the oocyte population collected and subjected to IVM that would have been identified as unsuitable.

Although the localization of Fluo-4 fluorescence was primarily observed in the peri-cortical region and exhibited a uniform distribution in MI and MII oocytes with comparable AFI's to that observed in bovine oocytes, the fluorescence intensity of canine oocytes in the DEG and/or GV-GVBD meiotic stages was more intense and exhibited localized accumulation of free intracellular Ca^{2+} in the peri-and sub-cortical regions of the ooplasm, that were interpreted as associated with early events of apoptosis and/or cell death. Also, both DEG and GV-GVBD grades had oocytes distributed throughout the curve (Fig. 3.28), whereas MI and MII oocytes were primarily confined to the lower end of the curve, and within the predicted range of potential optimal selection efficiency. Finally, considering the many insufficiencies related to selection of high quality canine oocytes and successful IVM, this technique could prove useful for optimizing oocyte selection and resources for in vitro studies.

CHAPTER V

CONCLUSIONS

The ultimate test of oocyte competency from in vitro studies is the successful maturation, fertilization, embryo development, implantation, gestation and finally, birth of live, healthy offspring. For in vitro studies, the achievement of successful outcomes at each of these developmental stages is sensitive and can be problematic, due to the number of physiological events in oocyte maturation that remain unknown. In this investigation, additional details related to oocyte selection have been developed that may provide a means to non-invasively increase the efficiency of identifying oocytes with a range of predicted competency for the bovine. Further, knowledge derived from analysis of bovine oocytes has been applied to the canine oocytes in which physiological processes related to oocyte development and maturation remains relatively unexplored (as compared to human, rodents and other domestic mammals), and has only recently been aggressively investigated. Here, baseline data related to functional endpoints of cellular function were identified using 3 different fluorescence probes that provided the potential to improve oocyte selection criteria. Further, application of the WOW system that was originally designed for IVC of embryos, was adapted for IVF with successful outcomes for both bovine and canine oocytes.

In conclusion, the primary objective of these investigations was accomplished, i.e., *to non-invasively identify specific, functional molecular markers that may relate to oocyte competency.* While additional improvements to the techniques described herein will be necessary to better optimize this experimental approach, future development of image analysis and multiphoton microscopy could significantly advance the area of oocyte selection in ART for academic research, commercial and clinical settings.

REFERENCES

Abeydeera LR, Wang WH, Cantley TC, Prather RS, Day BN. 1999. Glutathione content and embryo development after in vitro fertilization of pig oocytes matured in the presence of a thiol compound and various concentrations of cysteine. Zygote 7(3):203-210.

Acevedo N and Smith GD. 2005. Oocyte-specific gene signaling and its regulation of mammalian reproductive potential. Front Biosci. 10:2335-45.

Albertini DF. 2003. Origins and manifestations of oocyte maturation competencies. Reprod Biomed Online 6(4):410-415.

Albertini DF and Barrett SL. 2003. Oocyte-somatic cell communication. Reprod Supp 61:49-54.

Albertini DF and Barrett SL. 2004. The developmental origins of mammalian oocyte polarity. Semin Cell Dev Biol 15:599-606.

Allen E, Pratt JP, Newell QU, Bland, LJ. 1930. Human ova from large follicles; including a search for maturation divisions and observations on atresia. Am J Anat 46(1):1-53.

Andersen AC and Simpson ME. 1973. Follicular growth and degeneration. In The Ovary and Reproductive Cycle of the Dog (Beagle). Los Altos, CA: Geron-X, Inc. p 76-90.

Anderson JE, Matteri RL, Abeydeera LR, Day BN, and Prather RS. 2001. Degradation of maternal cdc25c during the maternal to zygotic transition is dependent upon embryonic transcription. Mol Reprod Dev 60:181-188.

Batten BE, Albertini DF and Ducibella T. 1987. Patterns of organelle distribution in mouse embryos during pre-implantaion development. Am J Anat 178:204-213.

Bavister BD and Yanagimachi R. 1977. The effects of sperm extracts and energy sources on the motility and acrosome reaction of hamster spermatozoa in vitro. Biol of Reprod 16:228-237.

Bavister BD and Squirrell J. 2000. Mitochondrial distribution and function in oocytes and early embryos. Hum Reprod 15 (Supp. 2):189-198.

Beijerink NJ, Kooistra HS, Dieleman SJ, and Okkens AC. 2004. Serotonin antagonist-induced lowering of prolactin secretion does not affect the pattern of pulsatile secretion of follicle-stimulating hormone and luteinizing hormone in the bitch. Reproduction 128:181-188.

Bing YZ, Nagai T, Rodriguez-Martinez H. 2001. Effects of cysteamine, FSH, and estradiol-17β on in vitro maturation of porcine oocytes. Theriogenology 55:867-876.

Blondin P and Sirard MA 1995. Oocyte and follicular morphology as determining characteristics for developmental competence in bovine oocytes. Mol Reprod Dev 41(1):54-62.

Bolamba D, Floyd AA, McGlone JJ, and Lee VH. 2002. Epidermal growth factor enhances expression of connexin 43 protein in cultured porcine preantral follicles. Biol Reprod 67:154-160.

Boni R, Cuomo A, and Tosti E. 2002. Developmental potential in bovine oocytes is related to cumulus-oocyte complex grade, calcium current activity and calcium stores. Biol Reprod 66:836-842.

Boni R, Gualtieri R, Talevi R, Tosti E. 2007. Calcium and other ion dynamics during gamete maturation and fertilization. Theriogenology 68S:S156-S164.

Bukovsky A, Caudle MR, Svetlikova M, Wimalasena J, Ayala ME, and Dominguez R. 2005. Oogenesis in adult mammals, including humans. Endocrine 26(3):301-316.

Burton GJ, Hempstock J, and Jauniaux E. 2002. Oxygen, early embryonic metabolism and free radical-mediates embryopathies. Reprod Biomed Online 6(1):84-96.

Cain JL, Lasley BL, Cain GR, Feldman EC and Stabenfeldt. 1989. Induction of ovulation in bitches with pulsatile or continuous infusion of GnRH. J Reprod Fertil Supp. 39:143-147.

Carroll, J and Swann K. 1992. Spontaneous cytosolic calcium oscillations driven by inositol triphosphate occur during in vitro maturation of mouse oocytes. J Biol Chem 267(16):11196-11201.

Castellani C. 1973. Spermatozoan biology from Leeuwenhoek to Spallanzani. J Hist Biol 6:37-68.

Chian RC, Niwa K and Nakahara H. 1992. Effect of sperm penetration in vitro on completion of first meiosis by bovine oocytes arrested at various stages in culture. J Reprod Fertil 96:73-78.

Choi YH, Love LB, Varner DD, and Hinrichs K. 2004. Factors affecting developmental competence of equine oocyte after intracytoplasmic sperm injection. Reproduction 127:187-194.

Christie DW, Bell ET. 1971. Endocrinology in the oestrous cycle in the bitch. J Small Anim Pract. Jul;12(7):383-9.

Ciotti PM, Notarangelo L, Morselli-Labate AM, Felletti V, Porcu E and Venturoli. 2004. First polar body morphology before ICSI is not related to embryo quality or pregnancy rate. Hum Reprod 19(10):2334-2339.

Concannon PW, McCann JP, and Temple M. 1989. Biology and endocrinology of ovulation, pregnancy and parturition in the dog. J Reprod Fertil Supplement. 39 3-25.

Concannon, PW. 2002a. Methods for induction of estrus in dogs using gonadotropins, GnRH or dopamine agonists. Proceedings of the 27th World Small Animal Veterinary Association Congress, Granada, Spain. URL (http://www.vin.com/proceedings/Proceedings.plx?CID=WSAVA 2002).

Concannon, PW. 2002b. Physiology and clinical parameters of pregnancy in dogs. Proceedings of the 27th World Small Animal Veterinary Association Congress, Granada, Spain. URL (http://www.vin.com /proceedings/Proceedings.plx?CID=WSAVA2002&PID=2681.

Concannon P.W. and Verstegen J. 2005. Some unique aspects of canine and feline female reproduction important in veterinary practice. Proceedings of the 30th World Small Animal Veterinary Association, Mexico City, Mexico. URL (http://www.vin.com/proceedings/Proceedings.plx?CID= WSAVA2005&Category=&PID=10995&O=Generic).

Corrada Y, Castex G, Sosa Y and Gobello C. 2003. Secretory patterns of prolactin in dogs: Circannual and ultradian rhythms. Reprod Domest Anim 38:219-223.

Damiani P, Fissore RA, Cibelli JB, Long CR, Balise JJ, Robl JM and Duby RT. 1996. Evaluation of developmental competence, nuclear and ooplasmic maturation of calf oocytes. Mol Reprod Dev 45:521-534.

Dedov VN, Cox GC, Roufogalis. 2001. Visualisation of mitochondria in living neurons with single-and two-photon fluorescence laser microscopy. Micron 32:653-660.

de Matos DG, Furnus CC, Moses DF, Martinez AG, Matkovic M. 1996. Stimulation of glutathione synthesis of in vitro matured bovine oocytes and its effect on embryo development and freezability. Mol Reprod Dev 45(4):451-457

de Matos DG and Furnus CC. 2000. The importance of having high glutathione (GSH) levels after bovine in vitro maturation on embryo development: Effect of β-mercaptoethanol, cysteine and cystine. Theriogenology 53:761-771.

de Matos DG, Gasparrini B, Pasqualini SR, and Thompson JG. 2002. Effect of glutathione synthesis stimulation during in vitro maturation of ovine oocytes on embryo development and intracellular peroxide content. Theriogenology 57:1443-1451

de Moor CH and Richter JD. 1999. Cytoplasmic polyadenylation elements mediate masking and unmasking of cyclin B1 mRNA. EMBO J 18(8):2294-2303.

Dumollard R, Duchen M, and Carroll J. 2007. The role of mitochondrial function in the oocyte and embryo. Curr Top Dev Biol 77:21-49.

Edwards RG. 1962. Meiosis in ovarian oocytes of adult mammals. Nature 196:446-450.

Eichenlaub-Ritter U and Peschke. 2002. Expression in vivo and in vitro growing and maturing oocytes: Focus on regulation of expression at the translational level. Hum Reprod Update 8(1):21-41.

England GCW, Verstegen JP, Hewitt DA. 2001. Pregnancy following in vitro fertilization of canine oocytes. Vet Rec 148 20-22.

Fair T, Hyttell P, Greve T. 1995. Bovine oocyte diameter in relation to maturational competence and transcriptional activity. Mol Reprod Dev 42:437-442.

Fan HY and Sun QY. 2004. Involvement of mitogen-activated protein kinase cascade during oocyte maturation and fertilization in mammals. Biol Reprod 70:535-547.

Farstad W. 2000. Assisted reproductive technology in canid species. Theriogenology 53(1):175-186.

Fatehi AN, Zeinstra EC, Kooij RV, Colenbrander B, Bevers MM. 2002. Effect of cumulus cell removal of in vitro matured bovine oocytes prior to in vitro fertilization on subsequent cleavage rate. Theriogenology 57:1347-1355.

Feldman EC and Nelson RW. 2004. Ovarian cycle and vaginal cytology. In Kersey R and LeMelledo D, editors. Canine and Feline Endocrinology and Reproduction 3rd ed. St. Louis, MO: W.B. Saunders Company p 752-773.

Fein A and Terasaki M. 2005. Rapid increase in plasma membrane chloride permeability during wound resealing in starfish oocytes. J Gen Physiol. 126(2):151-9.

Fortune JE. 2003. The early stages of follicular development: Activation of primordial follicles and growth of preantral follicles. Animal Reproduction Science 78:135-163.

Furnus CC, deMatos DG, and Moses DF. 1998. Cumulus expansion during in vitro maturation of bovine oocytes: Relationship with intracellular glutathione level and its role on subsequent embryo development. Mol Reprod Dev 51:76-83.

Gandolfi F, Luciano AM, Modina S, Ponzini A, Pocar P, Armstrong DT, and Lauria A. 1997. The in vitro developmental competence of bovine oocytes can be related to the morphology of the ovary. Theriogenology 48:1153-1160.

Ge L, Sui HS, Lan GC, Liu N, Wang JZ, Tan JH. 2008. Co-culture with cumulus cells improves maturation of mouse oocytes denuded of the cumulus oophorus: Observations of nuclear and cytoplasmic events. Fertil Steril Jan 10. [Epub ahead of print].

Gee KR, Brown KA, Chen WN, Bishop-Stewart J, Gray D, Johnson I. 2000. Chemical and physiological characterization of fluo-4 Ca(2+)-indicator dyes. Cell Calcium. 27(2):97-106.

Gitlin S. 2003. Oocyte biology and genetics revelations from polar bodies. Reprod Biomed Online 6(4):403-409.

Gobello C and Corrada Y. 2003. Biotechnology in canine reproduction: An update. Analecta Veterinaria 23(1):30-37.

Gordo AC, Rodrigues P, Kurokawa M, Jellerette T, Exley GE, Warner C, Fissore R. 2002. Intracellular calcium oscillations signal apoptosis rather than activation in in vitro aged mouse eggs. Biol Reprod 66:1828-1837.

Gosden RG. 2002. Oogenesis as a foundation for embryogenesis. Mol Cell Endocrinol 186:149-153.

Gunter TE, Yule DI, Gunter KK, Eliseev RA, Salter JD. 2004. Calcium and mitochondria. FEBS Letters 567:96-102.

Harrop AE. 1956. A review of canine artificial insemination. JAVMA 129:564-567

Harvey AJ, Kind KL, and Thompson JG. 2002. REDOX regulation of early embryo development. Reproduction 123:479-486.

He CL, Damiani P, Parys JB, Fissore RA. 1997. Calcium, calcium release receptors, and meiotic resumption in bovine oocytes. Biol Reprod. 57(5):1245-55.

Hendriksen PJM, Vos PLAM, Steenweg WNM, Bevers MM, Dielman SJ. 2000. Bovine follicular development and its effect on the in vitro competence of oocytes. Theriogenology 53:11-20.

Hewitt DA.1997. Oocyte maturation and fertilization in the bitch; the use of in vitro culture. Ph.D. Thesis. University of London.

Hewitt DA and England GCW. 1998. The effect of oocyte size and bitch age upon oocyte nuclear maturation in vitro. Theriogenology 49 957-996.

Holst PA and Phemister RD. 1971. The prenatal development of the dog: Preimplantation events. Biol Reprod 5:194-206.

Homa ST. 1995. Calcium and meiotic maturation of the mammalian oocyte. Mol Reprod Dev 40(1):122-34.

Hinrichs K and Williams KA. 1997. Relationships among oocyte-cumulus morphology, follicular atresia, initial chromatin configuration and oocyte meiotic competence in the horse. Biol Reprod 57:377-384.

Hyttel P, Farstad W, Mondain-Monval M, Bakke Lajord K, and Smith AJ. 1990. Structural aspects of oocyte maturation in the blue fox (*Alopex lagopus*). Anat Embryol 181:325-331.

Hyttel P, Fair T, Callesen H and Greve T. 1997. Oocyte growth capacitation and final maturation in cattle. Theriogenology 47:23-32.

Inaba T, Tani H, Gonda M, Nakagawa A, Ohmura M, Mori J, Torii R, Tamada H and Sawada T. 1998. Induction of fertile estrus in bitches using a sustained-release formulation of a GnRH agonist (luprolide acetate). Theriogenology 49:975-982.

Jalkanen L and Lindeberg H. 1998. Successful embryo transfer in the silver fox. Anim Reprod Sci 54 139-147.

Jang G, Kim MK, Oh HJ Hossein MS, Fibrianto YH, Hong SG, Park JE, Kim JJ, Kim HJ, Kang SK, Kim DY, Lee BC. 2007. Birth of viable female dogs produced by somatic cell nuclear transfer. Theriogenology 67(5):941-947 [Epub 2006].

Jang G, Hong SG, Oh HJ, Kim MK, Park JE, Kim HJ, Kim DY, Lee BC. 2008a. A cloned toy poodle produced from somatic cells derived from an aged female dog. Theriogenology 69(5):556-63.

Jang G, Oh HJ, Kim MK, Fibrianto YH, Hossein MS, Kim HJ, Kim JJ, Hong SG, Park JE, Kang SK, Lee BC. 2008b. Improvement of canine somatic cell nuclear transfer procedure. Theriogenology 69(2):146-54.

Jöchle W and Andersen AC. 1977. The estrous cycle in the dog: A review. Theriogenolgy 7(3):113-40.

Johnston SD, Root Kustritz MV and Olson PNS. 2001. Canine pregnancy. In Kersey, R, editor. Canine and Feline Theriogenology. Philladelphia, PA: W.B. Saunders Company p 66-104.

Kalab P, Srsen V, Farstad W, Krogenaes A, Motlik J, Hafne A-L. 1997. MAP Kinase activation and RAF-1 synthesis in Blue fox oocytes is controlled by cumulus granulosa cells. Theriogenology 47 400 abstract.

Kaneko T, Iuchi Y, Kawachiya S, Fujii T, Saito H, Kurachi H and Fujii J. 2001. Alteration of glutathione reductase expression in the female reproductive organs during the estrous cycle. Biol Reprod 65:1410-1416.

Kim MK, Fibrianto YH, Oh HJ, Jang G, Kim HJ, Lee KS, Kang SK, Lee BC, Hwang WS 2004. Effect of β-mercaptoethanol or epidermal growth factor supplementation on in vitro maturation of canine oocytes collected from dogs with different stages of the estrus cycle. J Vet Sci5(3):253-258.

Kim MK, Jang G, Oh HJ, Yuda F, Kim HJ, Hwang WS, Hossein MS, Kim JJ, Shin NS, Kang SK, Lee BC. 2007. Endangered wolves cloned from adult somatic cells. Cloning and Stem Cells 9(1):130-137.

Kobayashi M, Lee ES, Fukui Y. 2006. Cysteamine or beta-mercaptoethanol added to a defined maturation medium improves blastocyst formation of porcine oocytes after intracytoplasmic sperm injection. Theriogenology 65(6):1191-1199.

Kooistra HS, Okkens AC, Bevers MM, Popp-Snijders C, van Hafften B, Dieleman SJ, and Schoemaker J. 1999. Concurrent pulsatile secretion of luteinizing hormone and follicle-stimulating hormone during different phases of the estrous cycle and anestrus in beagle bitches. Biol Reprod 60:65-71.

Kraemer DC, Kinney GM, and Schriver MD. 1982. Embryo transfer in dogs and cats. Proceedings of the 2nd International Congress of Embryo Transfer in Mammals. In Embryo Transfer in Mammals, 2nd International Congress, Annecy. Foundation Marcel Merieux, Lyon, France. pp 223-233.

Krogenaes A, Nagyova E, Farstad W, and Hafne AL 1993. In vitro maturation of blue fox oocytes and cAMP production in oocyte-cumulus cell complexes. Theriogenology 39 250 abstract.

Larson DR, Zipfel WR, Williams RM, Clark SW, Bruchez MP, Wise FW and Webb WW. 2003. Water-soluble quantum dots for multiphoton fluorescence imaging in vivo. Science 300 (5624):1434-1436.

Lee BC, Kim MK, Jang G, Oh HJ, Yuda F, Kim HJ, Shamim MH, Kim JJ, Kang SK, Shatten G, and Hwang WS. 2005. Dogs cloned from adult somatic cells Nature 436:641-642.

Lee HS, Yin XJ, Jin YX, Kim NH, Cho SG, Bae IH, Kong IK. 2006. Germinal vesicle chromatin configuration and meiotic competence is related to the oocyte source in canine. Anim Reprod Sci Dec 17 [Epub].

Lee JH, Yoon SY, Bae IH. 2004. Studies on Ca^{2+} channel distribution in maturation arrested mouse oocytes. Mol Reprod Dev 69(2):174-85.

Leibfried L and First NL. 1979. Characterization of bovine follicular oocytes and their ability to mature in vitro. J Anim Sci 48(1):76-86.

Lindeberg H. 2003. Embryo technology in the farmed European pole cat (*Mustela putorius*). Ph.D. Dissertation University of Kuopio, Helsinki, Helsinki.

Liu RH, Li YH, Jiao LH, Wang XN, Wang H and Wang WH. 2002. Extracellular and intracellular factors affecting nuclear and cytoplasmic maturation of porcine oocytes collected from different sizes of follicles. Zygote 10:253-260.

Lonergan P, Rizos D, Gutierrez-Adan A, Fair T, and Boland MP. 2003. Oocyte and embryo quality: Effect of origin, culture conditions and gene expression patterns. Reprod Domest Anim 38:259-267.

Longeran P and Fair T. 2008. In vitro-produced bovine embryos: Dealing with the warts. Theriogenology 69(1):17-22.

Luberda Z. 2005. The role of glutathione in mammalian gametes. Reprod Biol 5(1):5-17.

Luciano AM, Lodde V, Beretta MS, Colleoni S, Lauria A, Modina S. 2005. Developmental capacity of denuded bovine oocyte in a co-culutre system with intact cumulus –oocyte complexes: Role of cumulus cells, cyclic adenosine 3',5'-monophosphate, and glutathione. Mol Reprod Dev 71(3):389-97.

Luvoni GC, Luciano AM, Modina S, Gandolfi F. 2001. Influence of different stages of the oestrous cycle on cumulus-oocyte communications in canine oocytes: Effects on the efficiency of in vitro maturation. J Reprod Fertil Supp 57 141-146.

Maedomari N, Kikuchi K, Ozawa M, Noguchi J, Kaneko H, Ohnuma K, Nakai M, Shino M, Nagai T, Kashiwazaki N. 2007. Cytoplasmic glutathione regulated by cumulus cells during porcine oocyte maturation affects fertilization and embryonic development in vitro. Theriogenology 67(5):983-993.

Mahi CA and Yanagimachi R. 1976. Maturation and sperm penetration of canine ovarian oocytes in vitro. J Exp Zool 196 189-196.

Marks CA, Brzozowski M, Zurek H and Clark M. 2002. Control of fertility in the red fox (*Vulpes vulpes*): Effect of a single oral dose of cabergoline in early pregnancy. Reprod Fert and Dev 14:29-33.

Matzuk MM, Burns KH, Viveiros MM, and Eppig JJ. 2002. Intercellular communication in the mammalian ovary: Oocytes carry the conversation. Science 296:2178-2180.

McEvoy TG, Coull GD, Broadbent PJ, Hutchinson JSM, and Speake BK. 2000. Fatty acid composition of lipids in immature cattle, pig and sheep oocytes with intact zona pellucida. J Reprod Fertil 118:163-170.

McLellan ME, Kajdasz ST, Hyman BT, and Bacskai BJ. 2003. In vivo imaging of reactive oxygen species specifically associated with thioflavine S-positive amyloid plaques by multiphoton microscopy. J Neurosci 23(6):2212-2217.

Memili E and First NL. 1999. Control of gene expression at the onset of bovine embryonic development. Biol Reprod 61:1198-1207.

Metcalfe SS. 1999. Assisted reproduction in the bitch. M.S. Thesis, Monash University, Victoria, Australia.

Motlik J, Crozet N and Fulka J. 1984. Meiotic competence in vitro of pig oocytes isolated from early antral follicles. J Reprod Fertil 72:323-328.

Nickson DA, Boyd JS, Eckersall PD, Ferguson JM, Harvey MJA and Renton JP. 1993. Molecular biological methods for monitoring oocyte maturation and in vitro fertilization in bitches. J Reprod Fertil Supplement 47 231-240.

O'Malley CD. 1956. On the genesis of the ovum of mammals and of man. Isis 47(2):117-153.

Onclin K, Murphy B and Verstegen JP. 2002. Comparisons of estradiol, LH and FSH patterns in pregnant and non-pregnant beagle bitches. Theriogenology 57:1957-1972.

Otoi T, Yamamoto K, Noyama N, Tachikawa S, and Suzuki T. 1997. Bovine oocyte diameter in relation to developmental competence. Theriogenology 48:769-774.

Otoi T, Fujii M, Tanaka M, Ooka A and Suzuki T. 1999. Effect of serum on the in vitro maturation of canine oocytes. Reprod Fertil and Dev 11 387-390.

Otoi T, Fujii M, Tanaka M, Ooka A and Suzuki T. 2000. Canine oocyte diameter in relation to meiotic competence and sperm penetration. Theriogenology 54 535-542.

Otoi T, Ooka A, Murakami M, Karja NWK, and Suzuki T. 2001. Size distribution and meiotic competence of oocytes obtained from bitch ovaries at various stages of the oestrous cycle. Reprod Fertil and Dev 13:151-155.

Otoi T, Willingham L, Shin T, Kraemer DC and Westhusin M. 2002. Effects of oocyte culture density on meiotic competence of canine oocytes. Reproduction 124:775-78.

Otoi T, Shin T, Kraemer DC, Westhusin M. 2007. Role of cumulus cells on in vitro maturation of canine oocytes. Reprod Domest Anim. 42(2):184-9.

Ownby C. 2000. Histology: Female reproductive system. URL (http://instruction.cvhs.okstate.edu/Histology/fr/HiFRp01.htm.

Patterson GH, Knobel SM, Arkhammar P, Thastrup O, Piston DW. 2000. Separation of the glucose-stimulated cytoplasmic and mitochondrial NAD(P)H responses in pancreatic islet beta cells. PNAS 97:5203-5207.

Perez-Armendariz EM, Saez JC, Bravo-Moreno JF, Lopez-Olmos V, Enders GC, and Villalpando I. 2003. Connexn43 is expressed in mouse fetal ovary. Anat Rec 271A(2):360-7.

Pertoft H, Laurent T, Laas C, Kagedl L. 1978. Density gradients prepared from colloidal silica particles coated by polyvinylpirrolidone (Percoll). Ann Biochem. 88:271 -282.

Pickard B, Dean W, Engemann S, Bergmann K, Fuermann M, Jung M, Reis A, Allen N, Reik W, and Walter J. 2001. Epigenetic targeting in the mouse zygote marks DNA for later methylation: A mechanism for maternal effects in development. Mech Dev 103:35-47.

Picton H, Briggs D and Gosden R. 1998. The molecular basis of oocyte growth and development. Mol Cell Endocrin 145:27-37.

Picton HM. 2001. Activation of follicle development: The primordial follicle. Theriogenology. 55(6):1193-210.

Pincus G and Enzmann EV. 1935. The comparative behavior of mammalian eggs in vivo and in vitro. J Exp Med 62:665-675.

Reynaud K, Fontbonne A, Marseloo N, Thoumire S, Chebrout M, Viaris de Lesegno C, and Chastant-Maillard S. 2005. In vivo meiotic resumption, fertilization and early embryonic development in the bitch. Reproduction 130:193-201.

Rice GC, Bump EA, Shrieve DC, Lee W, Kovacs M. 1986. Quantitative analysis of cellular glutathione by flow cytometry utilizing monochlorobimane: Some applications to radiation and drug resistance in vitro and in vivo. Cancer Res. 46(12 Pt 1):6105-10.

Rocha A, Randel RD, Broussard JR, Lim JM, Blair RM, Roussel JD, Godke RA, Hansel W. 1998. High environmental temperature and humidity decrease oocyte quality in *Bos taurus* but not in *Bos indicus* cows. Theriogenology 49:657-665.

Rodrigues BA and Rodrigues JL. 2003 Meiotic response of in vitro matured canine oocytes under different proteins and heterologous hormone supplementation Reprod Domest Anim 38(1):58-62.

Saint-Dizier M, Salomon JF, Petit C, Renard JP, Chastant-Maillard S. 2001. In vitro maturation of bitch oocytes: Effect of sperm penetration. J Reprod Fertil Suppl. 2001;57:147-50.

Saint-Dizier M, Reynaud K and Chastant-Maillard S. 2004. Chromatin, microtubules, and kinases activities during meiotic resumption in bitch oocytes. Mol Reprod Dev 68:205-212.

Salamone DF, Damiani P, Fissori RA, Robl JM, Duby RT. 2001. Biochemical and developmental evidence that ooplasmic maturation of prepubertal bovine oocytes is compromised. Biol Reprod 64(6):1761-1768.

Senger, PL. 2003. Reproductive cyclicity. In Pathways to Pregnancy and Parturition. Pullman, WA: Current Conceptions, Inc. p 151.

Sergeev IN and Norman AW. 2003. Calcium as a mediator of apoptosis in bovine oocytes and preimplantation embryos. Endocrine 22(2):169-76.

Shettles LB. 1958. Corona radiata cells and zona pellucida of living human ova. Fertil Steril 9:167-170.

Shrieve DC, Bump EA, Rice GC. 1988. Heterogeneity of cellular glutathione among cells derived from a murine fibrosarcoma or a human renal cell carcinoma detected by flow cytometric analysis. J Biol Chem. 5;263(28):14107-14.

Skinner MK. 2005. Regulation of primordial follicle assembly and development. Hum Reprod Update 11(5) 461-471.

Sokolowski JH. 1977. Reproductive patterns in the bitch. Vet Clin North Am. 7(4):653-66.

Songsasen N, Yu I and Leibo SP. 2002. Nuclear maturation of canine oocytes cultured in protein-free media. Mol Reprod Dev 62:407-415.

Songsasen N, Yu I, Gomez M, and Leibo SP. 2003. Effects of meiosis-inhibiting agents and equine chorionic gonadotropin on nuclear maturation of canine oocytes. Mol Reprod Dev 65:435-445.

Squirrell JM, Wokosin DL, White JG, and Bavister BD. 1999. Long-term two-photon fluorescence imaging of mammalian embryos without compromising viability. Nature Biotechnology 17:763-767.

Squirrell JM, Schramm RD, Paprocki AM, Wokosin DL and Bavister BD. 2003. Imaging mitochondrial organization in living primate oocytes and embryos using multiphoton microscopy. Microsc Microanal 9:190-201.

Srsen V, Kalous J, Nagyova E, Sutovsky P, King WA, and Motlik J. 1998. Effects of follicle-stimulating hormone, bovine somatotrophin and okadaic acid on cumulus expansion and nuclear maturation of blue fox (*Alopex lagopus*) oocytes in vitro. Zygote 6(4):299-309.

Steeves TE and Gardner DK. 1999. Metabolism of glucose, pyruvate, and glutamine during the maturation of oocytes derived from pre-pubertal and adult cows. Mol Reprod Dev 54:92-101.

Stojkovic M, Machado S, Stojkovic P, Zakhartchenko V, Hutzler P, Goncalves P, and Wolf E. 2001. Mitochondrial distribution and adenosine triphosphate content of bovine oocytes before and after in vitro maturation: Correlation with morphological criteria and developmental capacity after in vitro fertilization and culture. Biol Reprod 64:904-909.

Sturmey RG and Leese HJ. 2003. Energy metabolism in pig oocytes and early embryos. Reproduction 126:197-204.

Szabo PL. 1967. Ultrastructure of the developing dog oocyte. Anatom Rec 157:330.

Tarazona AM, Rodriguez JI, Restrepo LF and Olivera-Angel M. 2006. Mitochondrial activity, distribution and segregation in bovine oocytes and embryos produced in vitro. Reprod Dom Anim 41:5-11.

Tedor JB and Reif JS. 1978. Natal patterns among registered dogs in the United States. JAVMA 172(10):1179-85.

Tesoriero JV. 1981. Early ultrastructural changes of developing oocytes in the dog. J Morphol 168:171-179.

Thibault C**,** Szöllösi D**,** Gérard M. 1987. Mammalian oocyte maturation. Reprod Nutr Dev 27(5):865-96.

Tosti E, Boni R and Cumo A. 2000. Ca^{2+} current activity decreases during meiotic progression in bovine oocytes Am J Physiol Cell Physiol 297:C1795-C1800.

Tosti E. 2006. Calcium ion currents mediating oocyte maturation events. Reprod Biol and Endocrin 4:26.

Troiano L, Ferraresi R, Lugli E, Nemes E, Roat E, Nasi M, Pinti M and Cossarizza A. 2007. Multiparametric analysis of cells with different mitochondrial membrane potential during apoptosis bypolychromatic flow cytometry. Nat Protoc 2(11):2719-2727.

Valtonen M and Jalkanen L. 1993. Species-specific features of oestrous development and blastogenesis in domestic canine species. J Reprod Fertil Suppl. 47:133-137.

Vajta G, Peura TT, Holm P, Paldi A, Greve T, Trounson AO, Callesen H. 2000. New method for culture of zona-included or zona-free embryos: The well of well (WOW) system. Mol Reprod Dev 55:256-264.

Van Blerkom J. 1991. Mictrotubule mediation of cytoplasmic and nuclear maturation during the early stages of resumed meiosis in cultured mouse oocytes. PNAS 88:5031-5035.

Van Blerkom J, Davis PW and Merriam J. 1994. The developmental ability of human oocytes penetrated at the germinal vesicle stage after insemination in vitro. Hum Reprod 9:697-708.

Van Blerkom J, Davis P, and Lee J. 1995. ATP content of human oocytes and developmental potential and outcome after in-vitro fertilization and embryo transfer. Hum Reprod 10:415-424.

Van Blerkom J, Sinclair J, and Davis P. 1998. Mitochondrial transfer between oocytes: Potential applications of mitochondrial donation and the issue of heteroplasmy. Hum Reprod 1O:2857-2868.

Van Blerkom J, Davis P, Mathwig V, and Alexander S. 2002 Domains of high-polarized and low polarized mitochondria may occur in mouse and human oocytes and early embryos. Hum Reprod 17(2):393-406.

Van Blerkom J, Davis P, and Alexander S. 2003. Inner mitochondrial membrane potential ($\Delta\psi$m), cytoplasmic ATP content and free Ca^{2+} levels in metaphase II mouse oocytes. Hum Reprod 18(11):2429-2440.

Van Blerkom J. 2006. Regulatory roles for mitochondria in the peri-implantation mouse blastocyst: Possible origins and developmental significance of differential $\Delta\psi$m. Reproduction 131:961-976.

Van Blerkom J and Davis P. 2007. Mitochondrial signaling and fertilization. Mol Hum Reprod. 13(11):759-70. Epub 2007 Sep 23.

Van Blerkom J. 2008. Mitochondria as regulatory forces in oocytes, pre-implantation embryos and stem cells. Reprod Bioimed Online 16(4):553-569.

Verstegen JP, Onclin K, Silva LDM, and Concannon PW. 1998. Effect of stage of anestrus on the induction of estrus by the dopamine agonist cabergoline in dogs. Theriogenology 51:597-611.

Viaris De Lesegno C, Reynaud K, Pechoux C, Thomumire S and Chastant-Maillard S. 2008a. Ultrastructure of canine oocytes during in vivo maturation. Mol Reprod Dev 75:115-125.

Viaris De Lesegno C, Reynaud K, Pechoux C, Chebrout M and Chastant-Maillard S. 2008b. Ultrastructural evaluation of in vitro-matured canine oocytes. Reprod Fertil Dev. 20(5):626-39.

Wanke MM, Farina J, Loza MH, Rebuelto M and Concannon PW. 1996. Induction of estrus in bitches with normal and persistent anestrus using human menopausal gonadotropin (hMG). Theriogenology 47:935-942.

Westhusin M, Hinrichs K, Choi YH, Shin T, Liu L and Kraemer D. 2003. Cloning companion animals (Horses, cats and dogs). Cloning and Stem Cells 5(4):301-317.

Whitaker M and Patel R. 1990. Calcium and cell cycle control. Development. 108(4):525-42.

White N and Errington R. 2002. Multi-Photon Microscopy: Seeing more by imaging less. BioTechniques 33(2):298-305.

Wilding M, Dale B, Marino M, diMatteo L, Alviggi C, Pisaturo ML, Lombardi L and De Placido G. 2001. Mitochondrial aggregation patterns and activity in human oocytes and preimplantation embryos. Hum Reprod 16(5):909-917.

Wildt DE, Panko WB, Chakraborty PK, Seager SW. 1979. Relationship of serum estrone, estradiol-17-b and progesterone to LH, sexual behaviour and time of ovulation in the bitch. Biol Reprod 20:648-658.

Willingham-Rocky LA, Hanna CBM, Westhusin ME, Kraemer DC. 2002. Effects of porcine somatotropin and epidermal growth factor on the resumption of meiosis of canine oocytes matured in vitro. Theriogenology 57:742.

Willingham-Rocky LA, Hinrichs K, Westhusin ME, and Kraemer DC. 2003. Effects of stage of cycle and progesterone supplementation during culture on maturation of canine oocytes in vitro. Reproduction 126(4):501-8.

Willingham-Rocky LA, Golding MC, Wright JM, Kraemer DC, Westhusin ME, Burghardt RC. 2007. Cloning of GJA1 (connexin43) and its expression in canine ovarian follicles throughout the estrous cycle. Gene Expr Patterns 7(1-2):66-71 [Epub Jun 2006]

Wimsatt WA. 1975. Some comparative aspects of implantation. Biol Reprod 12:1-40.

Winger QA, Hill JR, Watson AJ, Westhusin ME. 2000. Characterization of a bovine cDNA encoding citrate synthase, and presence of citrate synthase mRNA during bovine pre-attachment development. Mol Reprod Dev 55(1):14-19.

Wongsrikeao P,Kaneshige Y, Ooki R, Taniguchi M, Agung B, Nii M, Otoi T. 2005. Effect of the removal of cumulus cells on the nuclear maturation, fertilization and development of porcine oocytes. Reprod Domest Anim. 40(2):166-70.

Wurth YA and Kruip ThAM. 1992. Bovine embryo production in vitro after selection of the follicle and oocytes. Proceedings of the 12th International Congress on Animal Reproduction, Hague, The Netherlands 1:387-389.

Yamada S, Shimazu Y, Kawaji M, Nakazawa M, Naito K & Toyoda Y. 1992. Maturation, fertilization and development of dog oocytes in vitro. Biol Reprod 46 853-858.

Yamada S, Shimazu Y, Kawano Y, Nakazawa M, Naito K, and Toyoda Y. 1993. In vitro maturation and fertilization of preovulatory dog oocytes. J Reprod Fertil Supplement. 47 227-229.

Yoshida M, Ishigaki K, Nagai T, Chikyu M, Pursel VG. 1993. Glutathione concentration during maturation and after fertilization in pig oocytes: Relevance to the ability of oocytes to form male pronucleus. Biol Reprod 49(1):89-94.

Yoshikuni M, Ishikawa K, Isobe M, Goto T, Nagahama Y. 1988. Synergistic actions of disulfide-reducing agents on 1-methyladenine-induced oocyte maturation in starfish. Dev Biol 128(1):236-239.

Zuelke KA, Jeffay SC, Zucker RM, and Perreault SD. 2003. Glutathione (GSH) concentrations vary with the cell cycle in maturing hamster oocytes, zygotes, and pre-implantation stage embryos. Mol Reprod Dev 64:106-112.

Zhou HM and Jin SY. 2007. Ca^{2+} cascade and meiotic resumption of the caprine primary oocyte. Reprod Domest Anim. 42(5):555-9.

VITA

LAURI WILLINGHAM-ROCKY
5900 Jack Finney Blvd.
Greenville, Texas 75402
(903) 268-2670
lwillingham@cvm.tamu.edu

Academic Background

2008 Ph.D., Texas A&M University, Department of Veterinary Integrative Biosciences
Major: Veterinary Anatomy
Dissertation Title: Evaluation of Oocyte Competency in Bovine and Canine Species Via Non-Invasive Assessment of Oocyte Quality

2001 M.S., Texas A&M University, Department of Animal Science
Major: Reproductive Physiology, Thesis Title: Canine Oocyte in vitro Maturation

1998 B.S., University of North Texas, Major: Biology

Publications

Willingham-Rocky LA, Golding MC, Wright JM, Kraemer DC, Westhusin ME, Burghardt RC. 2007. Cloning of GJA1 (connexin43) and its expression in canine ovarian follicles throughout the estrous cycle. Gene Expr Patterns 7(1-2):66-71 [Epub Jun 2006].

Willingham-Rocky LA, Hinrichs K, Westhusin ME, and Kraemer DC. 2003. Effects of stage of cycle and progesterone supplementation during culture on maturation of canine oocytes in vitro. Reproduction 126(4):501-8.

Otoi T, Willingham L, Shin T, Kraemer DC and Westhusin M. 2002. Effects of oocyte culture density on meiotic competence of canine oocytes. Reproduction 124:775-78.

Willingham-Rocky, LA. 2001. Canine oocyte in vitro maturation. M.S. Thesis, Texas A&M University.

Accepted GenBank Submissions

AY462223 Canis familiaris connexin 43 (Gja1) mRNA, complete cds